AGARD-R-798

AGARD

ADVISORY GROUP FOR AEROSPACE RESEARCH & DEVELOPMENT
7 RUE ANCELLE, 92200 NEUILLY-SUR-SEINE, FRANCE

AGARD REPORT 798

Aircraft Loads due to Turbulence and their Impact on Design and Certification

(Efforts avion dus à la turbulence atmosphérique et leurs impacts sur la conception et la certification)

This Publication was prepared at the request of the Structures and Materials Panel (SMP) of AGARD. Papers presented at a Workshop held in Lillehammer, Norway, 5 May 1994.

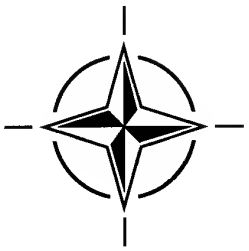

NORTH ATLANTIC TREATY ORGANIZATION

Published December 1994

Distribution and Availability on Back Cover

AGARD

ADVISORY GROUP FOR AEROSPACE RESEARCH & DEVELOPMENT
7 RUE ANCELLE, 92200 NEUILLY-SUR-SEINE, FRANCE

AGARD REPORT 798

Aircraft Loads due to Turbulence and their Impact on Design and Certification

(Efforts avion dus à la turbulence atmosphérique et leurs impacts sur la conception et la certification)

This Publication was prepared at the request of the Structures and Materials Panel (SMP) of AGARD. Papers presented at a Workshop held in Lillehammer, Norway, 5 May 1994.

North Atlantic Treaty Organization
Organisation du traité de l'Atlantique Nord

The Mission of AGARD

According to its Charter, the mission of AGARD is to bring together the leading personalities of the NATO nations in the fields of science and technology relating to aerospace for the following purposes:

- Recommending effective ways for the member nations to use their research and development capabilities for the common benefit of the NATO community;
- Providing scientific and technical advice and assistance to the Military Committee in the field of aerospace research and development (with particular regard to its military application);
- Continuously stimulating advances in the aerospace sciences relevant to strengthening the common defence posture;
- Improving the co-operation among member nations in aerospace research and development;
- Exchange of scientific and technical information;
- Providing assistance to member nations for the purpose of increasing their scientific and technical potential;
- Rendering scientific and technical assistance, as requested, to other NATO bodies and to member nations in connection with research and development problems in the aerospace field.

The highest authority within AGARD is the National Delegates Board consisting of officially appointed senior representatives from each member nation. The mission of AGARD is carried out through the Panels which are composed of experts appointed by the National Delegates, the Consultant and Exchange Programme and the Aerospace Applications Studies Programme. The results of AGARD work are reported to the member nations and the NATO Authorities through the AGARD series of publications of which this is one.

Participation in AGARD activities is by invitation only and is normally limited to citizens of the NATO nations.

Published December 1994

ISBN 92-836-0002-9

Printed by Canada Communication Group
45 Sacré-Cœur Blvd., Hull (Québec), Canada K1A 0S7

Preface

The study of the effects of atmospheric disturbances on the behaviour of aircraft started in about 1910. These disturbances which create discomfort for passengers and aircraft control problems for the pilots, are important dimensioning criteria in the field of structures.

The first regulatory requirements in this field appeared in the 1930's. Since this time, many other elements have intervened, in particular measurement of atmospheric disturbances (or their effect on aircraft), analysis of the disturbance structure, reduction of in-flight measurements, turbulence models, calculation of aircraft response, regulatory requirements, etc...

The AGARD Structures and Materials Panel has always been heavily involved in this field in particular, since the mid 80's, under the impetus of Dr. G. COUPRY. This renewal of interest comes from the development of transport aircraft towards wing configurations with high aspect ratios associated with flexible structures, the search for high-performance and optimized structures, the appearance of fly-by-wire controls and control laws, the development of computational power enabling more efficient simulation models using the results of measurements made on a large number of modern aircraft during commercial flights.

In this spirit and under the impetus of J. GLASER, the Structures and Materials Panel proposed an activity which led to the organisation of a Workshop on the theme: "Aircraft Loads due to Turbulence and their Impact on Design and Certification". This Workshop was held on 5 May 1994 as part of the 78th Meeting of the Structures and Materials Panel.

Concentrated into a single day, this Workshop brought together the world's leading specialists in structure calculations under the effect of atmospheric disturbances. It was an opportunity to link up and continue studies undertaken within other bodies such as the JAR Structure Study Group or the Gust Specialists' Committee whose last meeting was organized by the FAA in April 1994.

This document reproduces the papers presented. Many of them concerned the computation of the aircraft responses including high nonlinearities under the effect of a "continuous turbulence" type excitation. Given the recent nature of these studies, many complex theories and methods, which are sometimes very similar, are being developed, leading to the implementation of long and costly calculations. Developments for dealing with specific configurations were also presented: aircraft equipped with turboprops, aircraft equipped with external loads.

The discussions held within the scope of a round table at the end of the meeting gave rise to lively and fruitful exchanges and additional presentations (J. HOUBOLT) which allowed us to determine the main lines for orientating the future activities of the Structures and Materials Panel in this field.

Mr. D. CURBILLON
Sub-Committee Chairman

Préface

L'étude des perturbations atmosphériques sur le comportement des avions a commencé vers les années 1910. Si, pour les passagers des avions de transport, elles se manifestent par une sensation d'inconfort, et si, pour les pilotes, elles posent des difficultés de contrôle de l'avion, dans le domaine des structures, elles représentent un critère de dimensionnement important.

Les premières exigences réglementaires en la matière sont apparues autour des années 30. Depuis cette époque, de nombreux éléments sont intervenus, notamment la mesure des perturbations atmosphériques (ou de leurs effets sur avion), l'analyse de la structure des perturbations, la réduction des mesures en vol, les modèles de turbulence, le calcul de la réponse avion, les exigences réglementaires...

Le Panel des Structures et Matériaux de l'AGARD a toujours eu une activité importante dans ce domaine, en particulier depuis 1985 sous l'impulsion du Dr. G. COUPRY. Ce regain d'intérêt provient de l'évolution des avions de transport vers des configurations de voilure à grands allongements associées à des structures souples, de la recherche de structures performantes et optimisées, de l'apparition des commandes de vol électriques et des lois de pilotage, du développement des moyens de calcul autorisant des modèles de simulation plus performants utilisant les résultats des mesures effectuées sur un grand nombre d'avions modernes lors de vols commerciaux.

Dans cet esprit, et sous l'impulsion de J. GLASER, le Panel des Structures et Matériaux a proposé une activité qui a débouché sur l'organisation d'un atelier sur le thème : «Les charges avion liées à la turbulence atmosphérique et leur impact sur la conception et la certification». Cet atelier s'est tenu le 5 mai 1994 dans le cadre de la 78ème réunion du Panel des structures et matériaux.

Concentré sur une journée, cet atelier a permis de réunir les principaux spécialistes mondiaux du calcul des structures sous l'effet des perturbations atmosphériques. Il a été l'occasion de faire le lien et de poursuivre les réflexions menées dans d'autres organismes tels que le JAR Structure Study Group ou le Gust Specialists' Committee dont le dernier réunion a été organisé par le FAA en avril 1994.

Ce document donne le texte des différentes communications présentées. Pour une large part, elles concernent le calcul de la réponse des avions comportant de fortes non-linéarités sous l'effet d'une excitation du type «turbulence continue». Compte tenu du caractère récent de ces études, on assiste au développement de théories et méthodes nombreuses et complexes, parfois très voisines, aboutissant à la mise en œuvre de calculs longs et coûteux. Ont été également présentés, des développements pour traiter des configurations spécifiques : avions équipés de turbopropulseurs, avions équipés de charges externes.

La discussion menée dans le cadre d'une «table ronde», en fin de réunion, a été l'occasion d'échanges vivants et fructueux, de présentations complémentaires (J. HOUBOLT) qui ont permis de déterminer des axes de réflexions pour orienter les activités futures du Panel des Structures et Matériaux dans ce domaine.

M. D. CURBILLON
Président du sous-comité

Structures and Materials Panel

Chairman: Mr. R. Labourdette
Directeur Scientifique des
Structures
ONERA
29 Ave de la Division Leclerc
92320 Châtillon Cedex
France

Deputy Chairman: Dr. O. Sensburg
Deutsche Aerospace AG
Militaerflugzeuge
Postfach 80 11 60
81663 Munich
Germany

SUB-COMMITTEE MEMBERS

Chairman : Mr. M. CURBILLON
Adjoint au Chef de Dept Structures
AEROSPATIALE—Division avions
316, route de Bayonne—BP 3153
31060 TOULOUSE Cedex 03
France

Members :	D. Chaumette	—	FR	D. Paul	—	US
	L. Chesta	—	IT	H. Perrier	—	FR
	B. Eksi	—	TU	C. Perron	—	CA
	H. Försching	—	GE	R. Potter	—	UK
	R. Freymann	—	LU	E. Sanchiz	—	SP
	A.R. Humble	—	UK	N. Sandsmark	—	NO
	R. Labourdette	—	FR	O. Sensburg	—	GE
	M. Minges	—	US	D.L. Simpson	—	CA
	H. Ottens	—	NL			
	G. Papakonstantinou	—	GR			

PANEL EXECUTIVE

Dr Jose M. CARBALLAL, Spain

Mail from Europe:
AGARD-OTAN
7, rue Ancelle
92200 Neuilly-sur-Seine
France

Mail from US and Canada:
From USA and Canada
AGARD-NATO/SMP
PSC 116
APO AE 09777

Tel: (1) 4738 5790 & 5792
Telefax: (1) 4738 5799
Telex: 610176F

Contents

Overview of the Activities of the Ad Hoc Committee of International Gust Specialists

Terence J. Barnes
National Resource Specialist, Federal Aviation Administration
Northwest Mountain Region Hqs
1601 Lind Ave. (ANM - 105N), Southwest Renton
Washington 98055 - 4056, United States

1. SUMMARY

This paper presents the status of the work being undertaken by an international team of specialists to re-evaluate the gust criteria for future generations of commercial transports.

The international Ad Hoc Committee of Gust Specialists was formed in 1986, and established the following goals:

Criteria and means of compliance to be the same for FAR 25 and JAR 25.

Reduce the total number of criteria to be met.

Level of strength to be similar to current successful transports.

Ability to handle advanced technologies such as active controls and load alleviation.

Analytical work conducted by the specialists and reported at the annual meetings provided valuable background information to enable the Discrete Tuned Gust Method to be selected for the analysis of transport airplane dynamic loads due to discrete gust encounter.

Current and future work will concentrate on improved ways to account for loads due to continuous turbulence, and handle advanced technologies such as load alleviation which result in non linearity.

2. NOMENCLATURE

AGARD - Advisory Group for Aerospace Research and Development
ARAC - Aviation Rulemaking Advisory Committee
CAA-UK - UK Civil Aviation Authority
DSP - deterministic spectral procedure
FAA - US Federal Aviation Administration
FAR - US Federal Aviation Regulation
JAA - European Joint Aviation Authorities
JAR - European Joint Aviation Requirements
NACA - US National Advisory Committee for Aeronautics, now NASA
NASA - US National Aeronautics and Space Administration
MFT - matched filter theory
PSD - Power Spectral Density
SDG - statistical discrete gust
SSB - stochastic simulation based method

3. BACKGROUND

Since the recognition that turbulence produced significant structural loads (around 1915) there have been several significant steps in the development of gust criteria. The first gust criterion was the SHARP EDGED GUST formula. This was later modified to a formula specifying RAMP-PLATFORM GUSTS and later to ONE-MINUS-COSINE gusts. Finally, the criteria for CONTINUOUS TURBULENCE were developed.

Additional background and history on the development of the current FAA criteria are given in References 1 and 2.

In parallel with the development of criteria in the USA, various European Authorities developed their own criteria and added these as "National Variants" to the Joint Airworthiness Requirements of JAR 25.

The net result was that when the gust specialist's committee was formed, in order to certify a transport airplane to both FAR 25 and JAR 25, a manufacturer was required to consider and possibly perform seven separate gust analyses, and design to the most critical loads. These were :

Gust Load Formula
PSD Design Envelope
PSD Mission Analysis
JAR 12.5 Chord Dynamic Gust Analysis
CAA-UK Tuned Dynamic Gust Analysis
RLD Negative Gust
Round-the-clock Gust

Further background information is to be found in Reference 3.

As a result of ongoing Airworthiness Authority/ Industry cooperative activity and the removal of National Variants from JAR 25, the seven gust criteria have been reduced to four and modified as follows:

Tuned Discrete Gust
PSD Design Envelope
PSD Mission Analysis
Round-the-Clock Gust

Paper presented at a Workshop on "Aircraft Loads due to Turbulence and their Impact on Design and Certification" held in Lillehammer, Norway on 5 May 1994.

Even though this significant reduction in required analyses was a very positive step, earlier concerns raised by European Industry and Airworthiness Authorities regarding application of the PSD criteria of FAR 25 App G to European transports were still unresolved.

Furthermore, it was recognized that computer controlled systems such as gust alleviation would be under consideration on many projects, and thus the nonlinear effects of these systems would need to be included in any new gust analysis approach.

In the absence of definitive criteria, airplanes employing active load alleviation concepts such as the Lockheed L-1011 (Reference 4) and to the Airbus A-320 (Reference 5) used interim design criteria and analysis procedures which are not discussed in this paper.

4. DISCUSSION

The desire to provide gust analysis loads results which could be used directly in a stress analysis resulted in the consideration of analyses in the time domain first. These could then provide time correlated loads directly.

Each of the evaluations of new methods conducted and listed on Figure 1 will be discussed. Only key references are given for each method.

New Methods Proposed to Handle Discrete Gusts and Continuous Turbulence

Atmospheric Disturbance / Method	Discrete Gusts	Continuous Turbulence	Reference
Statistical Discrete Gust (SDG)	X	X	6
Tuned Discrete Gust (TDG)	X		JAR 25, Ch 13, Amdt 91/1
Matched Filter Theory (MFT)		X	8,9
Stochastic Simulation Based (SSB) Method		X	11
Deterministic Spectral Procedure (DSP)		X	12
Spectral Gust Method		X	13
Probability of Exceedance		X	14

Figure 1

Statistical Discrete Gust (SDG):
This method is unique in that it can handle both discrete gust events and continuous turbulence. The basic assumption of the SDG approach is that atmospheric turbulence can be represented by a series of 1-cosine shaped ramps applied in any order. The amplitude of each element is adjusted to reflect equal probability of occurrence by scaling element amplitude according to the element gradient length, H, to a power: $H^{1/3}$ for continuous turbulence and $H^{1/6}$ for extreme amplitude events.

It was first proposed by Glynn Jones in 1967, and reported in Reference 6.

Although developed in parallel with the Power Spectral Density (PSD) method, it was not evaluated as intensely, especially by US manufacturers.

Prior to proposing an in-depth evaluation of the SDG method by the manufacturers, the FAA requested NASA assistance in evaluating some of the major assumptions used in the SDG method. It was determined that for a given set of circumstances, the SDG continuous turbulence method produced essentially the same results as the PSD method, thus confirming the similarity between the $H^{1/3}$ scaling law used in SDG and the von Karman spectrum used in PSD (Reference 7).

An extensive evaluation by manufacturers of large and small transports in the US, Canada and Europe concluded that the method was not acceptable because of the laborious search procedure for the analysis of highly nonlinear systems, and the method was not recommended for consideration as a new Airworthiness Requirement.

However, this conclusion may have been premature, since no other method has been found which can efficiently handle continuous turbulence and highly non-linear systems, and the SDG method is also capable of handling both discrete and continuous turbulence.

Furthermore, since no single method was found to cover both discrete gusts and continuous turbulence, it was agreed that the existing situation of separate criteria would be continued, and each developed independently.

Tuned Discrete Gust (TDG):
The TDG method evolved from the method used to certify the Airbus A-320 (Reference 5) and includes three key elements.

A gust tuning law relating gust velocity to gust gradient distance in the same way as for the SDG method using the $H^{1/6}$ relationship.

A reference gust velocity based on in-flight recordings of transport airplane loads parameters in

normal operations. This results in a variation of reference gust velocity versus altitude.

A flight Profile Alleviation factor which accounts for the primary effects of the airplane operation by reducing the reference gust velocity at the lower altitudes for airplanes that predominantly cruise at high altitude.

The TDG method is part of the JAR and has been used for certification of several major programs, e.g., Airbus A330 and A340, and is part of the certification basis of the Boeing 777 and Cessna Citation X, among others. The FAA evaluates each new program individually, considering the equivalency of the TDG method to existing regulations.

Matched Filter Theory (MFT):
The MFT method identifies the gust velocity versus time profile which produces the maximum unit value of a specific load quantity.

Unit impulses of various strengths are applied through a von Karman filter to the known dynamics of an airplane, and the impulse responses of a given load quantity are ascertained. For that given load quantity, the load impulse response waveforms are reversed in time and played back through the gust filter and the airplane system to determine the critical load quantity in question and the associated correlated loads. The matched excitation or output waveforms are a function of the initial impulse strengths. The whole process is repeated for impulses of various strengths to determine the most critical load response together with the associated correlated loads.

With a nonlinear system, super position and other convenient features of linear MFT cannot be used, and a search procedure is the only practical means of finding a solution!

NASA reported results for time correlated loads for linear systems in Reference 8, and for nonlinear systems in Reference 9.

Stochastic Simulation Based (SSB) Method:
The SSB method uses a random white noise input signal fed through a von Karman filter to produce a gust velocity time history with a von Karman power spectrum which is applied to an airplane with linear or nonlinear systems.

Several simulations are performed. First, a search of time histories for a particular structural element load locates points in time where a peak load is within a specified range. The narrow response range is chosen for nonlinear systems to isolate the nonlinear nature of the airplane responses. Second, a sufficient amount of time prior to and following the peak load is selected, and the corresponding time history segments of the input excitation, the gust velocity, and the response waveforms are extracted.

The average waveforms of each type from this process converge to provide a gust velocity description that maximizes a given load quantity, hence that load quantity and the associated correlated loads are obtained.
Under a small contract with the FAA, NASA developed a SSB method to the same level as the MFT method and developed loads on a representative model with nonlinear systems, and compared the results and resources needed.

Reference 11 summarizes the SSB method and presents numerical results, and concludes that the approach requires excessive computer resources.

At the conclusion of this study the FAA accepted NASA's recommendations and released the computer code for MFT for industry evaluation (Reference 10).

Deterministic Spectral Procedure (DSP):
The Deterministic Power Spectral Procedure, DSP, was introduced by Jones and has been further developed by Noback (Reference 12). It can be regarded as the translation of the continuous turbulence power spectral density, PSD, method from the frequency domain into the space or time domain. The critical gust profile, giving maximum response for any given load quantity and correlated associated loads, is obtained directly. Noback has compared the method with Matched Filter Theory, and with direct simulation. It gives identical results to the power spectral approach for linear systems. Results have been obtained for a nonlinear system using equivalent gains to obtain the critical gust profile, and these results, also, have been compared with direct simulation.

Spectral Gust Method:
This is based on discrete gusts which have the correct power spectral density. Thus, the spectral gust method represents a direct translation of the PSD method into the time domain.

The method requires no optimization.

However, there can be several Spectral Gusts resulting in different design loads for nonlinear systems, depending on the definition of design load.

One solution might be to develop a few Spectral Gusts for the certification of each project, however, this would be a cumbersome process (see Reference 13).

Probability of Exceedance:
This method, which was proposed several years ago by Noback (Reference 14), determines limit loads for a nonlinear aircraft using the design envelope criterion. The method requires a time domain stochastic simulation of the pertinent responses to be evaluated for a number of input RMS gust intensities. The use of three gust intensities is suggested.

The criteria are defined so that the probability of exceeding the design load with the nonlinear system would be the same as the probability of exceeding the design load with a linear system. The result must be scaled to match linear traditional PSD results for a linear system.

5. FUTURE PLANS

Gust analysis methodology and design criteria are being worked by two overlapping committees. The Gust Specialists Committee defines, evaluates and makes recommendations to the ARAC FAA/JAA Loads Harmonization Working Group, which continues the process into possible rulemaking activity.

The tuned discrete gust analysis method, which handles isolated gusts, has followed this procedure, and was incorporated in JAR 25 at Amendment 91/1 effective 12 April 1991, and an FAA Draft NPRM has been prepared.

Activity to re-evaluate the Power Spectral Density gust analysis method, which handles continuous turbulence, and consider other methods such as Matched Filter Theory which can efficiently handle nonlinear systems, is in work in both committees.

The status of the various gust evaluations is given on Figure 2.

The following needs to be accomplished:

Complete re-evaluation of current PSD criteria of FAR 25, App G - U_{sigma} and mission analysis.

Complete evaluation of MFT one dimensional search method.

Recommend method for analysis of airplanes with nonlinear systems flying through continuous turbulence.

At the analysis level, consistent structural and aerodynamic modeling needs to be addressed.

In Reference 15, John Glaser of deHavilland Inc., Canada, proposed an AGARD study with the following title: "State-or-the-Art Methods in the Computation of Aircraft Gust Loads".

The proposed activity is described as follows:

The activities to date on the Flight of Flexible Aircraft in Turbulence have concentrated on the models of atmospheric turbulence and the determination of their properties from flight data recordings, the most familiar being the discrete, (1-cos) time domain gust model and the von Karman frequency domain or PSD gust model. The importance of the gust model is that it forms the "excitation" side of the equations of motion and the gust intensity value used is essential to ensuring an adequate level of design strength and therefore safety.

There are, however, other aspects in calculating gust loads that must be considered because of their potentially large influence on the design levels obtained. These have to do with aircraft modeling methods and the analytical procedures used. To date, little attention has been paid to these aspects within AGARD, or elsewhere for that matter. The following areas are offered as examples:

Flight mechanic modeling methods and the methods used to achieve appropriate flight stability characteristics.

Structural dynamic modeling methods.

The methods used to combine the flight mechanic and the structural dynamic equations of motion.

Computational techniques for solving the equations of motion.

The calculation of response loads from the solution for gust response.

A large variety of assumptions and approximations are made in the calculation of gust response loads that can strongly influence the loads results obtained. There is a clear need to identify where rigorous modeling methods and analytical procedures are required, to establish what those methods should be and to make those methods and procedures known so they can be applied uniformly throughout the industry.

But in recent years, the calculation of gust loads has become even more difficult with the advent of active flight control systems with their highly nonlinear characteristics. This has stimulated the investigation of a variety of new gust modeling methods, equivalent to the von Karman model, labeled SDG, MFT, DSP, DPSD, etc. These new methods are viewed by some gust loads analysts as being too complex to understand, to apply in routine calculations or to be accepted by airworthiness authorities.

There is a clear need to understand what effect nonlinear control systems (and other sources of nonlinearity) can have on gust design loads. If significant, it is important to have some simple but effective simulations of the von Karman model of continuous turbulence that can be accepted by industry and airworthiness authorities alike.

The purpose of this activity is to organize a workshop of gust loads specialists from industry, research establishments and airworthiness authorities to review the state-of the-art of gust loads computations with the view to identifying aircraft modeling methods and analysis procedures that can significantly influence design but are :

Inconsistently or incorrectly applied.
Inadequate to give reliable results.

Impractical or do not exist at all for current or emerging designs, in order to give framework and direction for a working group on gust loads methods.

The ultimate objective of this workshop is to establish a terms of reference for a working group that will be charged with establishing recommended design gust load methods, that will define those methods with demonstrations of their accuracy and effectiveness and that will issue the results of their work in a manual or AGARDOGRAPH.

The AGARD Working Group can work essentially independently of the other committees, and perform a useful function for the aviation community.

6. RECOMMENDATIONS

Incorporate TDG in FAR 25.

Continue evaluation of methods to develop design loads on airplanes with highly nonlinear control systems.

Possibly reconsider SDG if no other method can handle the problem of nonlinear control systems directly and efficiently.

Continue review of the current PSD method of FAR 25, Appendix G.

Define a limited number of patches of moderate/severe turbulence to be used to test the operation of airplane systems in the nonlinear range. These patches of turbulence could also be studied to determine the validity of the current assumptions, e.g., the I-cosine shape, and to determine if it would be possible to obtain an improved and much simplified time history characterization of design gusts that would work equally well for nonlinear as well as linear systems.

Proceed with the formation of an AGARD Working Group to review and recommend analytical modeling methods and procedures for dynamic gust analysis.

Continue to support the efforts to collect worldwide operational gust statistics from the current commercial fleet, and collect data from high altitude research aircraft to support the development of HSCT gust design criteria.

7. REFERENCES

I. H. N. Murrow, K. Pratt and J. Houbolt, "NACA/NASA Research Related to Evolution of U.S. Gust Design Criteria", AIAA Paper No. 89-1373 presented at the 30th SDM Conference in Mobile, Alabama, April 1989.

2. T. J. Barnes, "Current and Proposed Gust Criteria and Analysis Methods. An FAA Overview", AGARD Report 734- Addendum, 1987. Presented at the AGARD Workshop on the Flight of Flexible Aircraft in Turbulence, Cesme, Turkey, October 1987.

3. T. J. Barnes, "Harmonization of U.S. and European Gust Criteria for Transport Airplanes" presented at "ICAS 90" the 17th ICAS Congress, Stockholm, Sweden, September 1990.

4. J. D. Gould, "Effect of Active Control System Nonlinearities on the L-1011-3 (ACS) Design Gust Loads", AIAA Paper No. 85-0755 presented at the 26th SDM Conference in Orlando, Florida 1985.

5. G. Vinnicombe, A. Dudman and M. Hockenhull, "Gust Analysis of an Aircraft with Highly Non-Linear Systems Interaction", AIAA Paper No. 89-1377 presented at the 30th SDM Conference in Mobile, Alabama, April 1989.

6. J. G. Jones, "Statistical Discrete Gust Theory for Aircraft Loads, a Progress Report", RAE Technical Report 73167, 1973.

7. B. Perry, III, A. S. Pototzky, and J. A. Woods, "An Investigation of the 'Overlap' Between the Statistical-Discrete-Gust and the Power-Spectral-Density Analysis Methods", AIAA 30th Structures, Structural Dynamics and Materials Conference, Mobile, Alabama, April 3-5, 1989.

8. A. S. Pototzky and T. A. Zeiler, "Time-Correlated Gust Loads Using Matched Filter Theory and Random Process Theory - A New Way of Looking at Things", AIAA 30th Structures, Structural Dynamics and Materials Conference, Mobile, Alabama, April 3-5, 1989.

9. B. Perry, III, R. C. Scott, and A. S. Pototzky, "Update of NASA Research in Time-Correlated Gust Loads for Nonlinear Aircraft", prepared for Gust Specialists Meeting, La Jolla, California, April 22, 1993.

10. B. Perry, III, R. C. Scott, and A. S. Pototzky, "A Computer Program to Obtain Time Correlated Gust Loads for Nonlinear Aircraft Using the Matched Filter Based Method", DOT/FAA/CT-93/63.

11. R. C. Scott, A. S. Pototzky, and B. Perry, III, "Further Studies Using Matched Filter Theory and Stochastic Simulation for Gust Loads Prediction, presented at the AIAA 34th Structures, Structural

Dynamics and Materials Conference, La Jolla, California, April 1993.

12. R. Noback, "The Deterministic Power Spectral Density Method", National Aerospace Laboratory NLR, The Netherlands, NLR TP 92114L, prepared for Gust Specialists Meeting, Dallas, Texas, April 15, 1992.

13. M. Molzow, H. Lusebrink, and J. Brink-Spalink, "Proposal for a Spectral Gust Method", presented at the Gust Specialists Meeting, April 22, 1993, La Jolla, California.

14. R. Noback, "Definition of P.S.D. Design Loads for Nonlinear Aircraft", NLR TP 89016U, 1989.

15. J. Glaser, "Aircraft Loads Due to Turbulence and Their Impact on Design and Certification" Candidate AGARD Working Activity CA/04/90.

SUMMARY OF GUST EVALUATIONS - DISCRETE GUSTS

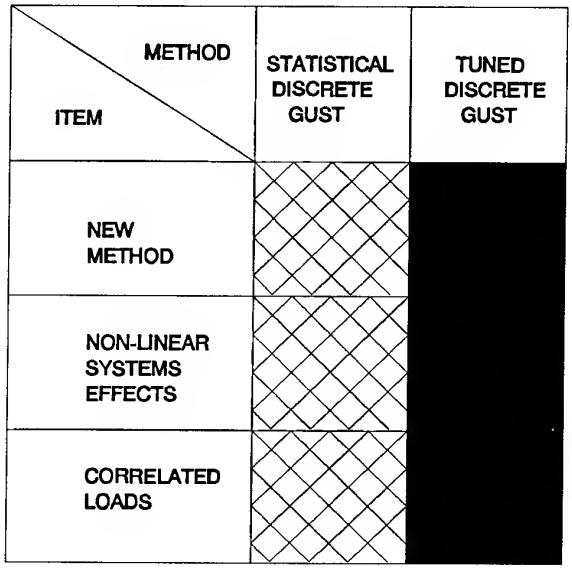

Key

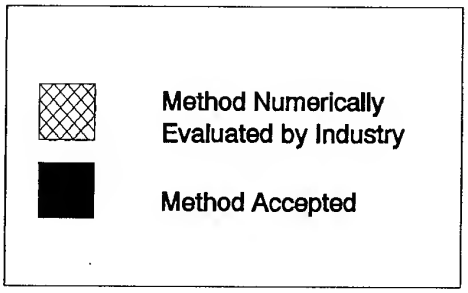

FIGURE 2A

SUMMARY OF GUST EVALUATIONS
CONTINUOUS TURBULENCE

METHOD / ITEM	STATISTICAL DISCRETE GUST	MATCHED FILTER THEORY	L-1011 METHOD	A-320 METHOD	REVIEW OF MISSION ANALYSIS	REVIEW OF P's and B's	REVIEW OF U_{sigma}
RE-EVALUATION OF FAR 25, APP G	▨				▨	▨	▨
NON-LINEAR SYSTEMS EFFECTS	▨	▨	■	■			
CORRELATED LOADS	▨	▨					

Key

▨ Method Developed

▨ Method Numerically Evaluated by Industry

■ Method Accepted

FIGURE 2B

The Impact of Non-linear Flight Control Systems on the Prediction of Aircraft Loads due to Turbulence

R.M. Warman
British Aerospace Airbus Limited
P.O. Box 77, Filton
Bristol, BS99 7AR
England

SUMMARY

During the past ten years the extensive use of electronic flight control systems has introduced a high level of non-linearity, to the behaviour of civil transport aircraft, in response to both pilot inputs and external influences such as turbulence. These systems that control, protect and, in some instances, alleviate the loads experienced by the aircraft have had a significant impact on the prediction of aircraft loads. There is an increasing need both to model control system non-linearity, to avoid designing control systems that degrade structural performance, and to demonstrate the effectiveness of alleviation systems for aircraft certification.

The introduction of non-linear flight control systems presents little problem when using time-based simulations to predict aircraft loads due to discrete gusts. Frequency domain, Power-Spectral Density (PSD), analysis used to predict aircraft loads due to Continuous Turbulence (CT), however, is severely restrictive, requiring a linear mathematical model of both the aircraft and control systems. Over the past ten-to-fifteen years various analysis techniques have been developed that provide time-based interpretations of the CT atmosphere and, therefore, means by which loads due to CT can be predicted for aircraft with non-linear flight control systems. Recent involvement in the design of Airbus aircraft has led to British Aerospace Airbus Limited taking an active role in both developing and using these non-linear analysis techniques.

By drawing on experience gained during the design of recent Airbus aircraft, the impact of non-linear flight control systems on the prediction of aircraft loads due to turbulence is discussed.

LIST OF SYMBOLS

$\underline{A}$, $\underline{A}_a$	inertia coefficient matrices.
$\underline{B}$, $\underline{B}_a$	aerodynamic damping coefficient matrices.
$\underline{C}$, $\underline{C}_a$	aerodynamic stiffness coefficient matrices.
$\underline{\delta}$	vector of control deflections.
$\underline{D}$	structural damping coefficient matrix.
$\underline{E}$	structural stiffness coefficient matrix.
$\mathcal{E}[x\|y=y_d]$	expected value of load x given that load y is at its design value, y_d.
$\Phi(\omega)$	normalised von Kármán power spectrum.
η_d	turbulence "probability" factor { $=U_\sigma/\sigma_w$ }.
$\underline{H}(j\omega)$	aircraft "closed-loop" frequency-response-function { $=\underline{Y}(j\omega)/u_g(j\omega)$ }.
$H_y(j\omega)$	frequency-response-function for load y, a member of $\underline{H}(j\omega)$ { $=y(j\omega)/u_g(j\omega)$ }.
$\underline{I}$	identity matrix.
K_{eq}	equivalent gain.
L	turbulence scale length.
$N[y_d]$	rate of exceedence of design load, y_d.
N_0	rate of positive going, zero crossings, for a linear model.
$p(\upsilon)$	probability density function of υ.
$\underline{q}$	modal coordinates (states).
ρ	air density.
ρ_{xy}	correlation coefficient between loads x and y.
$\underline{R}_c$, $\underline{R}_{ca}$	aerodynamic forcing vectors due to control surface deployment.
$\underline{R}_g$, $\underline{R}_{ga}$	aerodynamic forcing vectors due to turbulence.
σ_w	standard deviation (root-mean-square value) of turbulence, turbulence intensity.
σ_y	standard deviation (root-mean-square value) of load y.
T	turbulence time constant { $=L/V$ }.
U_σ	Design Envelope Analysis peak turbulence intensity.
u_{ce}	unit of computational effort.
u_g	turbulence input.
V	true airspeed.
ω	angular frequency.
$\underline{Y}$	"Interesting Quantity" vector containing load quantities, lift coefficients, accelerations, etc.
y	a load quantity, a member of $\underline{Y}$.
y_d	the design value of load y.

1.0 INTRODUCTION

The task of predicting aircraft flight loads due to turbulence has grown considerably over the past ten years, largely due to the extensive use of electronic flight control systems on modern civil transport aircraft.

Electronic flight control laws, with altitude and airspeed dependent gains, have meant that the use of extrapolation to focus on design critical flight regimes and aircraft configurations is not certain to identify the most critical loading conditions. Consequently, Design Envelope Analysis (DEA) requires a far more extensive coverage of the flight envelope and aircraft configurations than is required for an aircraft without electronic flight control systems. Non-linear flight control laws accentuate this problem.

The use of load alleviation systems has served to eliminate the concept of a "turbulence designed" aircraft or a "manoeuvre designed" aircraft by ensuring

Paper presented at a Workshop on "Aircraft Loads due to Turbulence and their Impact on Design and Certification" held in Lillehammer, Norway on 5 May 1994.

that envelope loads due to manoeuvres and envelope loads due to turbulence are of similar magnitude. Consequently, loads due to turbulence and manoeuvres must be analysed in equal depth throughout the design cycle.

The above observations serve to demonstrate both the importance and the increasing cost associated with the prediction of aircraft loads due to turbulence, for both the design and certification of an aircraft with non-linear flight control systems.

It has been the policy of Airbus Industrie to use DEA both to design and certificate its "fly-by-wire" aircraft. Consequently, all the following discussion will centre on the prediction of aircraft loads to establish a design envelope. For the purposes of this discussion the aircraft model is assumed linear and, when combined with a linear control system, forms the datum against which the impact of non-linear control systems are judged. However, much of the discussion is equally applicable for situations where the non-linearity is exhibited by the aircraft model.

2.0 THE DATUM MODEL OF THE AIRCRAFT

The manufacturers aim is to minimise the weight of the aircraft and thereby improve its performance and marketability, whilst airworthiness requirements exist to provide rules that are not necessarily rational, but that aim to ensure a safe structure based on a large database of past and present aircraft. The loads engineer must therefore strive to satisfy both requirements and accordingly choose modelling techniques of suitable complexity, accuracy and cost.

The model of the aircraft has developed over many years to a standard where, for the purposes of loads prediction, it adequately represents the aircraft. In general, flight tests have confirmed this although modification to the data, feeding into the model, is usually required to obtain a satisfactory match between the measured and predicted response. Prior to matching it is possible that some predicted aircraft loads will differ from measured aircraft loads by up to 20%, however the predicted trends in aircraft loads are usually accurate.

The aircraft model is not intended to "model the truth", rather to provide a reasonable representation of the aircraft that, in conjunction with other design parameters (e.g. factors of 1.5 between limit load and ultimate load), will ensure the structural integrity of the aircraft without yielding overweight designs. This does not imply that improvements to modelling techniques should not be sought, rather that all new methods must consider the accuracy and completeness of all model components; the purpose for which the model will be used and the external parameters that may influence the level of accuracy required.

2.1 The Mathematical Model of the Aircraft Model

Over many years the development of the mathematical model of the aircraft has been guided by:

- Its performance against flight test.
- The computing power available.
- The airworthiness requirements.
- The manufacturers desire to minimise weight.
- Design costs.

The model that has evolved combines both the structural and aerodynamic properties of the aircraft into a second order, linear, ordinary differential equation (1) described in terms of modal coordinates, i.e. all shapes that the aircraft can assume are represented by the sum of its natural vibration (mode) shapes, in various proportions. By eliminating the mode shapes that correspond to the higher frequencies of vibration it is possible to keep the aircraft equations of motion to a manageable size, with only minor degradation to accuracy.

$$\underline{A}\ddot{\underline{q}} + (\rho V\underline{B} + \underline{D})\dot{\underline{q}} + (\rho V^2\underline{C} + \underline{E})\underline{q} = \rho V\underline{R}_g u_g + \rho V^2\underline{R}_c\underline{\delta} \quad (1)$$

The aircraft "Interesting Quantity" (IQ) set comprises forces, moments, torques, accelerations, etc. at various stations within the aircraft structure and are recovered through an auxiliary equation (2) that sums the external forces acting on the structure. The forces and moments could also be recovered as the sum of internal forces, however this can prove unreliable when working with a limited number of mode shapes.

$$\underline{Y} = \rho V\underline{R}_{ga}u_g + \rho V^2\underline{R}_{ca}\underline{\delta} - \underline{A}_a\ddot{\underline{q}} - \rho V\underline{B}_a\dot{\underline{q}} - \rho V^2\underline{C}_a\underline{q} \quad (2)$$

2.2 The Introduction of a Flight Control System

The combination of the aircraft and control system is simulated by "wrapping" the control system equations around the aircraft dynamics represented by equations (1) and (2), see figure 1.

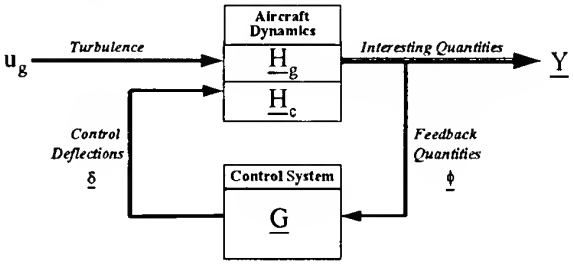

Figure 1. Aircraft simulation.

In the time-domain the aircraft equations are rearranged into state-space form and solved using a suitable integration method for first order, ordinary differential equations. The control system is modelled as a digital circuit driven by the feedback quantities (e.g. normal accelerations, pitch rate, etc.) that form a subset of the aircraft IQ set. At specified time-intervals within the simulation the IQ set is calculated; the control system activated and the commanded control deflections updated.

In the frequency-domain, the aircraft dynamics are described by Frequency-Response-Functions that relate the "Interesting Quantities" to the control and turbulence inputs, $\underline{H}_c$ and $\underline{H}_g$ respectively. Similarly, a linear control system is represented by a Frequency-Response-Function (FRF), $\underline{G}$. The "closed-loop" FRF, relating the IQ set to the turbulence input, is calculated using equation (3).

$$\underline{H}(j\omega) = \underline{H}_c(j\omega)\underline{\Gamma}(j\omega)\underline{G}(j\omega)\tilde{\underline{H}}_g(j\omega) + \underline{H}_g(j\omega) \quad (3)$$

$$\text{where } \underline{\Gamma}(j\omega) = \left[\underline{I} - \underline{G}(j\omega)\tilde{\underline{H}}_c(j\omega)\right]^{-1}$$

The embellishment, ~, denotes that the FRF contains only the feedback quantities.

The frequency-responses of the IQ set, hence the aircraft loads, are obtained via equation (4).

$$\underline{Y}(j\omega) = \underline{H}(j\omega)u_g(j\omega) \quad (4)$$

3.0 DESIGN ENVELOPE ANALYSIS

The current airworthiness requirements [1][2] request that two types of analyses are performed to predict aircraft flight loads due to turbulence. These comprise the prediction of loads arising from both discrete gust events and CT. In turn,

there are two alternative approaches to determining aircraft limit loads due to CT: Mission Analysis and DEA. It has been the policy of Airbus Industrie to use DEA to design and certificate its "fly-by-wire" aircraft, so this forms the basis for further discussion.

The concept of the Statistical Discrete Gust (SDG), introduced by Jones [3], attempted to combine the two analyses into a single analysis. However, the SDG has not been adopted as an airworthiness requirement and therefore offers little to the manufacturer, except maybe as a starting point for developing methods suitable for the prediction of loads for nonlinear aircraft models.

The Tuned Discrete Gust (TDG), comprising a series of "1-cosine" discrete gusts of varying gradient length, is used to predict loads due to discrete gust events and is best suited to a time-domain analysis. CT, however, is represented by a stationary, Gaussian, stochastic process for which the turbulence is described by the isotropic power-spectral density function attributed to von Kármán, equation (5). Consequently, for a linear aircraft model, CT analysis is best performed in the frequency-domain.

$$\hat{\Phi}(\omega) = \sigma_w^2 \Phi(\omega) = \sigma_w^2 T \left\{ \frac{1 + \frac{8}{3}(1.339T\omega)^2}{\left\{1 + (1.339T\omega)^2\right\}^{11/6}} \right\} \quad (5)$$

3.1 Tuned-Discrete Gusts

For a given design condition (e.g. aircraft configuration and flight point) the TDG requires the prediction of aircraft loads, due to a family of "1-cosine" discrete gusts of varying gradient length and amplitude, using a time-based analysis. DEA requires determination of the envelope (e.g. maximum and minimum) loads of all the design points considered. For design purposes, however, the maximum and minimum stresses, that are a function of the forces and moments acting at a given point in time, are of more importance. There are two ways that these stresses may be recovered.

1. Directly, by including stress quantities in the IQ set.
2. Indirectly, as a function of time-correlated loads.

The first method eliminates the need for time-correlated loads, but will require a complete turbulence analysis each time the structure is changed. The second method, albeit an approximation to the maximum and minimum stresses, enables structural designers to make modifications to local structure without recourse to further turbulence analyses.

For logistical and financial reasons the second method is preferred, so it is necessary not only to recover the envelope loads but, also, the loads over the rest of the aircraft that coincide (correlate) with the envelope values. Correlated load sets are easily obtained for time-based analyses by sorting through the load response time-histories.

The introduction of a non-linear flight control system has little impact on the discrete gust analysis techniques, only on the loads predicted.

Note 1: computational effort.
The calculation of a correlated load set, resulting from a single "1-cosine" discrete gust input, will be used as the base unit for a measure of computational effort. Typically, one unit of computational effort ($1u_{CE}$) represents the work required to establish a correlated set of, say, five-hundred "Interesting Quantities" from three seconds (approximately 200 time-points) of time-history response per IQ. For a given aircraft configuration and flight point, a TDG analysis comprising a family of, say, sixteen "1-cosine" gusts will require $16u_{ce}$ (sixteen units of computational effort).

3.2 Continuous Turbulence, Random Process Theory

For a given design condition and a linear aircraft model, the prediction of aircraft loads due to CT uses a frequency-domain analysis, often referred to as Random Process Theory (RPT). The aircraft is subjected to turbulence that conforms to the von Kármán power spectrum (5) and a statistical design load is determined through a "probability" factor, η_d, that relates the design load, y_d, to the root-mean-square value of the load, σ_y [4].

$$y_d = \eta_d \sigma_y = \overline{A}_y \eta_d \sigma_w = \overline{A}_y U_\sigma \quad (6)$$

where

$$\overline{A}_y = \frac{\sigma_y}{\sigma_w} = \sqrt{\frac{1}{\pi}\int_0^\infty \left|H_y(j\omega)\right|^2 \Phi(\omega) d\omega} \quad (7)$$

The CT problem was originally assumed to be linear, so the "probability" factor, η_d, and the turbulence intensity, σ_w, were combined into the single value of U_σ defined in the airworthiness requirements [1][2] as a function of altitude and airspeed.

Since the design load is determined on a statistical basis, the correlated loads can be determined on the basis of "equal probability", Noback [5]. The correlated load set represents the expected values of the other loads when the envelope load equals its design value, y_d. For a linear aircraft model the response of all loads to Gaussian turbulence will also be Gaussian, so the loads, y_j, that correlate to the design load, $y_i = y_d$, are given by the conditional expectation:

$$\mathcal{E}\left[y_j | y_i = y_d\right] = y_d \rho_{y,y_i} \frac{\sigma_{y_j}}{\sigma_{y_i}} \quad (8)$$

which, for the linear aircraft model, yields

$$\mathcal{E}\left[y_j | y_i = y_d\right] = \frac{U_\sigma}{\overline{A}_{y_i}} \int_0^\infty H_{y_j}(j\omega) H_{y_i}^*(j\omega) \Phi(j\omega) d\omega \quad (9)$$

A single CT analysis, for a given aircraft configuration at a given flight point, will involve the calculation of the aircraft "closed-loop" FRF (3) at, say, 400 frequencies. The frequency -responses of the "Interesting Quantities" are obtained using equation (4) and the correlated set formulated by integration using equations (6) through to (9). This requires about $10u_{ce}$ (ten units of computational effort).

Note 2: for a linear system, Matched Filter Theory (MFT) [6] offers an equivalent time-based approach to that of RPT. For a linear aircraft, however, RPT requires less computational effort and is, therefore, the preferred approach.

The unsuitability of RPT for non-linear problems means that alternative methods must be sought to deal with non-linear flight control systems. Consequently, the prediction of aircraft loads due to CT is where the introduction of non-linear flight control systems has had most impact on the methods used. Before discussing this further, however, the following two items will be addressed:

- The definition of the turbulence intensity for stochastic analysis using the "principle of equivalent safety".
- Non-linear flight control systems and the types of non-linear problem encountered.

4.0 "PRINCIPLE OF EQUIVALENT SAFETY"

It was noted in section 3.2 that for CT DEA, due to the assumption of linearity, the value of the turbulence intensity, σ_w, was combined with a "probability" factor, η_d, to yield a single value, U_σ, that is defined in the airworthiness requirements [1][2] as a function of aircraft speed and altitude.

$$U_\sigma = \eta_d \sigma_w \quad (10)$$

The choice of U_σ for DEA is founded on the basis of achieving a constant frequency of exceedence of load at all altitudes [4] and by choosing a frequency of exceedence of design load that experience has shown to be safe. Stochastic based, non-linear, analyses that utilise the "principle of equivalent safety" (i.e. maintain a statistical level of safety consistent with the linear definition of design load) require knowledge of the turbulence intensity, σ_w. Turbulence intensities are not defined for DEA, however they are for mission analysis [4]: turbulence is defined as a quasi-stationary, Gaussian, process with the same von Kármán power spectrum, but with a slowly varying root-mean-square intensity with a probability density function (11).

$$p(\sigma_w) = \sqrt{\frac{2}{\pi}}\left\{\frac{p_1}{b_1}\exp\left(\frac{-\sigma_w^2}{2b_1^2}\right) + \frac{p_2}{b_2}\exp\left(\frac{-\sigma_w^2}{2b_2^2}\right)\right\} \quad (11)$$

The parameters: p_1, p_2, b_1 and b_2 are specified in the airworthiness requirements [1][2].

The normalised rate of positive going exceedences (12) of the design load, y_d, for a given turbulence intensity is derived from a formula attributed to Rice [7].

$$\frac{N[y_d,\sigma_w]}{N_0} = \exp\left(\frac{-U_\sigma^2}{2\sigma_w^2}\right) \quad (12)$$

More importantly, the frequency of exceedence of the design load is obtained by integrating the product of equations (11) and (12) over the range of turbulence intensities.

$$\frac{N[y_d]}{N_0} = \int_0^\infty \frac{N[y_d,\sigma_w]}{N_0} p(\sigma_w) d\sigma_w \quad (13)$$

Noback [8] and Vinnicombe et al. [9] have demonstrated that exceedences of the design load are dominated by the "storm turbulence", represented by p_2 and b_2 in equation (11), and that the values of turbulence intensity contributing to exceedence of the design load are concentrated in a narrow band, as seen in figure 2.

The value of η_d that corresponds to the turbulence intensity contributing most to the exceedence of design load for a given flight point is given by equation (14).

$$\eta_{max} = \frac{U_\sigma}{\sigma_{max}} = \sqrt{\frac{U_\sigma}{b_2}} \quad (14)$$

A true, stochastic, non-linear analysis, based on the "principle of equivalent safety", would require many simulations using differing turbulence intensities, guided by the rate of frequency of exceedence variation, with turbulence intensity, shown in figure 2. Equation (13) would then be used to generate the rate of exceedence curves necessary to establish the non-linear design load. Clearly this is an impractical approach, therefore alternatives must be sought.

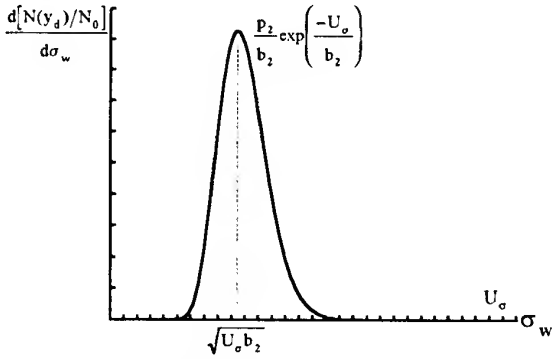

Figure 2. Contribution of turbulence intensity to design load.

Vinnicombe et al. [9] found that, for their particular non-linear problem, it was adequate to define a single value for the "probability" factor, η_{max} (e.g. η_{max}=3), using equation (14) for a load critical flight point. Equation (10) was then used to define turbulence intensities at other flight points.

An alternative, suggested by Noback [8], is to perform a non-linear analysis for several turbulence intensities and use a weighted average (based on the curve in figure 2) of the resulting loads to determine the non-linear design load.

The choice of turbulence intensity is not always straight forward and will depend very much on the aircraft and the nature of the non-linear problem. If the chosen turbulence intensity does not exercise the non-linearity then design loads will be biased towards those for a linear model, the converse is also true. *Clearly, this introduces an ambiguity into non-linear stochastic methods that is best addressed on a problem by problem basis, although there is a need for guidance within a future CT airworthiness requirement.*

5.0 NON-LINEAR CONTROL SYSTEMS

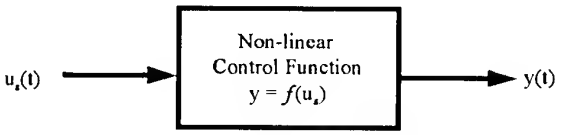

Figure 3. Non-linear control function.

Control system non-linearity manifests itself in an assortment of ways. In the context of turbulence analysis, the major non-linear problems encountered within the Airbus electronic flight control systems may be categorised as follows, with reference to figure 3.

"Unidirectional switching"

This type of non-linearity involves switching from, say, a normal flight control function to a flight protection function (e.g. stall protection). Switching to the protection function is triggered by the turbulence and reversion to the normal flight control function is only possible with pilot intervention. Consequently, a turbulence analysis, that does not permit pilot intervention, will

start in the normal control function, but may end within the protection function. For discrete turbulence events the behaviour of the system is typified by equations (15) and (16).

$$\left.\begin{aligned} u_g(t=0)=0 \quad &\text{and} \quad y(t=0)=0 \\ u_g(t\to\infty)=0 \quad &\text{and} \quad y(t\to\infty)\neq 0 \end{aligned}\right\} \quad (15)$$

$$f(u_g) \neq f(-u_g) \quad (16)$$

"Additive laws"
These functions involve the operation of additional control laws in combination with the normal flight control laws and are typified by load alleviation systems. The alleviation function is activated by the turbulence and will cease operation when the turbulence subsides. The behaviour of the system, for discrete turbulence events, is governed by equations (16) and (17).

$$\left.\begin{aligned} u_g(t=0)=0 \quad &\text{and} \quad y(t=0)=0 \\ u_g(t\to\infty)=0 \quad &\text{and} \quad y(t\to\infty)=0 \end{aligned}\right\} \quad (17)$$

"Elemental Non-linearity"
This is the existence of non-linear control law elements, such as limits and rate limits, within a control law function. In general the behaviour of this non-linearity is governed by equations (16) and (17).

The type of non-linear problem will influence the method used to predict aircraft loads.

6.0 METHODS FOR NON-LINEAR CT ANALYSIS

A multitude of non-linear methods have been developed that enable the prediction of loads. All are based on alternative realisations of the spectral properties of the atmosphere modelled by equation (5) and are categorised as:

- RPT based stochastic methods.
- Time-domain stochastic methods.
- Deterministic "spectral" gust methods.
- Deterministic "worst-case" gust methods.

Some of the more well-known methods in each category are summarised in figure 4, the computational effort required to predict design loads, for a given aircraft configuration at a given flight point, is indicated by the left hand scale. The four categories of method are discussed in more detail in the subsequent sections.

6.1 RPT Based Stochastic Methods

These methods require linearisation of the non-linear problem and the use of RPT as outlined in section 3.2. The linearisation can take two forms:

- *Direct removal the non-linear function:* currently this is the only means available for dealing with "unidirectional switching" non-linearities and involves replacing one CT analysis by two, i.e. a CT analysis is performed independently for both the normal flight control function and the protection function.

  Direct removal of "elemental non-linearity" is only possible if, in the context of a turbulence analysis, the non-linearity has no influence on the aircraft response. This is often the case for limits that restrict control surface movement, i.e. commanded control deflections, arising from turbulence, are usually well within such limits.

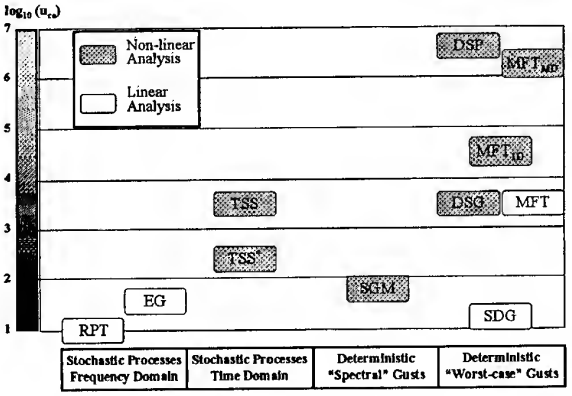

RPT	Linearisation and Random Process Theory
EG	Linearisation with Equivalent Gain, *Noback [10]*
SDG	Statistical Discrete Gust, *Jones [3]*
SGM	Spectral Gust Method, *Lusebrink et al. [11]*
TSS	Time-plane Stochastic Simulation
TSS*	Modified TSS, *Vinnicombe et al. [9]*
DSG	Design Stochastic Gust, *see note 3*
MFT	Matched Filter Theory, *Prototzky et al. [6]*
MFT_{1D}	MFT 1-dimensional search, *Prototzky et al. [12]*
MFT_{MD}	MFT multi-dimensional search, *Prototzky et al. [12]*
DSP	Discrete Spectral Procedure, *Jones [13]*

Figure 4. Methods for non-linear CT analysis.

- *Replacing a non-linear element by an Equivalent Gain (EG):* In cases of "elemental non-linearity", where the influence of the non-linearity on the aircraft response is significant, it is possible to approximate the non-linear element by an equivalent gain (see figure 5), provided that the non-linearity is an anti-symmetric function.

$$K_{eq} = \frac{2}{\sigma_v (K_{eq})^2} \int_0^\infty v f(v) p(v) dv \quad (19)$$

$$\text{provided that } f(v) = -f(-v) \quad (20)$$

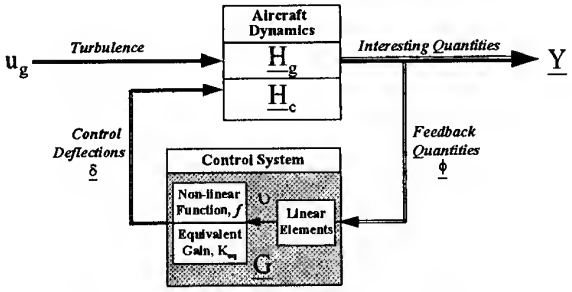

Figure 5. "Elemental non-linearity" represented by an equivalent gain.

Again the use of RPT is enabled, however, the root-mean-square value, σ_v, of the input into the non-linear element is a function of the aircraft "closed-loop" FRF, equation (3) which, in turn, is a function of the equivalent gain, hence equation (19) must be solved iteratively. Consequently, the computational effort is greater than that for the linear RPT analysis. If there is more than one significant non-linearity, then both the complexity of the method and the computational effort will increase. Equation (19) also implies knowledge of the turbulence intensity and the reader is referred to the discussion in section 4.0.

The described frequency-domain techniques require amongst the lowest amount of computational effort of all the methods for CT analysis, but are only suitable for a very limited set of non-linear problems.

6.2 Time-based Stochastic Methods

Time-based stochastic methods require the generation of a random time-history, or time-histories, that conform to the power-spectral density of the atmosphere described by equation (5). The Time-based Stochastic Simulation (TSS) requires generation of sufficient length of random turbulence time-history so that the spectral properties are adequately represented and the turbulence probability distribution function is Gaussian to at least three standard deviations. This turbulence history is used as an input to a time-simulation using the techniques outlined in section 2.2. Non-linear design loads may then be computed either directly, using auto-correlation functions, or by using the "principle of equivalent safety", based on frequency of exceedence of design load, Noback [14].

In an attempt to reduce computational effort, Vinnicombe et al. [9] used shorter simulation times and introduced the concept of a linear reference model to compensate for any statistical distortion present in the ensuing analysis. The non-linear design load is defined as that which has the same normalised rate of exceedence as the design load, for the linear reference model, given by equation (6).

TSS methods, that use the "principle of equivalent safety" to determine the design load, offer no direct means of obtaining correlated loads, so approximate methods must be sought, i.e. an averaging technique may be applied.

The computational effort required for TSS methods borders on the limits of practicality within existing design parameters and, in this respect, the alternative offered by Vinnicombe et al. is more acceptable.

6.3 Deterministic "Spectral" Gust Methods

Deterministic, time-based, methods differ from the stochastic time-based methods because the spectral properties of the turbulence are represented by a discrete gust. In the case of the "spectral" gust no attempt is made to tune the gust shape to the dynamics of the aircraft and the method does not adhere to the "principle of equivalent safety". These methods offer a deterministic representation of equation (5), however, the "spectral" gust is not unique. In general, these methods are computationally practical within the design environment.

6.4 Deterministic "Worst-Case" Methods

Deterministic "Worst-case" methods derive from the "matched filter principle" introduced by Papoulis [15] and involve the evaluation of deterministic inputs that satisfy a prescribed energy constraint and that maximise the response of a given load. Like the "spectral" gust methods, the "worst-case" gust offers a deterministic representation of equation (5) but, in this case, the response is tuned to the dynamic characteristics of the aircraft. "Worst-case" methods require a constrained optimisation procedure (for non-linear problems) to determine the "worst-case" gust: each gust is tuned to the load quantity in question. Consequently, these techniques require considerable amounts of computational effort, 10,000 to 100,000 times that required for a RPT analysis, depending on the complexity and completeness of the search.

Note 3: The Design Stochastic Gust (DSG), as shown in figure 4.0, is an approximate "worst-case" method (based on the "worst-case deterministic input" developed by Jones [16]) for a non-linear aircraft. The "critical gust input" for a linearised model is determined and then used as an input to the non-linear model.

7.0 NON-LINEAR CT DEA

It was noted in the introduction that the electronic flight control laws, in particular non-linear flight control laws, have served to increase, maybe double, the computational effort required to predict aircraft loads for both the design and certification of modern civil transport aircraft. It is essential that the methods employed to deal with the prediction of aircraft loads for the non-linear aircraft ensure the structural integrity of the aircraft without requiring unrealistic levels of computational effort.

Note 4: A DEA for an aircraft with an electronic flight control system may require consideration of several hundred design conditions (e.g. flight point, mass configuration and aerodynamic configuration) per design loop and require that both CT and TDG analyses are performed.

There is no single prediction method for CT analysis that satisfies design needs for all types of non-linear problem, i.e. there are no methods for dealing with "unidirectional switching" (except that described in section 6.1) unless an assumption is made regarding pilot intervention. This problem is not unique to CT analysis, but presents less of a problem when performing a discrete gust analysis.

"Worst-case" methods are impractical in the design environment unless the size of the IQ set is severely restricted and the coverage of the flight envelope significantly reduced, thus jeopardising structural integrity. Alternatively design timescales and costs will be increased, thus jeopardising the manufacturer's ability to produce cost-effective designs. Given the "state-of-the-art" in computing, these methods are too complex to be justified: the model of the atmosphere is at best approximate and the accuracy of the mathematical model (refer to section 2.0) used to represent the aircraft does not justify the complexity and computational effort required for a "worst-case" approach. Added to this there is no guarantee that the "worst-case" gust found by these methods is, in fact, the "worst-case" and the probability of encountering such a gust in flight is likely to be extremely remote.

The more practical non-linear prediction methods will require less than 1000 units of computational effort. Of these, the equivalent gain method provides one of the simplest approaches, but is very limited its application: the non-linearity must obey equation (20). This method has been employed in the design of recent Airbus aircraft to account for the effect of a limit within the autopilot control system. The equivalent gain method, however, is not suitable for the "additive law" associated with gust load alleviation systems.

The effectiveness of the A320 Gust Load Alleviation Function (GLAF) was demonstrated using the modification to the TSS method developed by Vinnicombe et al. [9]. In the case of the A320 GLAF the loads due to CT, in general, fell below the design envelope, so the problems of producing correlated load sets, associated with the method, were not unduly restrictive. Where correlated loads were required it was possible to consider only local parts of the structure and use approximate methods based on either the DSG or averaging of the load responses resulting from the TSS analysis.

In both the above examples, the effect of the non-linearity was not known prior to undertaking the non-linear analysis.

In fact, it is not an easy task to predict what effect a particular non-linearity will have on the aircraft loads, i.e. it is not unreasonable to assume that a GLAF will reduce wing up-loads, since this is its purpose, however the effect of the system on, say, tail loads is far less predictable. It is quite often the case that a non-linearity will both reduce and increase loads compared to those predicted for a linear representation of the system. Consequently, it is difficult to judge whether or not a linearised model provides, at least, a conservative estimation of all loads, so it is necessary to look closely at the problem. Even if a linearised model is conservative for all loads it may be in the manufacturer's interest to exploit the non-linearity. This is clearly the case for gust load alleviation systems where the clear objective is to reduce the wing up-loads, hence the overall aircraft weight. Whatever the situation, there is clearly a need for the manufacturer to establish the effect of all control system non-linearities on the predicted loads. The procedure adopted by British Aerospace Airbus Limited has been:

1. Linearise the problem and use RPT to perform a DEA to identify critical flight conditions for the linear model.
2. Study the results and make a judgement on which non-linearities, if any, may have a significant effect on the aircraft response.
3. Use a selection of methods, suitable for the non-linearity in question, to assess its influence.

   Note 5: for recent Airbus aircraft, use of the DSG method (see note 3) for a reduced set of "Interesting Quantities" has proved to give a good indication of the influence of the non-linearity and of the expected change in design loads. Both TSS and EG methods were also used for the autopilot non-linearity, eventually the EG method was selected for DEA. In the case of the A320, the TSS method was developed, see Vinnicombe et al. [9], and eventually used to demonstrate the effectiveness of the GLAF for certification. In all cases the EG, TSS and DSG demonstrated a similar influence on aircraft loads for the non-linearity in question.

   Note 6: if the existing "worst-case" analysis techniques have any place in future turbulence analysis it would be at this stage of the design process where the cost may be tolerable. They would, however, only be used to corroborate the validity of other methods.
4. Determine whether or not there is a need to model the non-linearity and, if so, choose the most practical method for use in the ensuing DEA.

8.0 CONCLUSION

The impact of non-linear flight control systems on the prediction of aircraft loads due to turbulence has been two-fold:

- There is an ambiguity regarding interpretation of the CT airworthiness requirements that has led to the development of an assortment of methods based on different assumptions.
- The cost to the manufacturer of the loads prediction process has risen and is likely to continue to rise.

It is not the intention to address the airworthiness requirements within this paper, however, there is an urgent need both to eliminate the ambiguity and to ensure the structural integrity of future designs. The CT DEA requirements were founded on the "principle of equivalent safety", so it would seem that a stochastic based analysis remains the most suitable for dealing with non-linear aircraft. On the other hand, it may be that a "worst-case" approach is preferred as the basis for a future requirement. If this is so, practical methods for predicting loads must first be established. In either case there is a need for clarification of the CT airworthiness requirements, for non-linear aircraft, and for the development of methods that will provide practical means of compliance.

Stochastic based processes currently border on the limits of practicality, it may be expected however that advances in computing will make these methods practical for the design of the next generation of civil transport aircraft. Even so, there still remains the problems of correlated loads and the treatment of the turbulence intensity.

Given the current "state-of-the-art" in computing it is unlikely that "worst-case" gust methods will provide a practical approach to loads prediction for the next generation of civil transport aircraft. "Worst-case" approaches lose the balance between complexity, accuracy and cost; the accuracy of the mathematical model and the model of the atmosphere do not warrant such complexity.

The intention of this paper is to give an industrial view of the impact of non-linear flight control systems on the prediction of aircraft loads due to turbulence. It does not recommend a particular method for dealing with non-linear problems, on the contrary it is believed that the method used should be tailored to the problem in hand.

It is hoped that the reader has gained an insight into both the problems encountered, when predicting aircraft loads due to turbulence for a non-linear aircraft model, and the way that these problems are currently addressed by British Aerospace Airbus Limited. At the same time there is a need for a review of the CT airworthiness requirements and for the continuing development of non-linear analysis techniques that provide practical means of compliance. Such methods must balance both complexity and computational effort against other modelling assumptions and external parameters. It should be remembered that the analyses discussed within this paper are for establishing limit loads and that there is a factor of one-and-a-half (1.5) between these and the ultimate design loads.

REFERENCES

1 Anon. *Federal Airworthiness Regulations, Part 25, Airworthiness Standards: Transport Category Aeroplanes*. Federal Aviation Administration.

2 Anon. *Joint Airworthiness Requirements, JAR-25, Large Aeroplanes*. Civil Aviation Authority.

3 Jones, J.G. *On the Formulation of Gust-Load Requirements in Terms of the Statistical Discrete Gust Method*. Technical Memorandum FS 208, RAE Farnborough, 1978.

4 Hoblit, F.M., Paul, N., Shelton, J.D. & Ashford, F.E. *Development of a Power-Spectral Gust Design Procedure for Civil Aircraft*. Technical Report ADS-53 (under contract FA-WA-4768 for the FAA), Lockheed-California Company, USA, 1966.

5 Noback, R. *The Generation of Equal Probability Design Load Conditions for Random Loads, Using the P.S.D. Method*. Memorandum SB-82-018 U, NLR, Netherlands, 1982.

6 Prototzky, S., Zeiler, T.A. & Perry III, B. *Time Correlated Gust Loads Using Matched Filter Theory and Random Process Theory - A New Way of Looking at Things*. NASA TM-101573, USA, 1989.

7 Rice, S.O. *Mathematical Analysis of Random Noise*. In *Selected Papers on Noise and Stochastic Processes*, Dover Publications Inc., New York, 1954.

8 Noback, R. *SDG, PSD and the Nonlinear Airplane*. Technical Report NLR MP 88018 U, NLR, Netherlands, 1988.

9 Vinnicombe, G., Hockenhull, M., Dudman, A.E. *Gust Analysis of an Aircraft with Highly Non-linear Systems Interaction*. AIAA paper, AIAA-89-1377, 30th AIAA/ ASME/AHS/ASC Structural Dynamics and Materials Conference, USA, 1989.

10 Noback, R. & Blaauboer, C. *The Determination of Gust Loads on Nonlinear Aircraft Using a Power Spectral Density Approach*. Technical Report 80123 U, NLR, Netherlands, 1980.

11 Lusebrink, H. & Brink-Spalink, J. *Treatment of Nonlinear Systems by Time-plane Transformed C.T. Methods: The Spectral Gust Method*. Paper to be presented at the AGARD workshop on *Aircraft Loads due to Turbulence and their Impact on Design and Certification*, Lillehammer, Norway, 1994

12 Scott, C., Prototzky, S. & Perry III, B. *Maximised Gust Loads for a Nonlinear Airplane using Matched Filter Theory and Constrained Optimization*. NASA TM-104138, USA, 1991.

13 Jones, J.G. *Formulation of Design Envelope Criterion in Terms of Deterministic Spectral Procedure*. Technical Memorandum SS 9, RAE Farnborough, 1990.

14 Noback, R. *The Deterministic Power-Spectral-Density-Method for Nonlinear Systems*. Technical Report NLR TP 92342 L, NLR, Netherlands, 1992.

15 Papoulis, A. *Maximum Response with Input Energy Constraints and the Matched Filter Principle*. In *IEEE Transactions on Circuit Theory*, pages 175-182, 1970.

16 Jones, J.G. *On the Implementation of Power-Spectral Procedures by the Method of Equivalent Deterministic Variables - Part I Analytical Background*. Technical memorandum FS(F) 485, RAE Farnborough, 1982.

Effets Gyroscopiques et Aérodynamiques des Propulseurs sur les Charges des moteurs d'avions en conditions turbulentes

Gyroscopic and propeller aerodynamic effects on engine mounts dynamic loads in turbulence conditions

J.M.Saucray
Département Etudes Générales-Structures
AEROSPATIALE
316,route de Bayonne 31620 Toulouse cedex 03 FRANCE

1. RESUME

Cet article traite du calcul des charges structurales des parties motrices lorsque les caractéristiques inertielles, les vitesses de rotation élevées et les grands déplacements, induisent un impact important des efforts d'origine gyroscopique. Une méthode directe, intégrée aux équations de la dynamique, pour le calcul des efforts gyroscopiques, en fonction des moments d'inertie polaires, des vitesses de rotation et des vitesses de précession est présentée et comparée à la procédure simplifiée de superposition sur la base des vitesses angulaires mesurées au centre de gravité moteur. Les résultats obtenus traduisent une bonne cohérence entre les deux méthodes de calcul, pour les moments de tangage et de lacet. Les fonctions de transfert présentées mettent en évidence l'importance des effets gyroscopiques sur le modèle dynamique, d'où un impact significatif sur l'ensemble des efforts moteur, aussi bien pour le jet que pour le turbopropulseur. D'autre part, l'impact des forces d'origine aérodynamique sur les hélices, induites par la réponse des propulseurs aux perturbations atmosphériques, est examiné. Les hypothèses retenues, la méthode de calcul et les résultats obtenus sont présentés.

1'. ABSTRACT

this paper deals with the problem of calculating loads on engines and their supporting structures when inertial characteristic, high engine speeds, large displacements, imposed by extreme atmospheric disturbances, give an important impact of gyroscopic effect. A direct method integrating the gyroscopic action in Lagrange's equations as a function of the polar moment of inertia, engine revolution speed and precession speed is presented and compared to the more common practice of superimposing gyroscopic effects on the basis of the angular speed calculated at the engine center of gravity. The results establish a good correlation between the two method on pitch and yaw moments on engine. On the other hand, tranfert funtion modifications due to groscopic effects, generate an increase of other loads for the direct method calculations, for both the turboprop and the turbojet aircraft. Effects of the aerodynamic force of the propeller due to the engine response are also examined.

2. INTRODUCTION

Les multiples phénomènes interférants dans la zone des parties motrices des avions de transport, phénomènes thermiques et dynamiques, géométrie très perturbée, siège de multiples interactions aérodynamiques entre les éléments en présence: fuselage, nacelle, mât, voilure, déflecteurs, surfaces mobiles... etc, en font une zone dont les modélisations sont particulièrement difficiles à appréhender. La quantité et la finesse des études menées tant par les motoristes que par les avionneurs en sont la preuve.

Le calcul des efforts généraux pour la prévision des charges limites et extrêmes est tributaire de la modélisation mise en place, avec une sensibilité plus ou moins aiguë aux variations des paramètres caractéristiques.

Ainsi, les dimensions importantes des ensembles propulsifs, les vitesses de rotations élevées, les structures de plus en plus souples, notamment la voilure, et les déplacements importants qu'elles impriment aux éléments tournants, sont autant de paramètres qui font que les moteurs et leurs éléments de liaison avec la voilure sont amenés à subir des efforts gyroscopiques et aérodynamiques non négligeables pour leur dimensionnement. De ce fait, les réglementations imposent la prise en compte de ces effets dans de nombreux cas de vols, dont les cas de turbulences atmosphériques (§25.371 pour la FAR et le JAR).

Dans ce cadre, cette étude présente l'influence des efforts inertiels gyroscopiques et des effets aérodynamiques des propulseurs, sur les charges structurales des parties motrices de deux avions de transport civil, un turbojet de type Airbus et un turbopropulseur de type ATR.

Paper presented at a Workshop on "Aircraft Loads due to Turbulence and their Impact on Design and Certification" held in Lillehammer, Norway on 5 May 1994.

3. AVANT-PROPOS - MODELISATION

Les avions traités étant de conception et de physionomie très différentes, les hypothéses et les modélisations adoptées le sont également. Dans le cas du turbopropulseur, le moteur étant en partie intégré à la voilure, ce dernier ne fait l'objet d'aucune modélisation aérodynamique particuliére. Il est représenté par plusieurs masses comportant 6 degrés de libertés chacune, dont le centre de gravité et le moyeu de l'hélice, que l'on utilisera pour l'intégration des forces d'origines gyroscopique et aérodynamique provenant du propulseur. A l'opposé, les parties motrices du turbojet étant séparées de la voilure par un mât, les nacelles sont modélisées par un prisme de base hexagonale formé de 36 pavés, permettant la définition de forces aérodynamiques instationnaires suivant les axes vertical et latéral. Dans ce cas, les efforts gyroscopiques sont évalués au niveau du centre de gravité du moteur. Pour les deux avions traités, les forces aérodynamiques sur les surfaces modélisées (voilure empennages,...) font l'objet d'un calcul instationnaire par la méthode dite des réseaux de doublets (Dubblet Lattice Method).

Cette modélisation suppose donc, pour les caractéristiques géométriques des moteurs, que le mouvement du point de réduction des efforts (moyeu ou centre de gravité) soit représentatif du mouvement des éléments en rotation, c'est à dire que les différents composants du moteur soient indéformables et que les axes de rotation restent alignés au cours du temps (pas de balourds).

D'autre part, la schématisation utilisée est limitée au demi avion et donc fondée sur une représentation symétrique de la structure. De même, seules les perturbations atmosphériques verticales et constantes en envergure sont traitées. Ceci représente une simplification importante compte tenu du problème étudié. En effet, le sens de rotation identique des moteurs gauche et droit, implique à travers les effets gyroscopiques, une dissymétrie dans la réponse dynamique de la structure, dissymétrie non modélisée dans notre cas.

Enfin, la représentation modale de la structure prend en compte les moteurs à l'arrêt, c'est á dire leur masse inerte. Les effets inertiels de gyroscope sont donc superposés à cette représentation.

La vitesse avion et le régime de rotation des moteurs (Ω) sont considérés comme constants lors du déroulement d'un calcul.

4. CALCUL DES EFFORTS GYROSCOPIQUES

4.1 Méthodes

Il est commun, pour le calcul des charges structurales, d'utiliser une représentation modale de la structure, théorique ou validée à partir d'essais de vibration au sol, les moteurs étant á l'arrêt. Les équations caractérisant la réponse dynamique de l'avion sont donc résolues sans prise en compte des effets gyroscopiques, qui sont simplement superposés á partir de la relation classique suivante, fournissant le moment gyroscopique de solides en rotation :

$$\vec{M}_{Gyr}(t) = I_p \; \vec{\Omega} \wedge \vec{\Omega}_p(t)$$

I_p étant le moment d'inertie polaire du solide en rotation,

Ω sa vitesse angulaire (régimes moteur),

$\Omega_p(t)$ la vitesse angulaire de précession

Une méthode plus précise, dont la théorie utilisée est présentée par Béatrix et Dat [2], permet la prise en compte directe des termes gyroscopiques dans les équations de Lagrange. L'intégration de ces moments au calcul de la réponse dynamique de l'avion souple à une rafale atmosphérique est brièvement rappelé dans ce qui suit.

Compte tenu des hypothèses formulées, les parties tournantes sont uniquement caractérisées par leur énergie cinétique, dont la dérivée s'écrit :

$$\frac{d}{dt}\left(\frac{\partial T}{\partial \dot{X}_i}\right) - \frac{\partial T}{\partial X_i} = [I]\left\{\ddot{x}\right\} + [G]\left\{\dot{x}\right\}$$

La représentation modale de la structure étant la même que pour la méthode initiale, les termes d'inertie classiques des parties tournantes sont déjá intégrés et il reste donc á ajouter à la modélisation le terme lié à la rotation et donc aux effets gyroscopiques : $[G]\left\{\dot{x}\right\}$

$[G]$ est une matrice carrée antisymétrique de coefficients constants sur les lignes et les colonnes correspondant aux degrés de libertés en tangage et lacet des points de réductions des déplacements de chaque élément tournant.

$$[G] = \begin{bmatrix} 0 & 0 & 0 & 0 \\ 0 & 0 & 0 & 0 \\ 0 & 0 & 0 & I_p\Omega \\ 0 & 0 & -I_p\Omega & 0 \end{bmatrix} \Bigg\} \begin{matrix} \text{degrés de} \\ \text{libertés} \\ \text{du point} \\ \text{moteur} \end{matrix}$$

La formulation de la dérivée par rapport au temps du vecteur des déplacements en fonction de la matrice des déformées unitaires modales $[\Phi]$ permet l'expression du terme gyroscopique dans la base modale et l'écriture matricielle du mouvement de l'avion dans la rafale est donc la suivante:

$$[M]\left\{\ddot{q}\right\} + \left[[C] + {}^t[\Phi][G][\Phi]\right]\left\{\dot{q}\right\} + [K]\left\{q\right\} = {}^t[\Phi]\left\{Fraf\right\}$$

(les matrices [M],[C] et [K] contiennent les termes aérodynamiques de mouvement)

4.2 Résultats

Ces deux méthodes, dites "par superposition effets gyroscopiques rajoutés" et "méthode à calcul intégré", ont été utilisées pour l'évaluation des efforts gyroscopiques de deux avions, représentatifs de leur catégories respectives, un turbopropulseur court-courrier de type ATR et un turbojet moyen courrier double couloir de type Airbus. D'autre part, les deux formes de perturbations atmosphériques exigées par les réglementations, la rafale discrète accordée et la turbulence continue ont été appliquées.

4.2.1 *Résultats obtenus pour le turbojet*

Une étude complète a été menée, fondée sur les cas définis lors des phases de conception et de certification de cet avion. Les charges moteur, au niveau du centre de gravité, sont présentées, dans les cas de poussée maximale continue, de poussée nulle et moteur à l'arrêt. Pour chaque effort et accélération, sont comparées les valeurs critiques obtenues dans chacun des cas de poussée, les effets gyroscopiques pouvant modifier la hiérarchie des cas traités. Seuls l'incrément d'effort dû à la perturbation atmosphérique est pris en compte à l'exclusion des charges dues au vol stationnaire en palier à Nz=1.

Les graphiques suivants présentent les résultats obtenus pour la rafale discrète par la méthode à calcul intégré. Les moteurs gauche et droit sont uniquement différenciés par l'inversion du sens de rotation, les intéractions entre les deux côtés n'étant pas considérée.

L'effet du couplage de la réponse dynamique avec le sens de l'effort gyroscopique apparaît à travers la comparaison de ces deux graphiques. On constate dans la majorité des cas, que les effets gyroscopiques modifient assez peu le comportement dynamique des moteurs de cet avion, et se superpose (>0 ou <0) au calcul moteur à l'arrêt. Seuls les efforts Fz, Mx et Mz mettent en évidence un couplage très différent entre les deux côtés, notamment à travers l'apparition d'un nouveau cas critique (n°1, 2 ou 3 dans les figures).

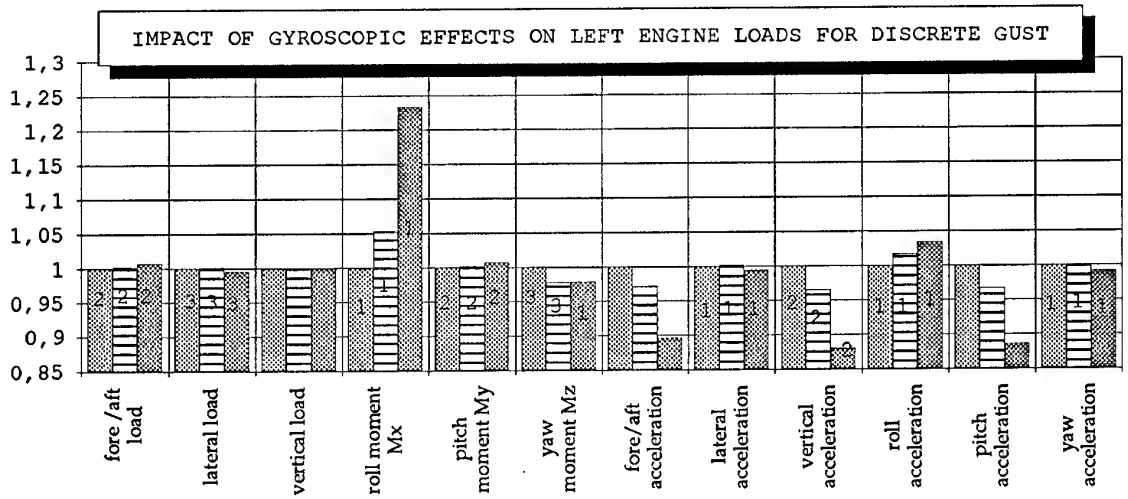

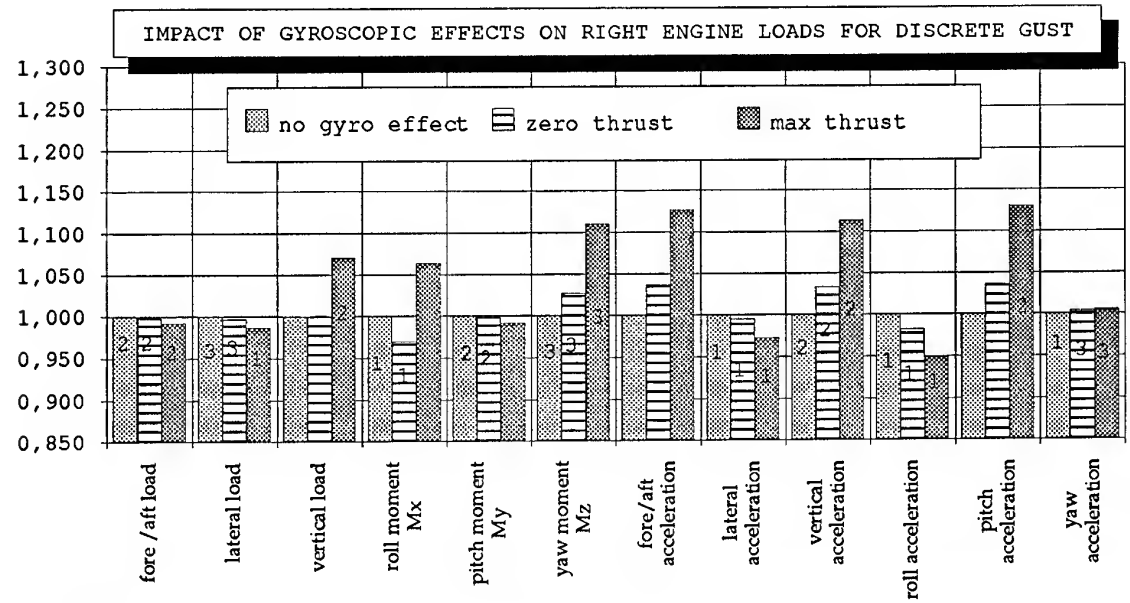

55% of critical case are still critical with gyroscopic

D'autre part, près de la moitié des critères (efforts ou accélérations) voient leur cas critiques modifiés par l'intégration des efforts gyroscopiques.

Une analyse identique a été effectuée dans le cas de l'excitation par la turbulence continue. Les graphiques suivants mettent en évidence un impact globalement moins important que pour la rafale discrète, limité dans ce cas à environ +5% sur le moteur gauche. On notera que la turbulence continue représente les cas dimensionnant pour la structure des parties motrices de cet avion.

Les résultats moteur droit sont comparés pour le cas à poussée maximale, aux valeurs pour le moteur gauche.

On remarque également le faible impact des cas à poussée nulle, ceci dû notamment aux régimes moteurs relativement faibles.

D'autre part, l' influence des effets gyroscopiques moteur sur les charges subies par la voilure et le fuselage a été évaluée.

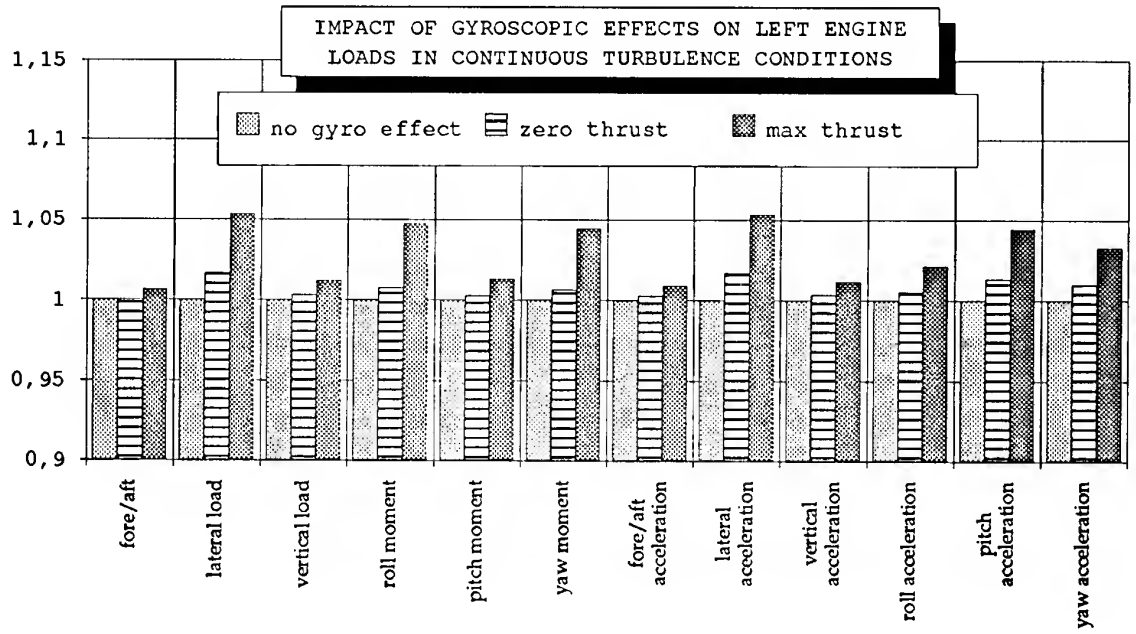

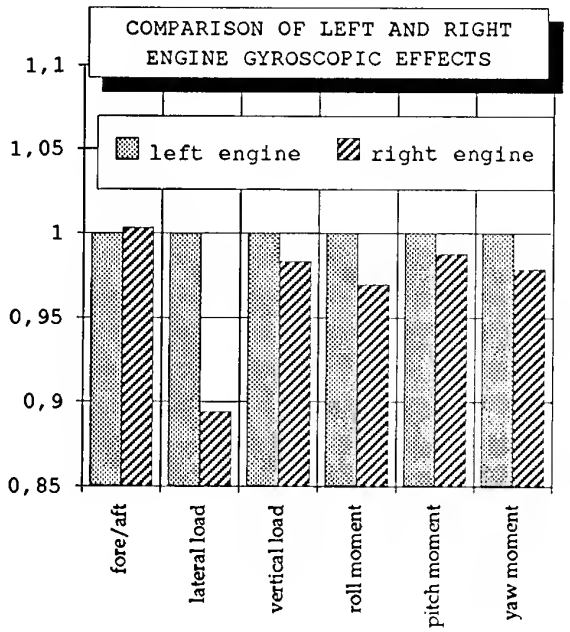

On note que cet impact, résultant du couplage entre les modes souples structuraux des parties motrices et ceux de la voilure et du fuselage s' avère très faible. On constate une variation des charges inférieure à 0,2% sur la quasi- totalité de la voilure et du fuselage. Seul le fuselage avant fait exception, où le facteur de charge vertical augmente de 0,9%. La vérification de cette hypothèse nous a permis de travailler à partir d'un modèle symétrique limité au demi-avion, chaque côté étant caractérisé par le sens donné à la rotation des moteurs.

Un point essentiel mis en évidence par ces résultats, est l'apport procuré par l'amplification des couplages modaux, sur les charges non soumises directement aux effets gyroscopiques. L'effort et l'accélération latérale (Fy et Ny) ainsi que le moment de roulie Mx pour la turbulence et l'effort et l'accélération verticale (Fz et Nz) ainsi que le moment de roulis Mx pour la rafale en sont

les meilleurs exemples. Non pris en compte par la méthode dite "par superposition efforts gyroscopiques rajoutés", on trouve des augmentations de l'ordre de 5 à 10%.

En ce qui concerne les charges directement associées aux efforts gyroscopiques, les moments de tangage My et de lacet Mz, les graphiques suivants présentent des tendances variables. Néanmoins, le faible impact sur le moment My et des niveaux enveloppes voisins pour le moment Mz, enregistrés pour la méthode "directe" et pour la méthode "par superposition", traduisent une assez bonne cohérence entre ces deux méthodes de calcul pour les avions traités, à la fois pour la turbulence continue et la rafale discrète. Dans le cas de la turbulence continue, le calcul des efforts gyroscopiques par la méthode dite "par superposition" à été effectué à partir de la relation suivante:

$$\sigma M_{Gyr} = I_p \; \rho_{M\Omega p} \; \vec{\Omega} \wedge \sigma\vec{\Omega}_p$$

σ représente l'écart type de la grandeur et

$\rho_{M\Omega p}$ le coefficient de corrélation entre la composante M de moment considéré et la vitesse angulaire Ωp correspondante.

COMPARISON OF GYROSCOPIC EFFECTS CALCULATION METHODS
- DISCRETE GUST -

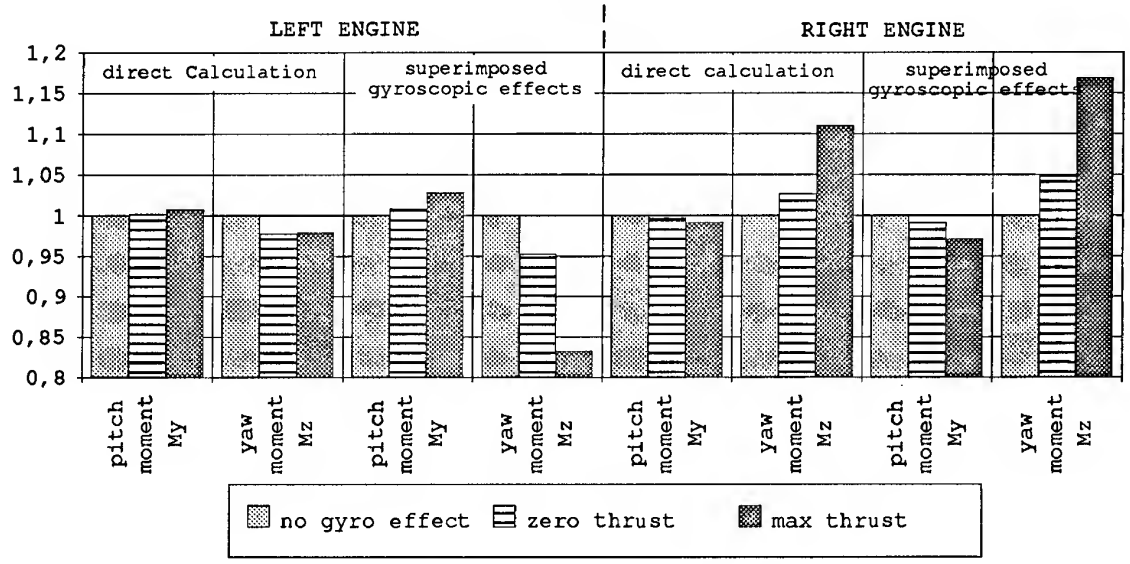

COMPARISON OF GYROSCOPIC EFFECTS CALCULATION METHODS
- CONTINUOUS TURBULENCE -

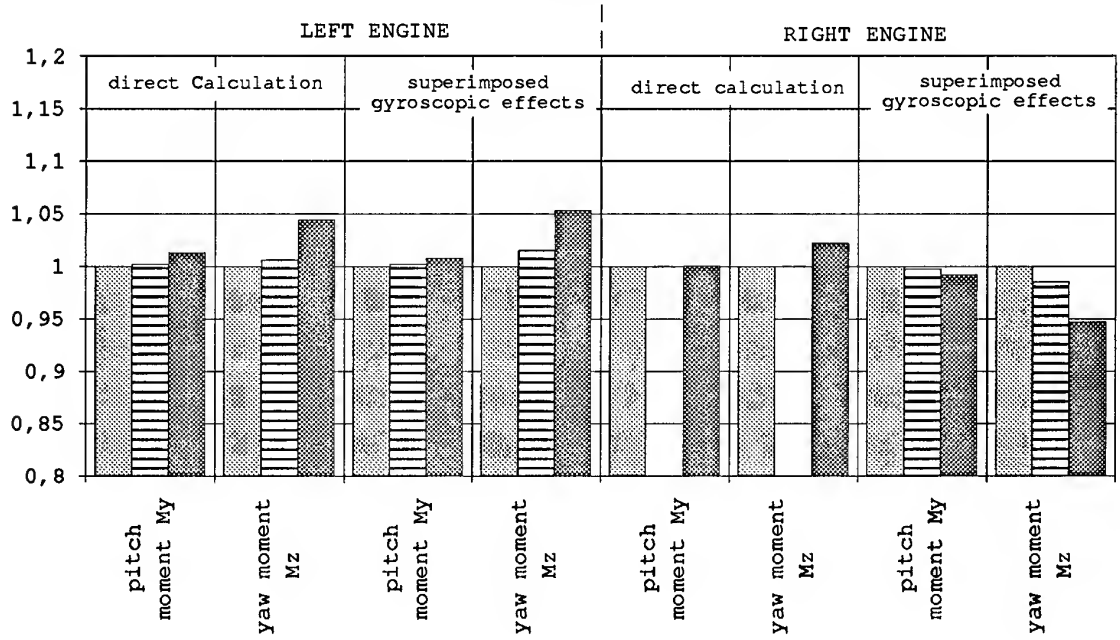

4.2.2 *Résultats obtenus pour le turbopropulseur*

L'étude menée sur cet avion, est fondée sur les cas déterminés comme critiques au niveau du centre de gravité moteur, lors de la certification de cet avion. Les efforts généraux au CdG moteur sont présentés dans les deux cas : moteur à l'arrêt, c'est à dire sans effets gyroscopiques et pour le régime 100% (environ 1200 tours/mn), légérement supérieur au régime de croisière égal à 86%. Les effets gyroscopiques induits par le propulseur sont intégrés dans le modèle, au niveau du moyeu de l'hélice.

De même que pour le turbojet, les comparaisons présentées portent uniquement sur l'incrément de charge induit par la perturbation atmosphérique, à l'exclusion des charges dues au vol en palier.

Pour le cas de la rafale discrète, les résultats obtenus par la méthode dite "à calcul intégré" pour les 4 premiers efforts (Tx, Ty, Tz, et Mx), et les deux sens de rotation des moteurs, seul l'effort latéral Fy met en évidence une sensibilité significative aux effets gyroscopiques, avec plus de 15% d'augmentation sur le moteur gauche, et un comportement symétrique pour le côté droit, les autres efforts ne présentant pas d'impact supérieur à 2%.
Les comparaisons sur les moments de tangage et de lacet sont présentés par les deux graphiques suivants, pour les deux sens de rotation et pour les deux méthodes de calcul "intégré" et "effets gyroscopiques rajoutés". On ne constate aucun impact significatif sur le moment de tangage My, et à l'opposé, un impact majeur sur le moment de lacet Mz. Les deux méthodes de calcul sont cohérentes aussi bien sur la tendance générale de l'impact que sur les niveaux rencontrés.

Les résultats obtenus pour cet avion, sont très différents de ceux présentés pour le turbojet, principalement du fait des différences de conception de l'assemblage moteur-mât-voilure. Le turbopropulseur se caractérise, comme la plupart des avions de ce type, par l'intégration du moteur à la voilure. Les mouvements du moteur induits par les déformations de la voilure sans fléche, sont donc essentiellement dans le plan vertical (déplacement suivant z et rotation en tangage). De ce fait, le mouvement coplanaire de la voilure, associé aux déformations du mât-moteur sont les sources essentielles de rotation de lacet au niveau du moteur. La différence d'impact entre le deux moments My et Mz, s'expliquent donc de façon assez classique, par le fait que la part gyroscopique My_g induite par rotation de lacet α_z du moteur, d'amplitude trés faible, est négligeable devant l'importance des efforts Tz et My résultant de la réponse de la voilure en flexion/torsion et de l'avion en pompage-tangage. A l'inverse, le moment gyroscopique Mz_g induit par ces mouvements de tangage est prépondérant devant le efforts Fy et surtout Mz d'origine principalement inertielle, résultant du mouvement de la voilure en coplanaire ou des déformation du mât-moteur en lacet.

La mise en évidence du contenu fréquentiel de la réponse dynamique est réalisée par les figures en pages suivantes, sur la base de réponses à plusieurs rafales discrètes de longueurs d'onde différentes mais de mêmes intensités, pour les efforts Tx max, Ty max, et Mz min. On constate des modifications dans le couplage des modes structuraux, se traduisant par des réductions (cas Tx) ou des augmentations de niveaux des charges (cas Ty et Mz) et par une modification de la fréquence critique (cas Mz).

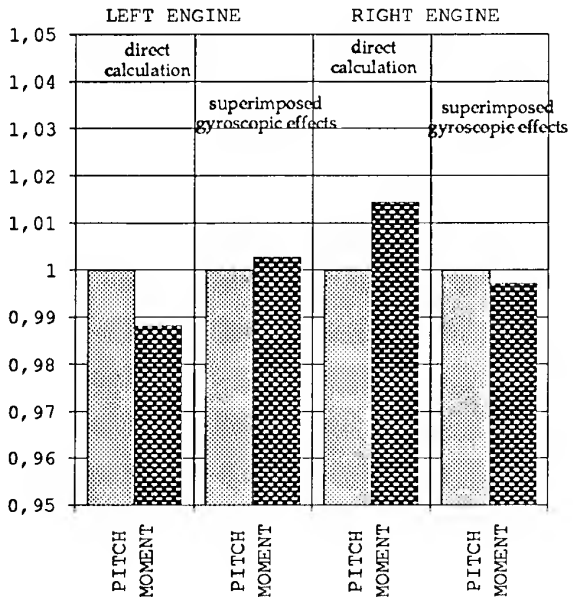

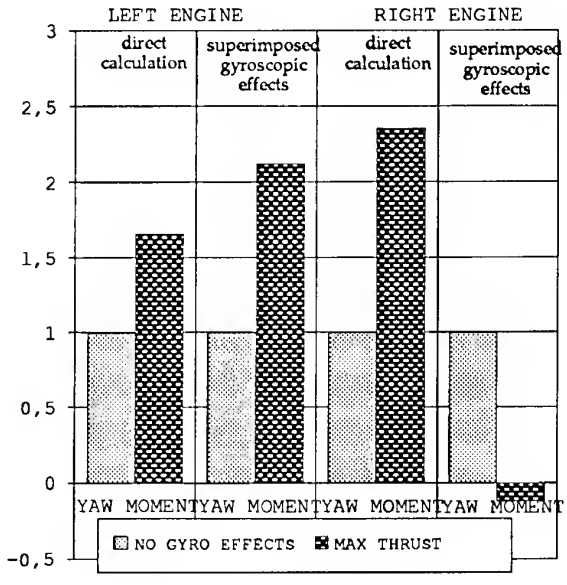

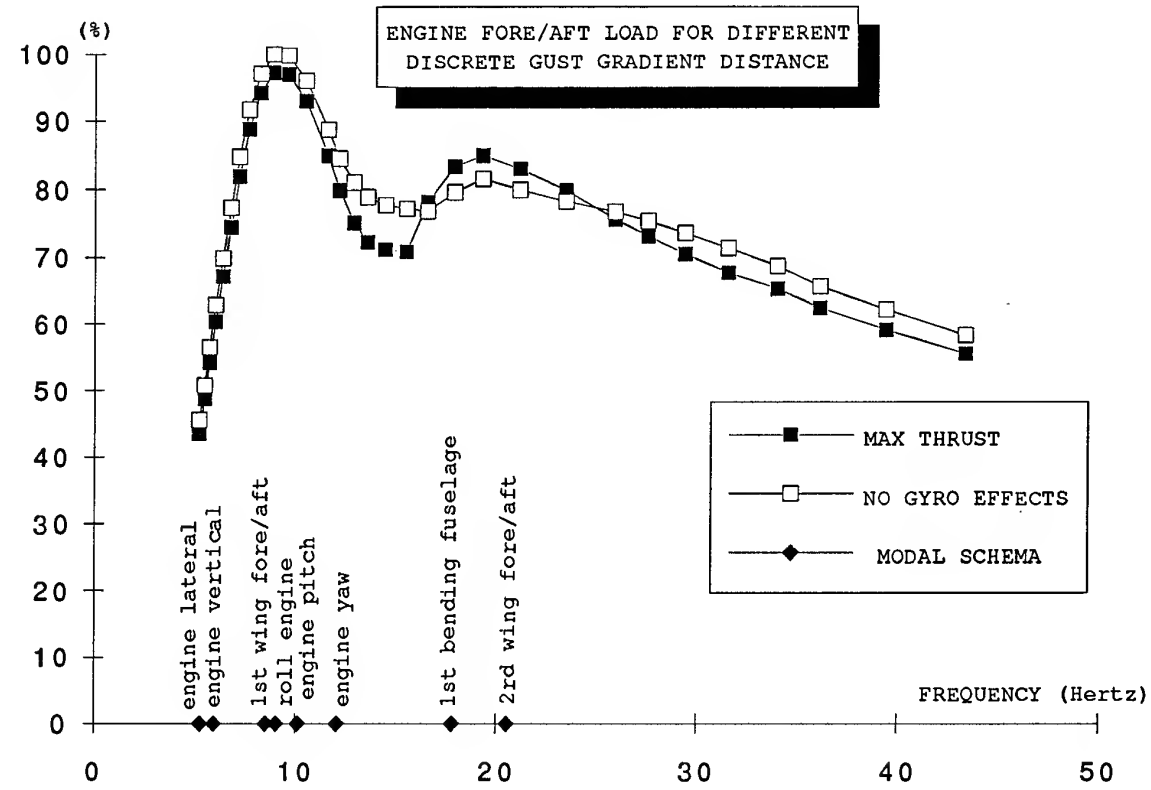
ENGINE FORE/AFT LOAD FOR DIFFERENT
DISCRETE GUST GRADIENT DISTANCE
(%)
100
90
80
70
60
50
40
30
20
10
0
MAX THRUST
NO GYRO EFFECTS
MODAL SCHEMA
engine lateral
engine vertical
1st wing fore/aft
roll engine
engine pitch
engine yaw
1st bending fuselage
2rd wing fore/aft
FREQUENCY (Hertz)
0
10
20
30
40
50

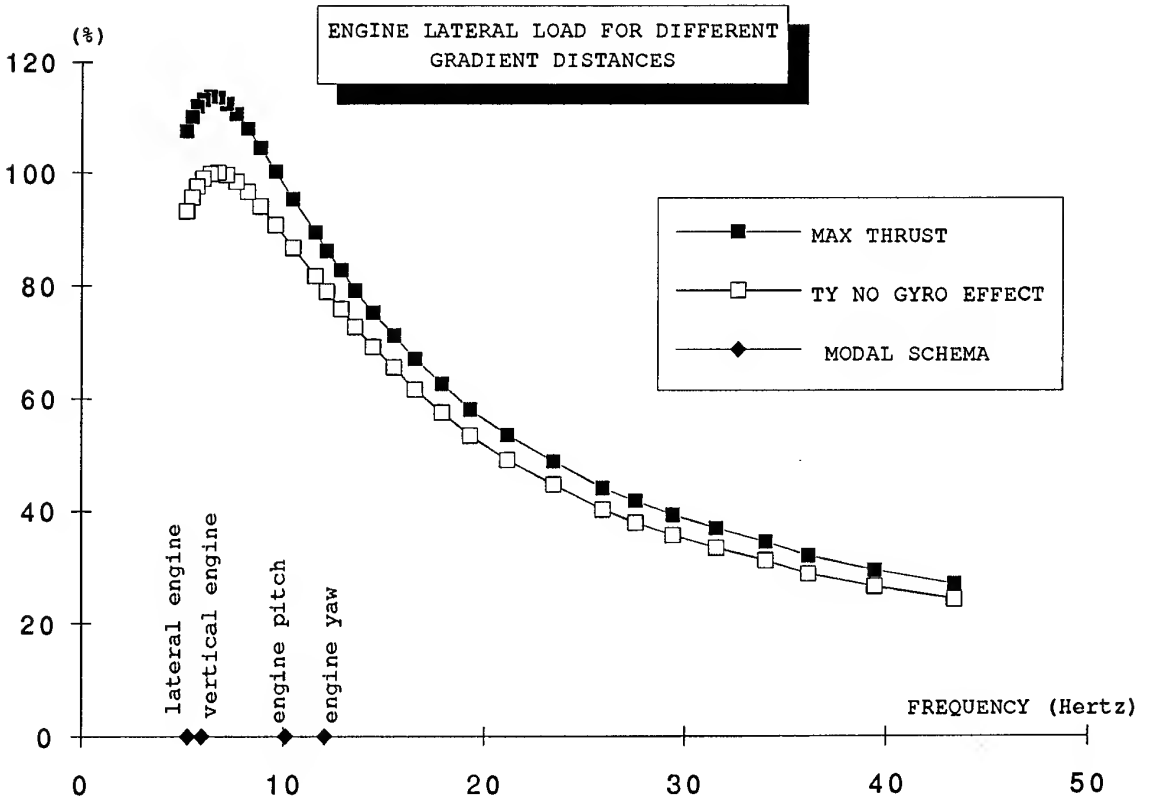
ENGINE LATERAL LOAD FOR DIFFERENT
GRADIENT DISTANCES
(%)
120
100
80
60
40
20
0
MAX THRUST
TY NO GYRO EFFECT
MODAL SCHEMA
lateral engine
vertical engine
engine pitch
engine yaw
FREQUENCY (Hertz)
0
10
20
30
40
50

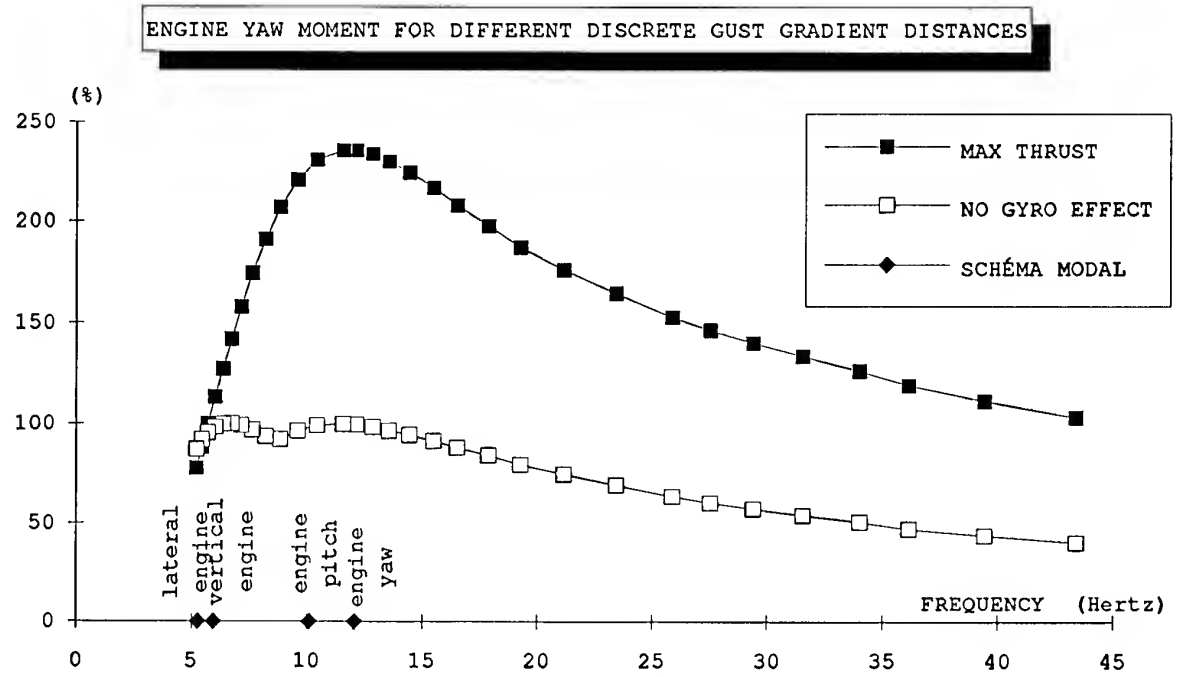

De même, les résultats obtenus sous une excitation par la turbulence continue sont présentés. D'une manière générale, les tendances ressenties pour la rafale discrète se confirment, notamment pour l'effort Ty (+8% côté gauche) et les efforts Tx, Tz, Mx, et My pour lesquels on rencontre peu ou pas d'impact, comme le montre la figure suivante. La principale différence se situe pour le moment Mz, pour lequel on ne retrouve pas l'amplitude de l'impact mis en évidence par les réponses à la rafale discrète. Le caractère spectral de la turbulence continue a certainement une influence importante dans ce résultat, et les fonctions de transfert pour les efforts Ty et Mz sont présentées. On remarque notamment la présence des modes de mouvement latéral du moteur (lateral engine~5Hz), de coplanaire voilure (1st wing fore-aft~7,8Hz), et l'apparition du mode de tangage moteur (engine pitch~10Hz) dans les cas avec effets gyroscopiques pour l'effort Mz. De même la participation du mode de lacet moteur (engine yaw~12Hz) est remplacé par le mode suivant, très similaire, mais comportant ses déformées latérales (lacet moteur et coplanaire voilure) en opposition de phase.

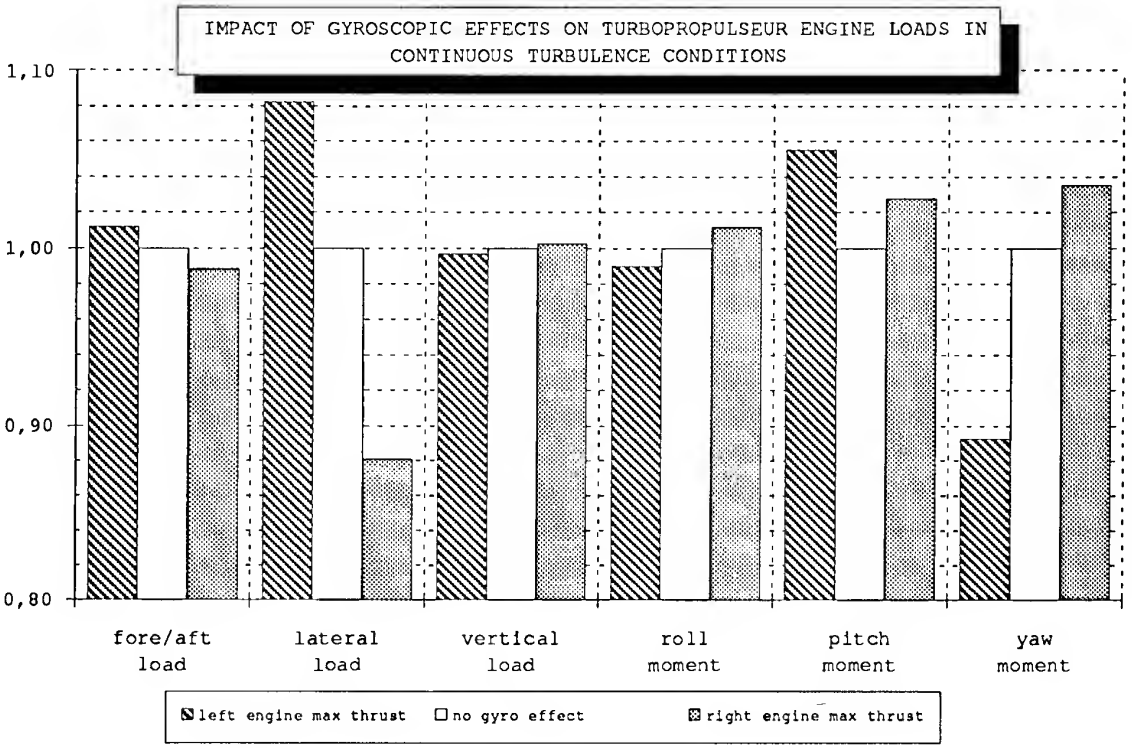

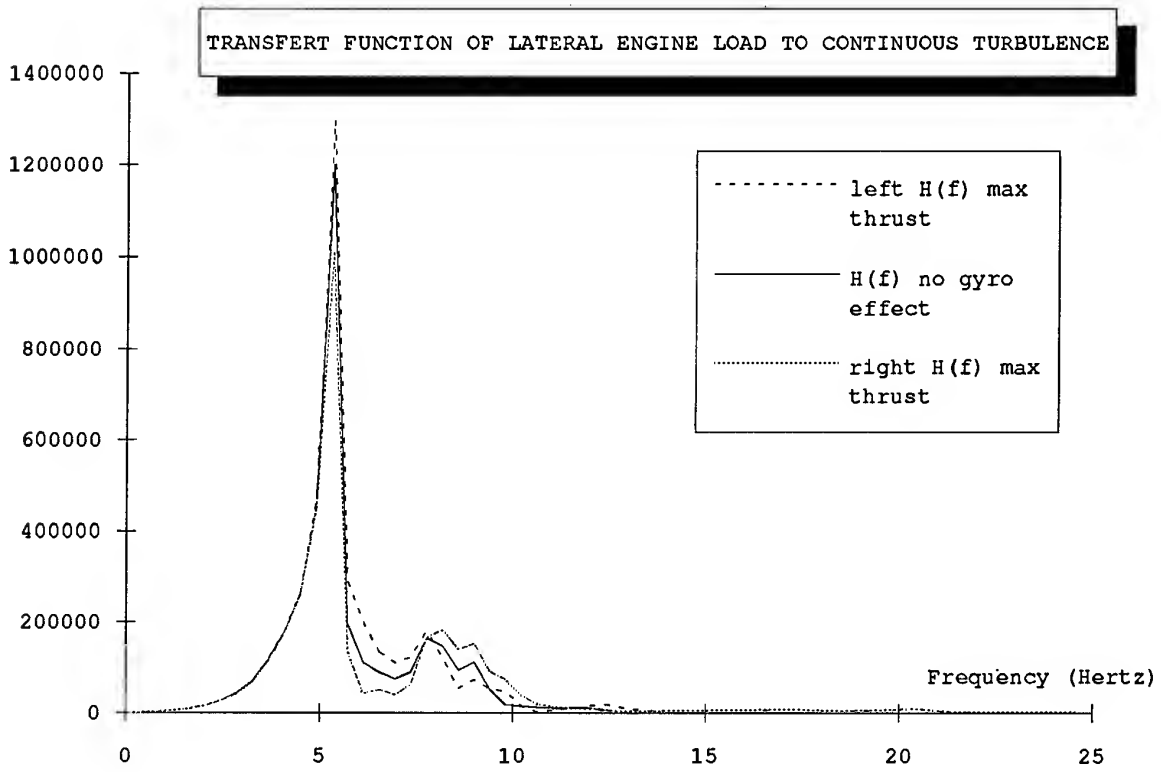
TRANSFERT FUNCTION OF LATERAL ENGINE LOAD TO CONTINUOUS TURBULENCE
1400000
1200000
1000000
800000
600000
400000
200000
0
0
5
10
15
20
25
Frequency (Hertz)
left H(f) max thrust
H(f) no gyro effect
right H(f) max thrust

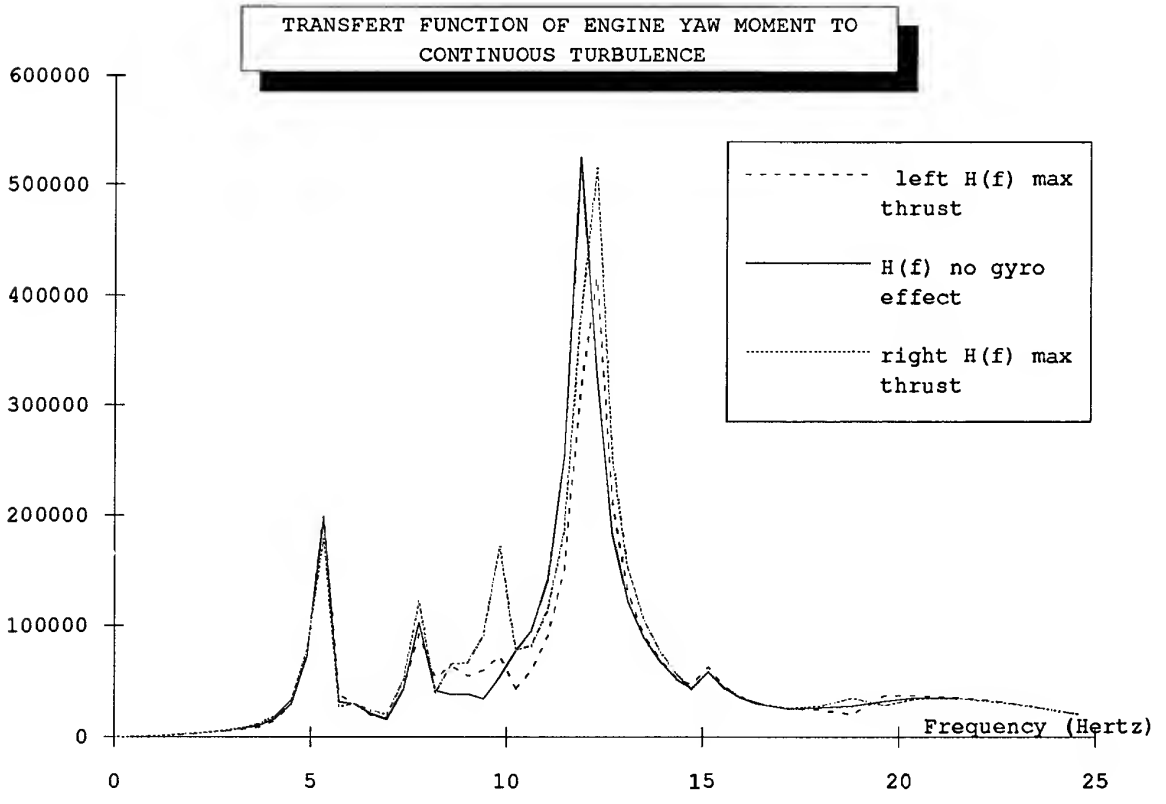
TRANSFERT FUNCTION OF ENGINE YAW MOMENT TO CONTINUOUS TURBULENCE
600000
500000
400000
300000
200000
100000
0
0
5
10
15
20
25
Frequency (Hertz)
left H(f) max thrust
H(f) no gyro effect
right H(f) max thrust

5. FORCES AERODYNAMIQUES DES PROPULSEURS

La théorie utilisée, est celle présentée par Houbolt et Reed [1], permettant le calcul quasi-stationnaire des efforts aérodynamiques sur les pales. Cette formulation est enrichie de l'effet de compressibilité de l'air et d'un effet instationnaire, modélisé par la fonction de Theodorsen, qui traduit le déphasage entre la variation d'angle d'attaque et la force aérodynamique correspondante sur la pale. Ces efforts résultent de la rotation du plan de l'hélice en tangage et en lacet, induite par les mouvements provenants de la réponse dynamique de la voilure, du mât ou du moteur aux perturbations extérieures.
Les hypothèses et la formulation retenues permettent l'intégration de ces termes aux équations de la dynamique de l'avion en vol exprimées dans la base modale.

5.1 Méthode

Pratiquement, les efforts sont calculés à partir de l'évaluation en écoulement compressible de l'effort local sur une tranche de pale en fonction de la vitesse de l'air et du point de vol. La vitesse de l'air sur la pale, considérée comme rigide dès lors qu'elle n'apparaît pas dans le schéma modal utilisé, est la composition de la rotation de l'hélice, de la vitesse avion et des vitesses induites par les réponses dynamiques de la voilure, du mât ou du moteur.

La figure suivante propose un schéma de cette modélisation.

De nombreux effets sont donc négligés, tels que l'impact des rafales atmosphériques sur les pales, les dissymétries, la variation du régime de rotation, de l'angle d'attaque des pales et des efforts de traction, les balourds, etc...

$$[K'''] = S \begin{bmatrix} -Cy_\psi & Cy_\theta & D/2\ Cy_q & D/2\ Cy_r \\ -Cz_\psi & Cz_\theta & D/2\ Cz_q & D/2\ Cz_r \\ -D.Cm_\psi & D.Cm_\theta & D^2/2\ Cm_q & D^2/2\ Cm_r \\ -D.Cn_\psi & D.Cn_\theta & D^2/2\ Cn_q & D^2/2\ Cn_r \end{bmatrix}$$

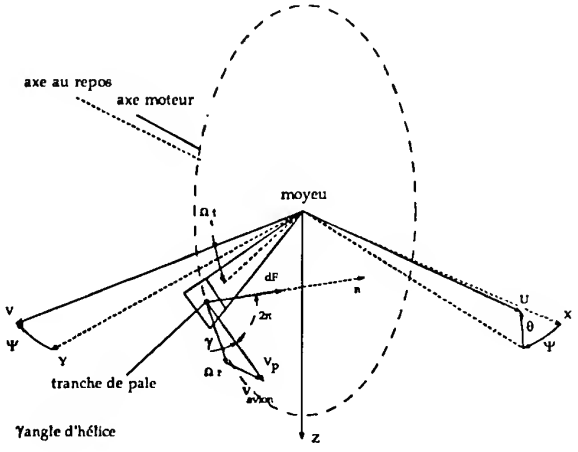

Le problème se pose donc d'intégrer ces efforts aérodynamiques au calcul de la réponse dynamique de l'avion souple à une rafale atmosphérique.

La vitesse de l'air sur une tranche de pale, étant exprimée en fonction du rayon local, des paramètres de position du moyeu et de leurs dérivées, la limitation aux termes du premier ordre permet la mise en place d'une expression relativement directe des efforts et moments élémentaires sur la tranche. La prise en compte des différentes pales (notamment les effets de symétrie autour de l'axe moteur) et l'intégration des efforts locaux sur le rayon des pales, permettent l'expression de l'effort global sous la forme d'une relation matricielle directement intégrable au second membre des équations de Lagrange (travaux de Béatrix et Dat [2]) :

$$\bar{q}\,[K'''] \left\{ \dot{x} \right\} \quad \text{et} \quad \bar{q}\,[K'] \left\{ x \right\} .$$

Les matrices de coefficients $[K''']$ et $[K']$ contiennent, pour les degrés de libertés du moyeu de l'hélice y, z, θ, Ψ (respectivement latéral, vertical, tangage et lacet), des termes que l'on peut rapporter aux gradients aérodynamiques correspondants de l'hélice :

degrés de liberté du moyeu moteur

	y	*z*	θ	ψ
	0	0	Cy_θ	Cy_ψ
	0	0	Cz_θ	Cz_ψ
	0	0	$D.Cm_\theta$	$D.Cm_\psi$
	0	0	$D.Cn_\theta$	$D.Cn_\psi$

$$[K'] = S \begin{bmatrix} 0 & 0 & Cy_\theta & Cy_\psi \\ 0 & 0 & Cz_\theta & Cz_\psi \\ 0 & 0 & D.Cm_\theta & D.Cm_\psi \\ 0 & 0 & D.Cn_\theta & D.Cn_\psi \end{bmatrix}$$

$\bar{q}$ étant la pression dynamique (DaN/m^2),
D le diamètre de l'hélice (m) et
S sa surface (m^2)

(X, Y, Z) repère lié à l'avion
(U, V, Z) repère lié au moteur, plan de l'hélice sous un déplacement θ et ψ respectivement tangage et lacet.

Les coefficients de ces deux matrices s'expriment de la façon suivante :

$Cz_\theta = -(4\ \Omega\ Cr/V)\ I1$; $Cz_q = (4\ \Omega\ Cr/V)\ J2$

$Cy_\theta = -(4\ \Omega\ Cr/V)\ J1$; $Cm_\theta = -(2\ \Omega\ Cr/V)\ J2$

$Cy_q = -(4\ \Omega\ Cr\ /V)\ I2$; $Cm_q = -(2\ \Omega\ Cr/V)\ I3$

$Cn_\theta = -(2\ \Omega\ Cr\ /V)\ I2$; $Cn_q = -(2\ \Omega\ Cr/V)\ J3$

De plus, les symétries des hélices autour de leur axe de rotation, permettent d'écrire les relations suivantes :

$Cy_\psi = -Cz_\theta$ $\qquad$ $Cm_\psi = -Cn_\theta$

$Cz_\psi = Cy_\theta$ $\qquad$ $Cn_\psi = Cm_\theta$

$Cy_r = -Cz_q$ $\qquad$ $Cm_r = -Cn_q$

$Cz_r = Cy_q$ $\qquad$ $Cn_r = Cm_q$

Les termes en gras dans les matrices [K'] et [K'''] proviennent de l'effet purement instationnaire, partie imaginaire de la fonction complexe de Theodorsen : F(k)+iG(k). Dans l'expression des gradients aérodynamiques, Cr est la corde dite "de référence" de la pale et V la vitesse de l'avion. Les termes I1, J1, I2, J2, I3 et J3, réalisent l'intégration sur l'ensemble de la pale des efforts élémentaires à partir des rayons courants adimensionnels (η=r/R) et de la corde locale C(η) (m) :

$$I1 = \frac{Np}{4}\frac{Cl\alpha}{2\pi}\mu^2\frac{Ar}{Cr}\int_{\eta_0}^{1}\frac{C(\eta)\ F(k)}{H(\eta,Mach,Ar)}\,d\eta$$

$$I2 = \frac{Np}{4}\frac{Cl\alpha}{2\pi}\mu\frac{Ar}{Cr}\int_{\eta_0}^{1}\frac{\eta^2\ C(\eta)\ F(k)}{H(\eta,Mach,Ar)}\,d\eta$$

$$I3 = \frac{Np}{4}\frac{Cl\alpha}{2\pi}\frac{Ar}{Cr}\int_{\eta_0}^{1}\frac{\eta^4\ C(\eta)\ F(k)}{H(\eta,Mach,Ar)}\,d\eta$$

Np étant le nombre de pales de l'hélice. L'effet de compressibilité est pris en compte à travers la fonction H(η,Mach,Ar) dépendant du nombre de Mach, de l'allongement de la pale (Ar) et de la position en envergure (η) de la tranche considérée :

$$H(\eta,Mach,Ar) = \frac{1}{\Omega R}\sqrt{(V^2+\Omega^2R^2\eta^2)}\ *$$

$$[\ 2 + Ar\sqrt{1 - M^2/V^2\ (V^2 + \Omega^2R^2\eta^2)}\ ]$$

en remarquant que le terme entre paranthèses représente le carré de la vitesse locale tangente à la pale dans le repère de l'hélice, et V^2/M^2 le carré de la célérité du son.

5.2 Résultats

L'évaluation de l'impact des effets aérodynamiques a ètè réalisée dans les mêmes conditions que celles décrites pour les effets gyroscopiques, limitées au cas du turbopropulseur, la méthode utilisée n'étant pas adaptée aux fans ou aux hélices carénées. Les résultats obtenus pour la turbulence continue sont présentés figure suivante. On remarque la variation importante des efforts Ty et Mz. La modification de comportement vis à vis du mode latéral moteur (lateral engine~5Hz) est mise en évidence sur les fonctions de transfert page suivante. Cet effet a été enregistré pour la plupart des cas traités (voilure vide ou pleine de carburant). A l'opposé, un impact très faible, inférieure à 3%, a été relevé pour la rafale discrète.

Les effets de compressibilité de l'air et d'instationnarité, ne modifient que très faiblement ces résultats.

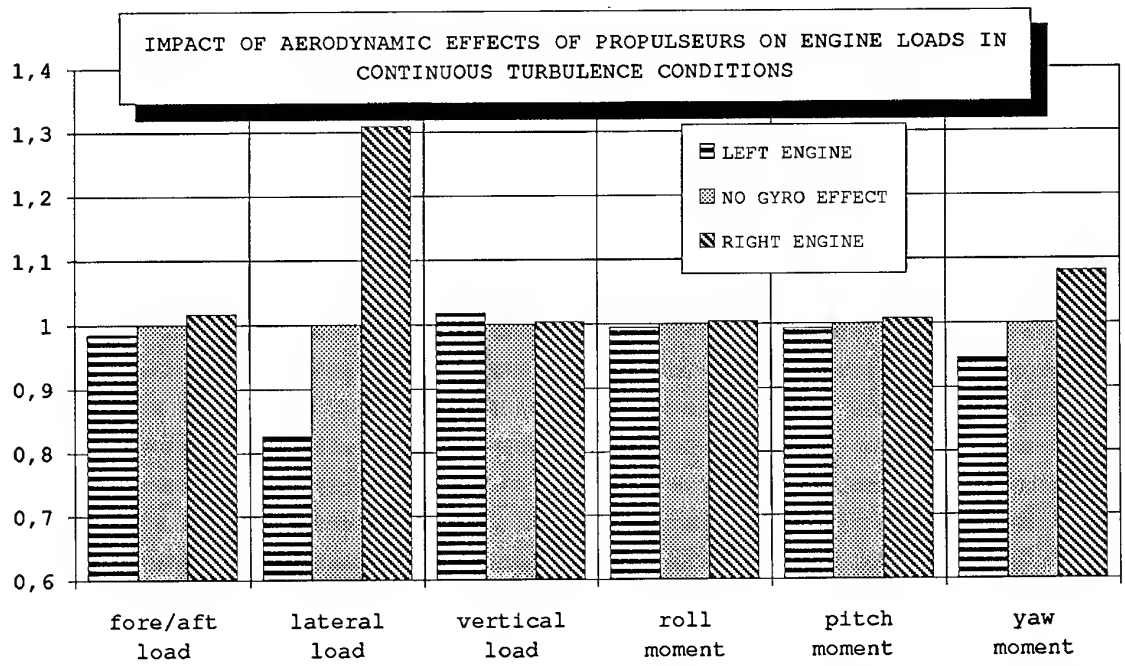

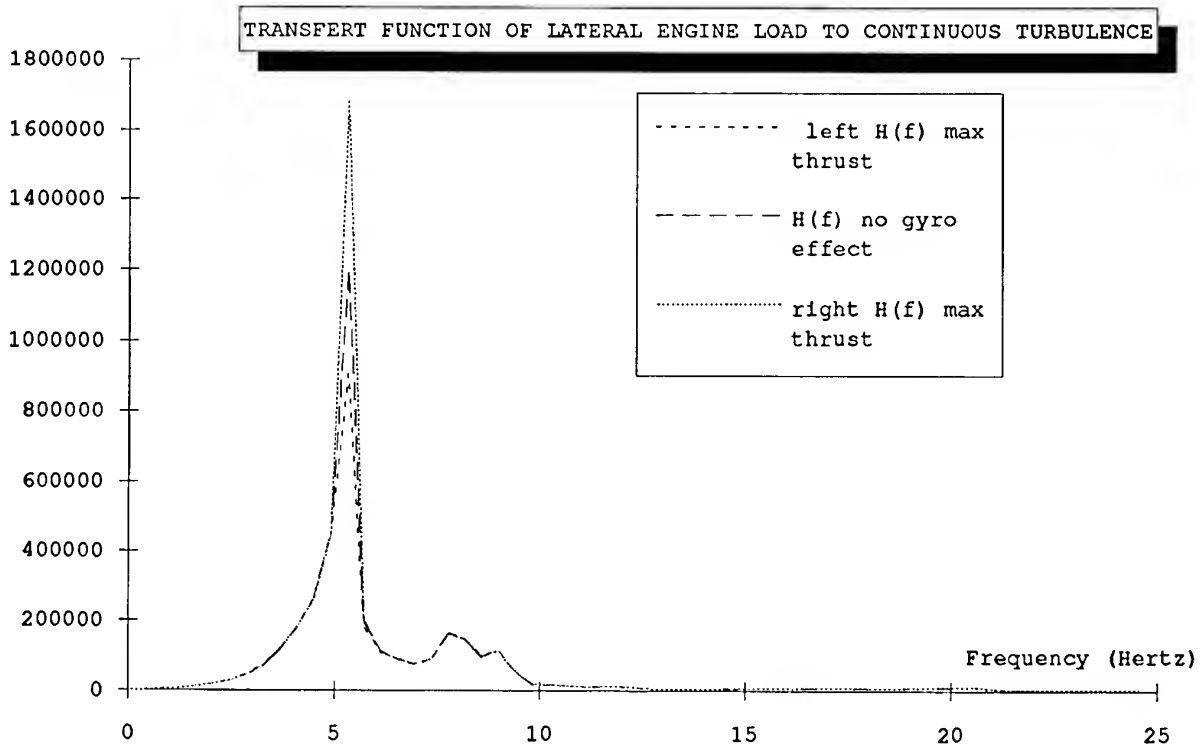

6. CONCLUSION

Les résultats obtenus sur l'impact des effets gyroscopiques sont significatifs, tant par les variations induites sur les charges moteur que par la modification du contenu en fréquence des réponses dynamiques calculées, ceci dans des proportions très liée à l'avion considéré. En ce qui concerne les moments de roulis et de lacet, My et Mz, malgré les différences dans la prise en compte de la réponse dynamique des moteurs, la comparaison entre la méthode dite "par superposition" et la méthode intégrant ces effets aux équations de la dynamique met en évidence des niveaux enveloppes globalement voisins ce qui traduit néanmoins, pour les avions étudiés, une assez bonne cohérence entre ces deux méthodes. On note également un impact induit parfois important sur les autres efforts moteur (notamment pour l'effort latéral Ty). La prévision des charges reste délicate, du fait de la grande sensibilité des résultats aux configurations massiques traitées, à l'intégration motrice et aux conditions de couplage.

En ce qui concerne la seconde partie, traitant des forces aérodynamiques sur les pales d'hélices, l'impact mis en évidence est généralement assez faible. On remarque néanmoins la modification de comportement du mode de déplacement latéral du moteur du turbopropulseur impliquant une augmentation significative des charges Ty et Mz dans le cas de la turbulence continue, augmentation non retrouvée dans pour la rafale discrète.

Un prolongement à cette étude serait la mise en œuvre des points suivants. Tout d'abord, un modèle asymétrique avion complet apporterait la prise en compte des effets antisymétriques entre les deux moteurs, donc des couplages différents négligés ici. De plus, les variations d'incidence induites par les rafales atmosphériques sont également génératrices de charges sur les pales, et l'évaluation de leur impact reste à effectuer.

Au delà de ces aspects, il doit être souligné, que la prévision des charges sur les parties motrices reste d'une complexité considérable, tant du fait de la modélisation de l'aérodynamiques locale, que de l'hypersensibilité des charges au modèle structural utilisé. Il apparaît également que, compte tenu de la complexité suplémentaire que les effets gyroscopiques ou aérodynamiques moteur, ajoutent au modèle de calcul, et à l'analyse des résultats, leur intégration doit être effectuée avec prudence à partir d'une connaissance suffisante des caractéristiques dynamiques du nouvel avion. La maîtrise de ces problèmes par la modèlisation utilisée actuellement à l'Aérospatiale, associée aux procédures de dimensionnement, à montrer assurer un bon niveau de sécurité aux éléments réalisant la liaison des parties motrices sur les avions.

7. REFERENCES

[1] J.C.Houbolt , W.H.Reed : Propeller-nacelle whirl fluter IAS paper n°61-34
[2] C.Beatrix, R.Dat : L'effet des hélices sur la stabilité aéroélastique. ONERA
[3] M.Lalanne, G.Ferraris : Rotordynamics. Prediction in engineering. John Wiley & sons

Treatment of Non−Linear Systems by Timeplane−Transformed C.T. Methods

The Spectral Gust Method

H. Lusebrink, J. Brink−Spalink
Deutsche Aerospace Airbus GmbH − Structural Dynamics
P.O. Box 95 01 09, D−21111 Hamburg, Germany

1. SUMMARY

The present paper discusses the problems, which occur when PSD/Continuous Turbulence (C.T.) gust methods, originally developed for linear dynamic gust analysis in the frequency plane, are applied to modern transport A/C with flight control systems, containing a variety of nonlinearities for signal shaping.
Power spectral density (PSD) gust velocity intensities are defined by the von Karman power spectrum in the frequency plane, scaled by the design gust intensity U_σ (RMS). This definition of gust in the frequency plane causes the basic problems for nonlinear dynamic analysis, in contrary to the timeplane defined Tuned Discrete Gusts.
Discrete Gust calculations show that aircraft nonlinearities cannot be neglected. To treat nonlinearities for C.T. there are basically three approaches (apart from linearization methods):

(SSB) **Stochastic Simulation Based Methods**

(timeplane stochastic simulation), usually in combination with exceedance rate based design load definition

(MFB) **Matched Filter Based Methods** ('Worst Case Gusts'):

For each load station, a search within a class of shape functions of prescribed 'spectral energy' is necessary to find that shape giving the highest load.

(SG) **Spectral Gust Method:**

Uses discrete gusts having exactly the von Karman spectrum, and computes the energy norm of the load time history.

A practical method for nonlinear C.T. method should have the following characteristics:

- give loads consistent to existing requirements (for linear aircraft),
- give correlated (balanced) loads
- straight−forward and economical, when applied for a large number of design cases to be calculated.

Since the SSB methods need long simulation times and give no balanced loads (together with exceedance rate counting), and the MFB methods are very expensive, the present paper proposes the SG method. It needs only one step to derive design loads, is consistent to Design Envelope Analysis and provides correlated loads.

2. INTRODUCTION

Continuous Turbulence (C.T.) gust design methods were introduced in the requirements (FAR/App. G, JAR/ACJ 25.305(d)), because the Discrete Gusts (DG) represented a too artificial description of atmosphere, not taking into account its randomness. The C.T. methods, first the Mission analysis (MA), later the simpler Design Envelope Analysis (DEA) are based on (von Karman) power spectral density description of gust velocity, and used frequency domain techniques to compute the loads.

The first problem with C.T. methods was to adjust the design gust intensity parameters: b_1, b_2, P_1, P_2 (for MA) or U_σ (for DEA) respectively, based on A/C designs with good structural safety records.

The next problem was the computation of balanced (correlated) loads, a demand from stress offices. Meantime this was solved, but only for DEA.

The third problem with C.T. methods since many years is how to treat aircraft nonlinearities. While aerodynamic nonlinearities can be linearized in a conservative manner, the control system nonlinearities (limiters, thresholds) of modern transport aircraft are more difficult to handle. Statistical linearization methods are not straight−forward. They need a two−step analysis procedure: First calculate Equivalent Gains, second: calculate design loads. The method is expensive and time consuming, if several such nonlinearities exist. The most adequate way to treat nonlinearities seems to be simulation in time domain. But time domain methods for C.T. introduce three new analytical problems:

- Unsteady aerodynamics have to be translated into time domain.
- Random gusts have to be realized in time domain or to be replaced by 'equivalent' discrete gust time histories.
- The specification of 'design load' from the corresponding load time history consistent with linear methods.

3. PROBLEM DESCRIPTION

The problem is the definition and computation of design loads for nonlinear aircraft subjected to random gusts.

Note that gust models, defined by Spectral Densities and intensity parameters and their time−plane realizations, are the most representative description of the atmosphere.

The nonlinearities can be found in:

- Controls (limiters, thresholds, actuator dynamics),
- Flight Mechanics (large rigid body motions)
- Aerodynamics (high angles of attack) linearization usually gives conservative loads
- Structure (free play, material, ...); usually not important for loads

Paper presented at a Workshop on "Aircraft Loads due to Turbulence and their Impact on Design and Certification" held in Lillehammer, Norway on 5 May 1994.

Resulting problems

Correct treatment of nonlinearities requires time domain methods, leading to following analytical difficulties

- -- Unsteady aerodynamics have to be translated into time domain.
  Solutions: [14]
  - -- rational function approximation (s−plane)
  - -- z−transform approach
- -- Random gusts have to be realized in time domain.
  Solutions:
  - -- Stochastic simulation
  - -- Worst Case Gusts (MFB, SDG,...)
  - -- Spectral Gusts
- -- The definition of 'design load ' for nonlinear systems needs further discussion.
  Solutions:
  - -- RMS load
  - -- MFB load
  - -- Exceedance probability based load
  - -- Spectral Gust based load

4. DISCUSSION OF POSSIBLE SOLUTIONS

(Lin) **Linearization**

This is the usual method today, when PSD methods (DEA or Mission Analysis) are applied. Linearization is achieved in case of saturation nonlinearities in control laws (yaw damper, load alleviation systems) by reducing the gains (conservative). In more general cases with isolated nonlinearities statistical linearization ("Equivalent Gain"−Method) is applied, which is appropriate for random gust .

Disadvantage: Not straight−forward, time consuming and expensive

(TSS) **Timeplane Stochastic Simulation**

A random gust shape u(t) is generated using

- --filtered (Gaussian) white noise, or
- --superposition of sinewaves with random phase and von Karman amplitudes and subsequent Inverse Fourier transform.

Then the nonlinear system is simulated in time domain (using rational function approximation of unsteady aerodynamics).

Disadvantage: high cost (long simulation times) ; balance ?

(MFB) **Matched Filter Based Methods** (NASA)

For each load quantity a "worst case gust" shape u(t) has to be found by evaluating

$$y_{des} = \frac{U_\sigma}{c} \max_{\|u\|_\Phi \le c^2} \max_t |y(t)|$$

where the "spectral energy"

$$\|u\|_\Phi = \frac{1}{2}\int_0^\infty |G(i\omega)|^2/\Phi(\omega)\, d\omega$$

(which is a measure for the "relative probability" $e^{-\|u\|_\Phi}$ [4]) is constrained.

The MFB methods are based on a variational principle (Cauchy−Schwarz Inequality), which for linear systems translates the RMS−norm of the DEA method into the max−norm of a load time history.

The MFB−1−Dimensional Search method [8] and the Statistical Discrete Gust method (SDG) are also based on this maximum principle.

Disadvantage: high cost (optimization for each load station is required)
(e.g. up to : 60 stations, each 12 responses;
to be done for : 40 mass cases, 10 velocities/altitudes)

(FPE) **Fokker Planck Equation**

The FPE represents a partial differential equation in the state variables (and t) for statistical properties of a stochastic differential equation [5, 6].

Disadvantage: extremely high cost

(Est) **Estimation methods**

Determine scaling factors = $\frac{nonlinear}{linear}$ from discrete gusts and apply them to linear PSD results.

Disadvantage: unknown accuracy, balance ?

(SG) **Spectral Gust Method (DA proposal)**

By a "Spectral Gust" we understand a discrete gust $u_G(t)$ with correct 'spectral density', i.e. simply the scaled impulse response of a gust filter G(s):

$$u_G(t) = \sqrt{\pi T}\ L^{-1}\ G(i\omega),\ .$$

T (= L/V) being a reference time. Then we define the design gust load by an energy norm of the load response y(t) due to a design Spectral Gust $u = U_\sigma\, u_G(t)$:

$$y_{des,SG} = \|y\|_t / \sqrt{T}, \qquad y(t) = y[U_\sigma u_G](t),$$

where $\|y\|_t = \left[\int_0^\infty |y(t)|^2\, dt\right]^{1/2}$, and U_σ $(= \sigma_w\, \eta_d)$ is the design gust velocity from the DEA method.

Then for linear systems it can be shown that the SG method is totally equivalent to the (balanced) DEA method in the frequency plane . Hence the SG method is a direct translation of the DEA method into time domain, which requires no optimization. We discuss the SG method in more detail in the next section.
Remark:
We have $\|u_G\|_t = \sqrt{T}$, and the natural selection T = L/V, τ = Vt/L, implies $\|U_\sigma u_G\|_\tau = U_\sigma$ and $y_{des,SG} = \|y\|_\tau$.

5. THE SPECTRAL GUST METHOD

It is well known that the discrete (1−cos) gust does not reflect correctly the power spectral density of atmosphere, see figure 1.

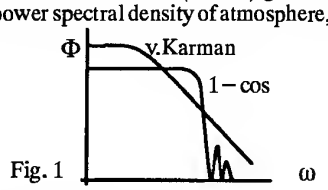

Fig. 1

Here, for reasons of comparison the discrete gust

$u(t) = \frac{1}{2}\,(1 - \cos(\Omega t))$, $\Omega = \pi V/H$, H = GustGradient, was periodically continued to get a nonvanishing power spectral density, which is defined for u(t) by [2]:

$$\Phi(\omega) = \lim_{T\Rightarrow\infty} \frac{1}{\pi T} \left| \int_{-T}^{+T} u(t)\, e^{-i\omega t}\, dt \right|^2$$

$$= \lim_{T\Rightarrow\infty} \frac{1}{\pi T} |U_T(\omega)|^2 .$$

This inconsistency of the spectral densities is one reason why Discrete Gust calculations and PSD methods cannot give comparable results.

In the following we derive "Spectral Gusts" u(t), i.e. discrete gusts having correct PSD (and the Laplace transform should exist).
Let T be the corresponding reference time (e.g. T=L/V, L the scale of turbulence). Then we require

$$\Phi_1(\omega) = \frac{1}{\pi T} |U(i\omega)|^2 ,$$

where $\Phi_1(\omega)$ is the given PSD, normalized by $\int_0^\infty \Phi_1 d\omega = 1$.

Now let G(s) be a normalized gust filter for Φ, i.e. a transfer function which generates random gusts with prescribed PSD from white noise. G(s) is a holomorphic function satisfying

$$\Phi_1(\omega) = |G(i\omega)|^2, \quad G(\bar{s}) = \overline{G(s)}.$$

Hence a normalized Spectral Gust is given by
$U_G(i\omega) = \sqrt{\pi T}\, G(i\omega)$, and in time domain by

$$u_G(t) = \sqrt{\pi T}\ \ L^{-1}\, G(s) .$$

It is simply a scaled impulse response of the gust filter G(s). Its energy norm is $\| u_G \|_t = \sqrt{T}$, $\| u_G \|_{t/T} = 1$, whereas the gust filter is normalized in frequency domain : $\| G \|_\omega = 1$

It should be remarked that there exist many gust filters; they are obtained from a special one by multiplication with a real, odd, analytic phase function $\psi(\omega)$:

$$G_\psi(i\omega) = G(i\omega)\ e^{i\psi(\omega)}.$$

Von Karman Spectral Gusts:

We apply this procedure to the normalized von Karman power spectrum

$$\Phi_K(\omega) = \frac{L}{\pi V}\, \frac{1 + \frac{8}{3}(1.339\omega L/V)^2}{\left[1 + (1.339\omega L/V)^2\right]^{11/6}}$$

Here L=2500 ft is the scale of turbulence. We found by means of Beta−Functions that the constant 1.339 can be replaced by

$$\frac{\Gamma(1/3)}{\Gamma(1/2)\ \Gamma(5/6)} = 1.338985279....$$

[Brink−Spalink, Sept. 1992].

Von Karman gust filters are given by

$$G(s) = \pm \sqrt{\frac{L}{\pi V}}\ \frac{1 \pm \sqrt{8/3}\ sT_0}{[1 + sT_0]^{11/6}}\ , \qquad T_0 = 1.339\frac{L}{V},$$

considering the different signs. Note that a minus sign in the denominator would give a time reversed impulse response (filter is not realizable). It is possible to transform these gust filters analytically into time domain [Lusebrink, Aug. 1990] : The denominator of form $(s - a)^{-n}$ has an inverse Laplace transform, and the numerator represents a differential operator. The resulting Spectral Gusts are quite simple:

$$u_G(t) = \pm\, c_0 \sqrt{\frac{T}{L/V}} \cdot e^{-t/T_0} \cdot \left(\frac{t}{T_0}\right)^{-1/6} \cdot \left(1 - c_1 \frac{t}{T_0}\right),$$

with constants $c_0 = \frac{5}{6}\sqrt{\frac{8}{3}} \,/\, \Gamma(\frac{11}{6})$, $c_1 = \frac{6}{5}\left(1 \pm \sqrt{\frac{3}{8}}\right)$

$\Gamma(11/6) = 0.940655858$, and $T_0 = 1.339L/V$, whereas T (=L/V) is the Spectral Gust reference time.
The singularity $t^{-1/6}$ is very mild; it can be approximated with arbitrary accuracy. Note that the impulse response of a Dryden filter or a rational function approximated von Karman filter does not have a singularity.
In case of a von Karman gust filter with an additional phase factor $e^{i\psi(\omega)}$, an analytical Inverse Fourier transform will not be possible in general. On the other hand a numerical transform will converge extremely slow, because $|G(i\omega)| \cong \omega^{-5/6}$ for the higher frequency band. But convergence can be accelerated by low pass filtering and numerical differentiation in time domain:

$$g(t) = \left(1 + k\,\frac{d}{dt}\right)\ L^{-1}\left\{\frac{1}{1 + k\,s}\ G(s)\right\} .$$

Mathematical Basis of the Spectral Gust Method

For linear systems with transfer function $H_y(s)$ the design load as used in DEA is defined by

$$y_{des,RMS} = U_\sigma\, \overline{A_y}, \qquad \overline{A_y} = \left[\int_0^\infty |H_y|^2 \Phi_K d\omega\right]^{1/2} .$$

If $G(i\omega)$ denotes a normalized gust filter, $|G|^2 = \Phi_1 (= \Phi_K)$, then $\overline{A_y}$ is the energy norm in frequency domain of the combined transfer function H_yG :

$$\overline{A_y} = \left[\int_0^\infty |H_yG|^2 d\omega\right]^{1/2} = \| H_yG \|_\omega .$$

To translate this into time domain we remember Parseval's theorem; its general form reads

$$\int_0^\infty u(t) \cdot v(t)\, dt = \frac{1}{2\pi} \int_{-\infty}^{\infty} \overline{U(i\omega)}\ V(i\omega)\, d\omega\ ,$$

where U(s), V(s) are the Laplace transforms of u(t), v(t). We get

$$\| H_yG \|_\omega =$$

$$= \left[\int_0^\infty \overline{H_yG}\ H_yG d\omega\right]^{1/2} = \left[\pi \int_{-\infty}^{\infty} |h_y * g|^2 dt\right]^{1/2}$$

$$= \sqrt{\pi}\ \| h_y * g \|_t$$

where $(h_y * g)(t)$ denotes the convolution of the impulse responses of $H_y(s)$ and G(s). Hence

$$y_{des,RMS} = U_\sigma \| H_yG \|_\omega = U_\sigma \sqrt{\pi}\ \| h_y * g \|_t .$$

For linear systems we may introduce a scaling factor c :

$$y_{des,RMS} = \frac{U_\sigma}{c}\sqrt{\pi}\ \| h_y * (c\ g) \|_t \ .$$

c corresponds to the reference time T as derived above: $c = U_\sigma\sqrt{\pi T}$. Now for nonlinear systems we define the Spectral Gust design load by

$$y_{des,SG} = \| y[U_\sigma u_G](t) \|_t \ / \ \sqrt{T} \ ,$$

where $u_G(t) = \sqrt{\pi T}\ \mathcal{L}^{-1}\ G(s)$ is a Spectral Gust and T (= L / V) is a reference time .

Note that for linear systems this definition is independent on U_σ , and independent on the selected gust filter G(s) . For linear systems it is totally equivalent to the DEA method in the frequency plane. Moreover, also the correlated loads from the DEA method can be defined in time domain, using Parseval's theorem once more:

$$z_y := z_{des}\ \varrho_{yz} \ , \quad \text{where}$$

$$\varrho_{yz} = \frac{\int_0^\infty y(t)\ z(t)\ dt}{\| y \|_t \ \| z \|_t}$$

is a correlation coefficient in time domain.

C. T. Design Load Definitions for nonlinear systems

In case of nonlinear systems the above definition will be dependent on the selected Spectral Gust. On the other hand no agreed definition exists in this case for random gusts. Possible definitions are:

-- the RMS gust load (used in the DEA method)
$y_{des} = \text{RMS}\ \{\ y\ [U_\sigma\ u_K(t)]\ \}$
with $u_K(t)$ = von Karman−filtered Gaussian unit white noise .

-- the MFB gust load (prescribed 'gust probability')
$y_{des} = \frac{U_\sigma}{c}\ \max_{\|u\|_\Phi \le c^2} \max_t |y(t)|$, $\quad c = U_\sigma$,

-- load with prescribed exceedance probability
$N_y(y_{des}) = N_{des}$ (used in Mission Analysis) ,
where $y(t) = y\ [u_K(t) \cdot U_\sigma/\eta_d]$,

-- the Spectral Gust based design load :
$y_{des,SG} = \| y \|_t / \sqrt{T}$, $\quad y(t) = y[U_\sigma u_G](t)$,

6. COMPARISON OF LOADS FROM VARIOUS METHODS

The nonlinear test model (open loop)

The best way to demonstrate the behaviour of the various nonlinear gust loads methods is to apply them to a nonlinear system, which is simple enough to compute results analytically, but complex enough to represent a broad class of systems (eigenfrequencies, dampings, nonlinearities). Our test model consists of a linear transfer function (harmonic oscillator, including load recovery) followed by a static quadratic nonlinearity (progressive) :

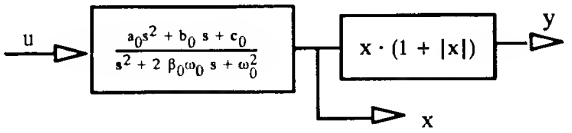

Hence the load response y(t) due to a general gust u(t) is

$$y(t) = f\ (\ \int_0^t h_x(t-\tau)\ u(\tau)\ d\tau\ ) = f\ (h_x * u)$$

where $h_x(t) = \mathcal{L}^{-1}\ H_x(s)$ and $f(x) = x \cdot (1 + |x|)$.

Using this 5−parameter model we can demonstrate the effects of different

-- gust inputs (random gust , Worst Case Gust, Spectral Gust), each with varying intensities

-- design load definitions:
y_{max} , σ_y , $\| y \|_2$, $N(y) = N_{des}$, and $P(\eta > y) = P_{des}$ [3].

-- nonlinearities: $f(x) = x \cdot (1 + |x|)^{\pm 1}$,

-- system damping: $\beta_0 = 0.10,\ 0.02$

Computation of RMS based design load (assuming Gaussian distribution)

The RMS−definition of design load as defined in JAR/ACJ 25.305(d) and based on FAA−ADS−53 , is given by

$$y_{des,RMS} = U_\sigma\ \overline{A}_y \ , \quad \overline{A}_y = \frac{\sigma_y}{\sigma_w} = \frac{\text{RMS}(y)}{\text{RMS}(u)} \ ,$$

where the design gust velocity $U_\sigma (= \sigma_w\ \eta_d)$ is prescribed as a function of altitude, but the gust velocity σ_w itself is not prescribed. But for nonlinear systems the $\overline{A}$ value depends on the gust velocity σ_w .
For our simple nonlinear model we can compute the RMS−based design load analytically, assuming Gaussian probability distribution of the gust velocity u(t):

$$p_u(u) = \frac{1}{\sigma_w (2\pi)^{1/2}}\ \exp\left(\frac{-u^2}{2\sigma_w^2}\right)$$

Then the linear response $x = H_x\ u$ has Gaussian distribution $p_x(x)$, with RMS $\sigma_x = \sigma_w\ \| H_x U \|_\omega$. Now the nonlinear response $y(t) = f(x(t))$ has a distorted Gaussian distribution:

$$p_y(y) = p_x(x)\ /\ \frac{\partial f(x)}{\partial x} \ , \text{where}\ \ y = f(x),$$

and f(x) is strictly increasing. We obtain

$$\sigma_y^2 = \int_{-\infty}^{\infty} y^2\ p_y(y)\ dy = \int_{-\infty}^{\infty} [f(x)]^2\ p_x(x)\ dx = \ldots$$

$$= \sigma_x^2[1 + \sqrt{32/\pi}\ \sigma_x + 3\sigma_x^2].$$

Here we have used the formulae

$$\int_0^\infty x^k\, e^{-\lambda x^2} dx = \frac{1}{2}\lambda^{\frac{-(k+1)}{2}}\ \Gamma\left(\frac{k+1}{2}\right),\quad \lambda > 0, k > -1 \text{ and}$$

$\Gamma(x+1) = x\Gamma(x)$, $\Gamma(1/2) = \pi^{1/2}$. Hence the RMS−design load is

$$y_{des,RMS} = U_\sigma \,\|H_x G\| \left[1 + \sqrt{32/\pi}\ \sigma_x + 3\sigma_x^2\right]^{1/2}$$

$$= x_{des}\left[1 + \sqrt{\frac{32}{\pi}}\,\frac{x_{des}}{\eta_d} + 3\left(\frac{x_{des}}{\eta_d}\right)^2\right]^{1/2},$$

which depends on gust intensity and nonlinearity.

Computation of MFB design load

The MFB design load for a nonlinear system H_y can be written as

$$y_{des,MFB} = \max_{\|w\| = U_\sigma\sqrt{\pi}} \max_t |y(t)|\ ,$$

where $y = y[u] = y[Gw]$. For our model $y = f(H * u)$. Now since f(x) is a monotonic function, the worst case gust for y(t) is the same as for x(t), hence

$$y_{des,MFB} = f(x_{des}) = x_{des}\,(1 + x_{des}), \quad \text{where}$$

$$x_{des} = x_{des,MFB} = x_{des,RMS} = U_\sigma \,\|H_x G\|_\omega$$

Computation of MFB−1DS design load

This simplified MFB−method was recently published by NASA including software [8]. Here the search for worst case gust is restricted to a 1−parameter family. The design loads obtained numerically will be slightly smaller than from the full MFB method.

Computation of Spectral Gust based design loads

The discrete gust used as input is a scaled Spectral Gust

$$U_\sigma\, u_G(t) = U_\sigma \sqrt{\pi T}\ \ L^{-1}\ G(s)$$

(see the analytical solutions in section 5). The corresponding Spectral Gust design load of our nonlinear system is

$$y_{des,SG} = \|f\,(h_x * (U_\sigma\, u_G)\|_t \,/\, \sqrt{T}, \quad (T = L/V).$$

This can be computed only numerically. The intensity U_σ and default system parameters

$\beta_0 = 0.10$, $\omega_0 = 4\ \pi$, $a_0 = c_0 = 0$, $b_0 = 1$,

were varied.

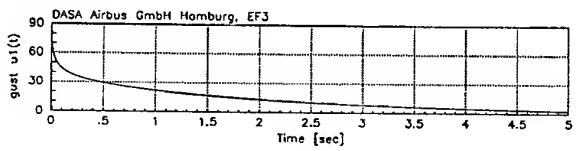

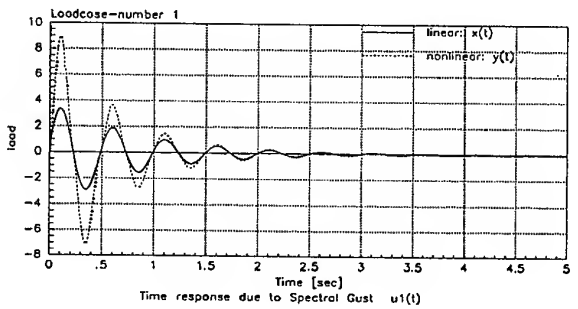

Time response due to Spectrol Gust u1(t)

Computation of exceedance rate based design load (for Gaussian distribution).

Based on timeplane stochastic simulation of the nonlinar aircraft with input process u(t) assumed to be stationary Gaussian with RMS(u) = σ_g (= $U_\sigma/3$ e.g.) given and output process y(t), the exceedance rate based design load $y_{des,EXC}$ is defined by the equation

$N_y(y_{des,EXC}) = N_{des}$ (= 1/50000h e.g.),

where N_{des} is a prescribed design frequency, and the function $N_y(y_1)$ denotes the exceedance rate of level y_1 for signal y(t) (number of crossings per unit time of level y_1 with positive slope).

For the linear subsystem $x = H_x(u)$ the exceedance rate is given by Rice's formula [1]

$$N_x(x) = N_{0,x}\ \exp\left(\frac{-x^2}{2\sigma_x^2}\right), \quad \text{where}$$

$$N_{0,x} = \frac{1}{2\pi}\,\frac{\sigma_{\dot x}}{\sigma_x} = \frac{\|i\omega H_x G\|}{2\pi\,\|H_x G\|}$$

is the "characteristic system frequency" for given PSD $\Phi_1 = |G(i\omega)|^2$; solving for x we get

$$x_{des,EXC} = \sigma_x\left[2\log\left(\frac{N_{0,x}}{N_{des}}\right)\right]^{1/2}.$$

For our nonlinear response, y(t) = f(x(t)), and from monotonicity of f(x) each x−crossing of level x1 corresponds to an y−crossing of level y1 = f(x1):

$N_y(y_1) = N_x(x_1)$, where $y_1 = f(x_1)$.

We obtain

$$y_{des,EXC} = f(x_{des,EXC}) = f(x_{des,RMS}\ \eta_{EXC/RMS})\ ,$$

where $x_{des,RMS} = \sigma_x \eta_d$ and

$$\eta_{EXC/RMS} = \frac{x_{des,EXC}}{x_{des,RMS}} = \frac{1}{\eta_d}\left[2\log\left(\frac{N_{0,x}}{N_{des}}\right)\right]^{1/2}$$

is a design load ratio for linear systems and Gaussian processes.

Note that $N_{0,x}$ is infinite if $|H_x(i\omega)|\,\omega^{2/3}$ is unbounded, since for the von Karman Spectrum $|G(i\omega)| \propto \omega^{-5/6}$; hence in our model $x_{des,EXC} = \infty$, if $a_0 \neq 0$.

Graphical presentation of design loads from variousmethods

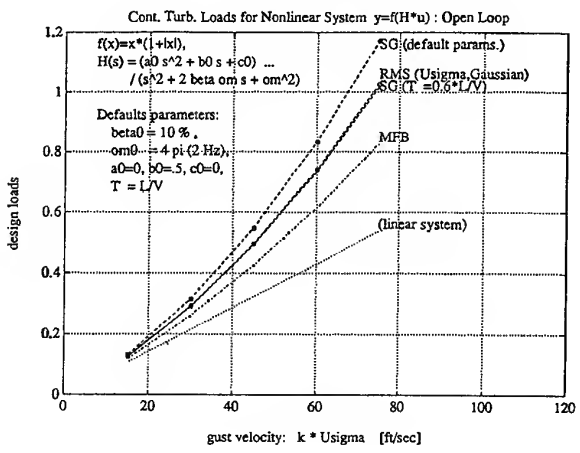

7. CONCLUSION

Based on discrete gusts having the 'correct' power spectral density,the Spectral Gust method represents a direct translation of the PSD method into time domain.

- --It requires no optimization (which is inherent in Worst Case Gust methods by definition) ,
- --The gust shape is independent of the load stations and their response characteristics. ...."the airplane does not generate the turhulence".. [1]
- --It produces loads consistent to DEA for linear A/C
- --It gives also correlated (balanced) loads
- --It is straight forward and very economical

The problem that several Spectral Gusts exist, leading to slightly different loads in case of nonlinear systems, reflects the lack of agreed definition of 'design load'. The selection of a Spectral Gust and a reference time T (varying the scale of turbulence) could be adopted, e.g. to the RMS definition, which was used in DEA .
The final Spectral Gust parameters are then ohtained from general studies during the means-of-compliance process.

8. REFERENCES

[1] HOUBOLT, J.C.
Suggestions for Improving Gust Design Procedures
75th AGARD-SMP Meeting, Lindau, 1992

[2] HOBLIT, F. M.,
Gust Loads on Aircraft: Concepts and Application,
AIAA, 1988, Washington

[3] NOBACK, R.
Definition of PSD Design Loads for Nonlinear Aircraft
NLR, TP 89016 U, 89117

[4] JONES, J.G.
Response of Linear Systems to Gaussian Process Inputs in Terms of Probability Functionals
RAE-TR-86028, 1986

[5] BHARUCHA-REID, A.T.
Elements of the Theory oF Markov Processes and ...,
McGraw-Hill 1960,

[6] STRATONOVICH R.L.
Topics in the Theory of Rrandom Noise
Vol.1, Gordon and Breach, 1963.

[7] SCOTT, R.C., POTOTZKI, A.S., PERRY, B.,III
Computation of Maximized Gust Loads for Nonlinear Aircraft Using Matched-Filter-Based Schemes
Journal of Aircraft, Vol 30, No. 5, 1993, pp. 763-768

[8] SCOTT, R.C., POTOTZKI, A.S., PERRY, B.,III
A Computer Program to Ohtain Time-Correlated Gust Loads for Nonlinear Aircraft Using the Matched-Filter-Based Method
NASA, Langley Research Center, Sept. 1993

[9] MOLZOW, M.
Gust Load Activities
AGARD-SMP, Lindau, Germany

[10] MOLZOW, M., LUSEBRINK, H.
BRINK-SPALINK,J.
Patches of Turbulence: The PSD Gust Method
AGARD-SMP, Lindau, Germany, Octoher 1992

[11] MOLZOW, M., LUSEBRINK, H.,
BRINK-SPALINK, J.
Proposal for a Spectral Gust Method
Gust Specialist Meeting,
La Jolla, California, April, 1993

[12] LUSEBRINK, H.
The Spectral Gust Method.- A Short Review -
LSD/EF3-09/94, 14.3.94

[13] BRINK-SPALINK, J.
Comparison of MFB Method and SG Method
LSD/EF3-08/94, 14.3.94
Response of Linear Systems to Gaussian Process Input in Terms of Probability Functional
RAE-TR-86028, 1986

[14] BRINK-SPALINK, J.
Fast Calculation of Root Loci for Aeroelastic Systems and Response in Time Domain.
AIAA-90-1156-CP

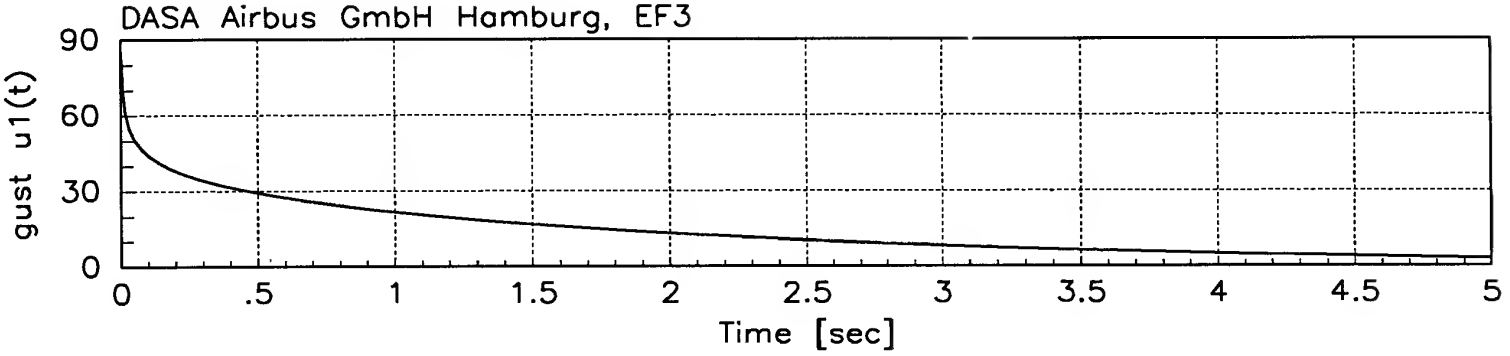

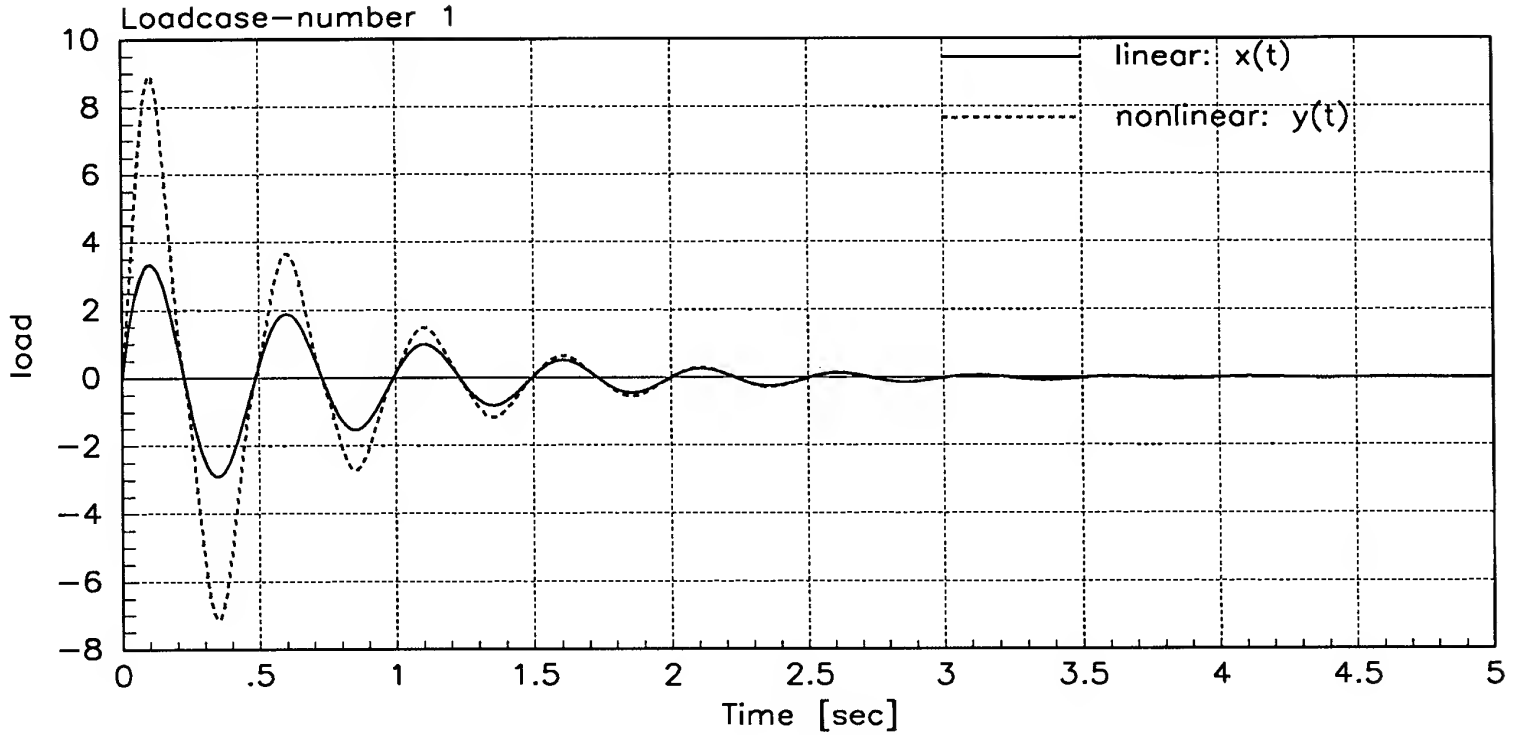

Time response due to Spectral Gust u1(t)

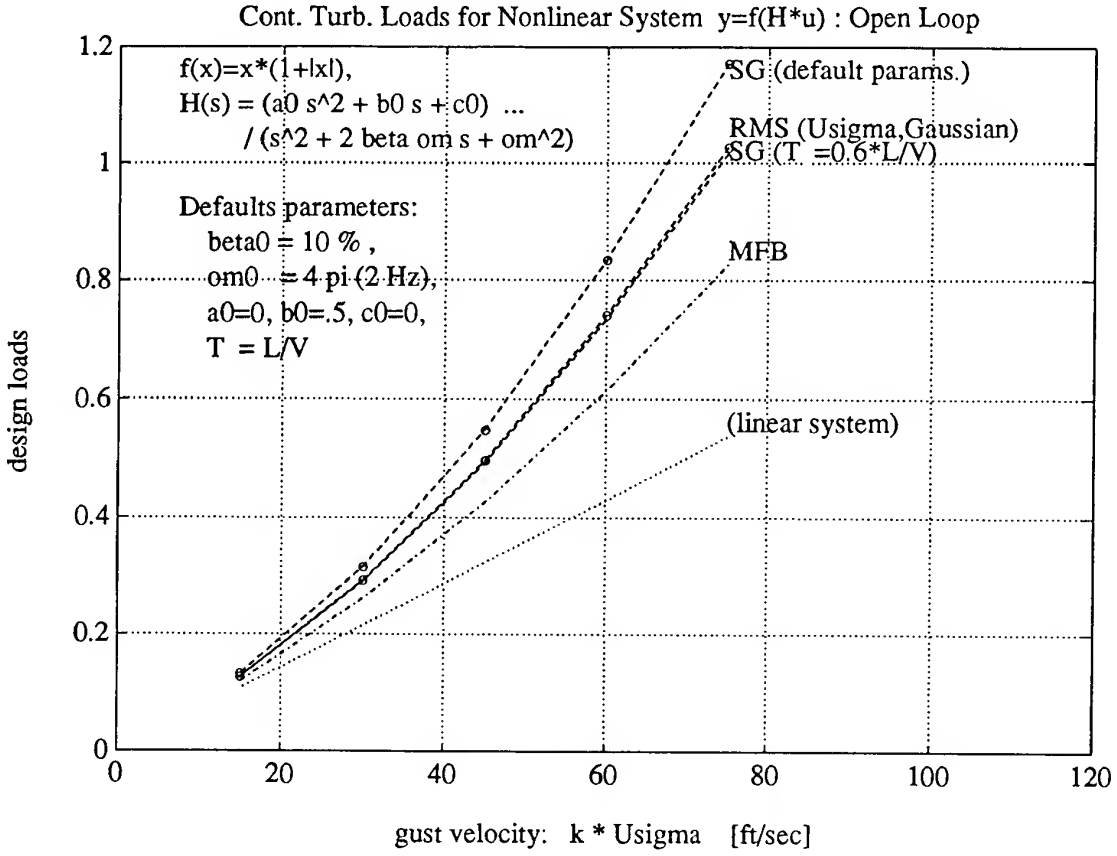
Cont. Turb. Loads for Nonlinear System y=f(H*u) : Open Loop
f(x)=x*(1+|x|),
H(s) = (a0 s^2 + b0 s + c0) ...
/ (s^2 + 2 beta om s + om^2)
Defaults parameters:
beta0 = 10 % ,
om0 = 4 pi (2 Hz),
a0=0, b0=.5, c0=0,
T = L/V
SG (default params.)
RMS (Usigma,Gaussian)
SG (T =0.6*L/V)
MFB
(linear system)
design loads
gust velocity: k * Usigma [ft/sec]
0
0.2
0.4
0.6
0.8
1
1.2
0
20
40
60
80
100
120

A STUDY OF THE EFFECT OF STORE UNSTEADY AERODYNAMICS ON GUST AND TURBULENCE LOADS.

M. Oliver
J. Casalengua
C. Maderuelo
Y. Camacho
H. Climent
Structural Dynamics Department
CONSTRUCCIONES AERONÁUTICAS S.A.
Getafe, 28906 Madrid, Spain

SUMMARY

Gust and turbulence loads are the most severe conditions for some parts of the aircraft, specially in the outboard wing region. The addition of external stores usually alleviates the gust/turbulence loads on the wing but becomes critical for other components as pylons and wing/pylon attachments.

Safety implications and all-weather envelope of current fighters force an accurate study of the gust/turbulence response of the aircraft for each store configuration. Inertia is the most important contribution of the store to the gust/turbulence loads. Nevertheless, store unsteady aerodynamics should be included if significantly changes the results of the gust/turbulence response.

This paper is devoted to the analytical study of the effect of store unsteady aerodynamics on gust/turbulence response. A large number of configurations have been included in the study. Several regulations to define the gust/turbulence excitation have been used.

1 INTRODUCTION

The effect of store aerodynamics in aeroelastic problems has been devoted mainly to study its influence in wing/store flutter. Published investigations started as early as 1949 [1], and continue over the time. A complete multivariate analysis can be found in [2].

On the other hand, very little published work concerning the effect of store aerodynamics in gust and turbulence loads is available. The reason may be in the fact that the addition of underwing external stores usually alleviates the gust/turbulence loads on the wing, while the flutter speed of the aircraft may be adversely affected because of the inertia, elastic and aerodynamic coupling between the wing and its stores.

Nevertheless, some parts of the airframe as wing-pylons attachments or the pylons themselves become critical with the addition of external stores. If the load envelope due to gust and turbulence overshoots the rest of loads envelope (manoeuvre, buffet, release...) as is the case using some current regulations, some pylon sizing cases will be product of gust and turbulence analyses. Therefore the accurate computation of the gust and turbulence responses is also a matter of safety in an all-weather flight envelope.

In the subsonic regime, current analysis standards [3]-[4] make possible to account for the wing/store unsteady aerodynamic coupling in gust and turbulence response while in the supersonic regime it is still an open question. The computation of the unsteady aerodynamic contribution of the store and the store/wing interference effect will increase significantly the cost of each single run and the associated engineer cost of data preparation, model validation and results evaluation. The economics of including store aerodynamics must be considered together with other technical aspects.

Due to the variety of stores that can be carried by a typical modern fighter and their derived configurations considering the release sequence (including failure cases), the total number of possible aircraft/store configurations is in the order of thousands. This constitutes a large amount of work for flutter analyses, because even using engineering judgement criteria several hundreds should be selected. In gust and turbulence response inertia is the most important contribution of the store to the pylon loads and therefore a significant reduction in the number of configurations to analyse can be made based on that parameter. It means that the inclusion of store unsteady aerodynamics in gust and turbulence loads calculation is feasible with current computers, and should be included if significantly changes the results of the gust and turbulence response, specially when changes are nonconservative.

Multivariate analysis of similar studies [2] has concluded that general guidelines can not be provided, only particular advices for use in a particular aircraft. Therefore, it has been preferred to deal directly with an actual set of external stores in an actual aircraft

Paper presented at a Workshop on "Aircraft Loads due to Turbulence and their Impact on Design and Certification" held in Lillehammer, Norway on 5 May 1994.

model.

The paper presents the general procedure followed to calculate the gust and turbulence load envelopes at monitoring stations. Some validations and sensitivity analysis of store aerodynamics are briefly outlined. The main part of the paper is devoted to present the effect of the store unsteady aerodynamics on gust/turbulence response by covering a large number of actual wing/store configurations first in single carriage and then in multiple carriage. The paper ends with conclusions and guidelines derived from the results of the analysis and description of some limitations of current methods.

2 GENERAL PROCEDURE

Loads acting on the aircraft due to the atmospheric turbulence are computed as response either to a tuned discrete gust or to continuous turbulence. A complete survey of vertical and lateral, "up" and "down", gust conditions, flight envelope points and mass configurations covering all possible airplane characteristics and current regulation requirements [9]-[12] have to be performed in the certification process. Nevertheless, for the intention of the present study it has been considered enough to analyse only tuned discrete gust and continuous turbulence vertical excitation (up and down) in one point in the subsonic regime.

2.1 Tuned discrete gust response

The tuned discrete gust definition used for the analysis corresponds to the requirements of the DEF STAN 00-970 regulations [9] which define the gust intensity without attenuation with gust length. Figure 1 shows the shape of the five different gust lengths used in the analyses, from 100.0 ft to 473.5 ft (25 $\bar{c}$, $\bar{c}$ = mean aerodynamic chord) with 66 f.p.s. of gust intensity. The loads obtained with this excitation are LIMIT loads.

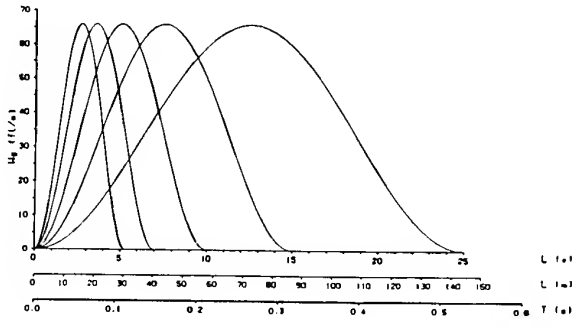

Figure 1: Tuned discrete $(1 - cos)$ gust

Linear behaviour of the structure is assumed. Therefore, the total loads are obtained adding up the transient loads due to the gust or turbulence response to the stationary loads due to the flight condition analysed. The flight condition considered in the results presented herein corresponds to the 1G level flight. MSC/NASTRAN aeroelastic capability [4] running in a CRAY XM-P computer and some internal CASA in-house codes have been used to obtain the transient response to the gust or turbulence excitation. A modal solution has been selected to reduce the computer time needed for the analysis. The dynamic equation defining the gust problem in the frequency domain is:

$$\left\{-\omega^2[M] + i\omega[B] + [K] + [Q]\right\}\{\xi\} = \{P(\omega)\} \quad (1)$$

where:

ω	Frequency
$[M]$	Generalized mass matrix
$[B]$	Generalized damping matrix
$[K]$	Generalized stiffness matrix
$[Q]$	Generalized aerodynamic coefficients
$\{\xi\}$	Generalized modal coordinates
$\{P(\omega)\}$	Generalized aero gust loads

The elements of $[M]$, $[B]$ and $[K]$ are obtained from the structural model. The unsteady aerodynamic theories (Doublet Lattice and Slender and Interference bodies method [5]-[8]) give the $[Q]$ matrix, as a function of Mach number and reduced frequency, in the frequency domain. A Fourier transform of the time histories defining the gust excitation is needed to obtain the aerodynamic loads $\{P(\omega)\}$. $\{\xi(\omega)\}$ is obtained as the solution of the system, and an Inverse Fourier Transform provides $\{\xi(t)\}$.

Back substitution gives the nodal displacement vector as:

$$\{x(t)\} = [\phi]\{\xi(t)\} \quad (2)$$

where $[\phi]$ is the modal matrix.

From this displacement vector, a quasi-static set of nodal gust loads can be obtained, at each time instant t, using the stiffness matrix $[K_{AA}]$:

$$\{F_g(t)\} = [K_{AA}]\{x(t)\} \quad (3)$$

This nodal loads distribution is summed up for each previously selected monitoring station (j) to obtain the resulting loads. Total loads are obtained summing up positive and negative incremental gust loads (to account for up and down gusts) to the stationary loads (1G loads).

$$F_{T_j}(t) = F_{s_j} \pm F_{g_j}(t) \quad (4)$$

Single gust load envelopes at each monitoring station are obtained from these time-histories for each gust length and aircraft configuration as shown in figure 2.

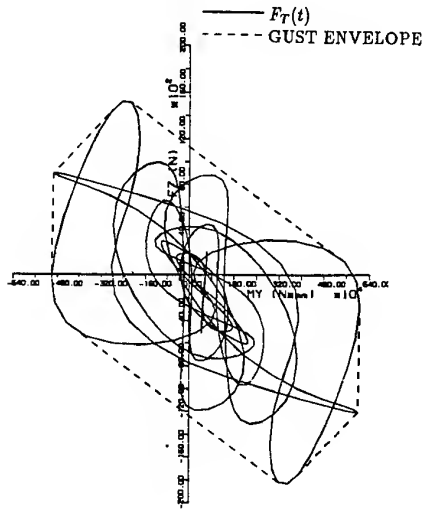

Figure 2: Typical single gust load envelope

Global gust load envelopes at each monitoring station are obtained "enveloping" single load envelopes for all gust lengths and airplane configurations. These gust loads are then compared with other envelopes (i.e. static loads) in order to select points to provide sets of nodal loads for checkstress. Figure 3 shows a typical pylon global gust load envelope compared with a a typical static load envelope. The gust envelope overshoots the static load envelope at some points. In this example, eight sets of nodal loads were provided.

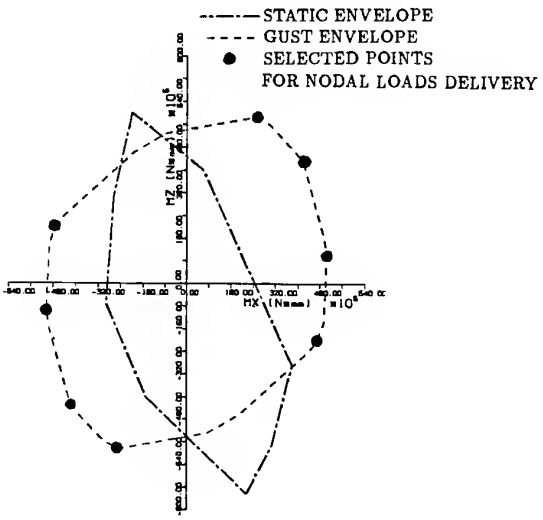

Figure 3: Typical pylon global gust load envelope with points for nodal loads delivery

2.2 Continuous turbulence response

For a fighter aircraft, current military regulations [10]-[11] require continuous turbulence analyses in the supersonic regime. This study has been focused in the subsonic regime, therefore the definition of the continuous turbulence model has been obtained following a civil regulation [12]. The continuous turbulence model used corresponds to the Von Karman Spectrum, with scale of turbulence L=2500 ft and 112.5 f.p.s. of gust intensity. Loads obtained with this excitation are LIMIT loads.

The airplane response to continuous turbulence is calculated by means of typical statistical approach of random analyses [13]. The unit Power Spectral Density (PSD) of airplane response ($S_j(\omega)$) can be computed from the unit PSD of the atmospheric turbulence ($S_a(\omega)$) using techniques of frequency response:

$$S_j(\omega) = |H_{ja}(\omega)|^2 \times S_a(\omega) \tag{5}$$

where $H_{ja}(\omega)$ is the frequency response of any physical variable u_j, due to an excitation source, Q_a that verifies the transfer function theorem:

$$u_j(\omega) = H_{ja}(\omega) \times Q_a(\omega) \tag{6}$$

where $u_j(\omega)$ and $Q_a(\omega)$ are the Fourier transforms of u_j and Q_a. The rms value ($\overline{A}$) of each response is computed as the squared root of the PSD area of the response:

$$\overline{A} = \sqrt{\frac{1}{2\pi}\int_0^\infty S_j(\omega)d\omega} \tag{7}$$

The limit loads are obtained as:

$$L = u_\sigma \times \overline{A} \tag{8}$$

Where L is the limit load and u_σ the gust intensity (112.5 fps), value that corresponds to the r.m.s. value of the gust velocity times a factor to account for peaks. In-house CASA programs are used to compute the rms values of the internal loads (shear force, bending moment and torsion moment) at the selected monitoring stations.

3 ANALYSIS CONDITIONS

All the results presented in this paper have been computed in the subsonic regime at Mach=0.8, sea level conditions and considering only vertical excitation.

3.1 Structural Models

The dynamic model used corresponds to an actual fighter aircraft model, with delta wing, foreplane, wing tip pod and four underwing stations to carry external stores. The model has been obtained by the assembly of several substructure models representing the main components of the aircraft. Normal mode frequencies and mode shapes have been validated using ground resonance test results.

The pylon models consist of a mass joined to the wing structure through a stiffness matrix with a reduced set of degrees of freedom, because the dynamic behaviour of the store is adequately represented by a few modes (pitch, yaw, lateral, roll etc.), that have also been validated with ground resonance test.

3.2 Aircraft Unsteady Aerodynamic Model

Unsteady aerodynamics has been calculated using Doublet Lattice method for lifting surfaces combined with Slender and Interference Body Methods for fuselage and tip pod [4]-[8].

Figure 4 gives a representation of the aerodynamic model. The wing aerodynamic model consists of a flat surface with 182 boxes and a body for the tip pod with 6 slender and interference elements. The number of boxes for the foreplane is 30. The fuselage model consists of 9 slender and interference elements. Values of $C_{L\alpha}$ and position of the wing pressure centre obtained for zero reduced frequency have been compared with the values obtained using more accurate steady aerodynamics methods and available wind tunnel results showing good correlation.

3.3 Monitoring stations definition

Monitoring stations have been defined covering all aircraft components. In gust/turbulence response, wing and pylon monitoring stations have received a special attention.

Four pylons located in four different spanwise positions of the wing structure have been considered:

Pylon	ID.	Spanwise position (%)
Inboard	(I/B)	32.0
Center	(CTR)	53.0
Outboard	(O/B)	71.0
Stub	(STUB)	87.0

For each pylon, several monitoring stations are defined, representing the loads acting on the store, store + launcher or store + launcher + pylon. The computed loads at each monitoring station are:

- F_y (Lateral Force)
- F_z (Vertical Force)
- M_x (Bending Moment)
- M_y (Pitch Moment)
- M_z (Yaw Moment)

Figure 5 shows a pylon monitoring station.

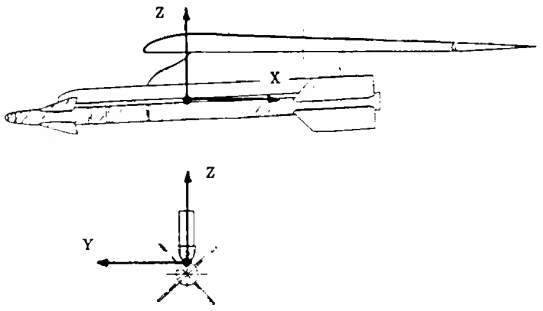

Figure 5: Pylon monitoring station.

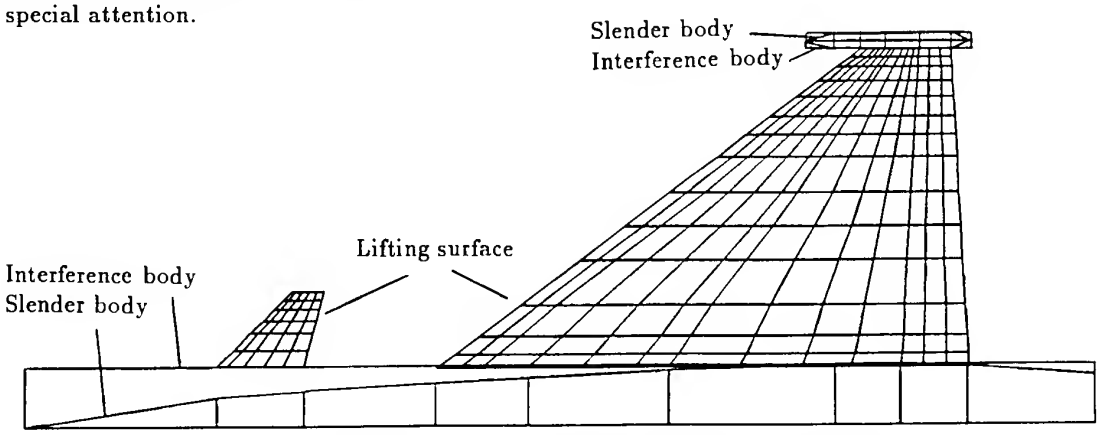

Figure 4: Aircraft Unsteady Aerodynamic Model

3.4 Sensitivity analysis to unsteady aerodynamic modelling of store and pylons

The loads convergence with unsteady aerodynamics model mesh has been verified with sensitivity analyses to number of:

- Slender body elements.
- Store fin boxes.
- Store canard boxes.
- Pylon boxes.

A quick convergence of loads has been observed with the number of slender body elements. Using as reference 25 slender body elements, 3 used to be enough in most of the cases to reproduce 98 % of body loads. In addition, no variation of loads has been observed above 10 slender body elements. For lifting surfaces, results have shown that relatively coarse meshes can be used for I/B, CTR and O/B pylon modelling while finer meshes should be used for STUB pylon, store fins and store canards.

3.5 External Stores Considered

The different type of external stores that can be carried in a fighter aircraft can be grouped, from the gust loads point of view, in three classes: fuel tanks, missiles and bombs. In general, heavy stores correspond to full fuel tanks while light stores are missiles.

The aerodynamic shape of the external fuel tanks corresponds to a slender body incorporating in some cases stabilizing fins. Missiles include both types of lifting surfaces: canards and fins to allow missile control. The third type of stores (bombs, equipment pods etc.) corresponds, in general, to stores with slender body without fins or control surfaces, and masses and cross-sectional areas that are between those of fuel tanks and missiles.

For this study, two types of external fuel tanks (one including stabilizing fins) have been considered. For missiles, a typical short range air-to-air missile has been considered in single or twin carrier configuration. For bombs, two typical heavy bombs have been analysed. The second bomb has been included in the study to allow the analysis of a twin bomb carrier.

Some functional assumptions have been performed to allocate the stores on the pylons. Usually, fuel tanks are carried at a unique underwing position with the adequate fuel system connections to allow fuel pumping from the fuel tanks. Missiles are located at the outboard regions of the wings. Bombs and pods can be carried at several spanwise positions, but in general, the heavier the store the more inboard is carried.

Table 1 describes the different stores considered in the analysis, the pylon or pylons where it has been assumed that these stores can be carried, weight and maximum cross section.

TYPE	ID.	UNDER WING STORES				W	SECT.
		I/B	CTR	O/B	STUB	(kg)	(m^2)
FUEL TANK	T1		X			1300.	0.430
	T2		X			920.	0.283
MIS-SILE	M				X	157.	0.014
	2M			X	X	297.	0.028
BOMB	B1	X	X	X		496.	0.139
	B2			X		263.	0.138
	2B2	X				591.	0.276

Table 1: External stores considered

Five of the seven stores are always carried in the same pylon. The twin missile carrier can be carried in two pylons and the B1 bomb in three pylons. This gives a total of 10 "single store" configurations. In addition large number of "multiple store" configurations can be arranged combining simultaneously the single ones.

3.6 Unsteady Aerodynamic Models for External Stores

Unsteady aerodynamics has been calculated using Doublet Lattice method for the pylon surfaces, store fins and canards, combined with Slender and Interference Body Methods (Images) for the underwing stores [4]-[8]. Full interference effects with the aircraft unsteady aerodynamic model have been taken into account.

The final unsteady aerodynamic models of pylons and stores have been obtained after the sensitivity analyses representing a balanced trade-off between economy and accuracy. Pylon lifting surfaces models are shown in figure 6 and store models in figure 7. The store models are not at the same scale to allow visibility of small stores details. Only slender models have been represented.

NOTE: current methods do not allow easy modelling of stores for which control surfaces are inside of interference body. Interference body section should match slender body maximum section, which in turn, should match store maximum section. Control surfaces close to longitudinal axis should be modelled translated outside the interference body with the associated problem of structural-aerodynamic interpolation. Figure 8 shows two typical stores that present this modelling problem, a laser guided bomb with canards and a balistic bomb with fins.

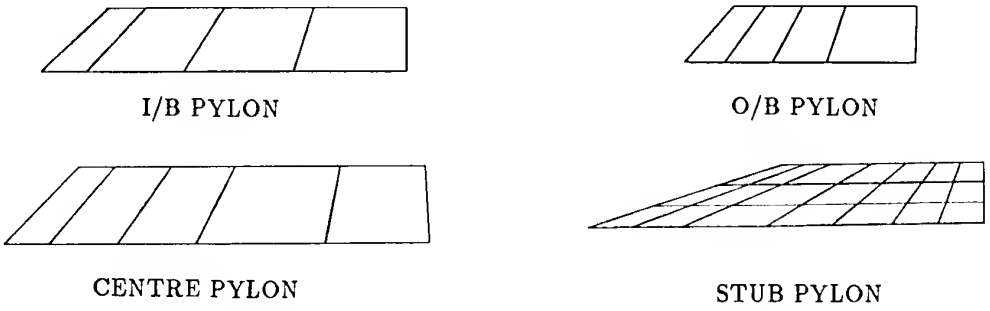

Figure 6: Pylons unsteady aerodynamic models

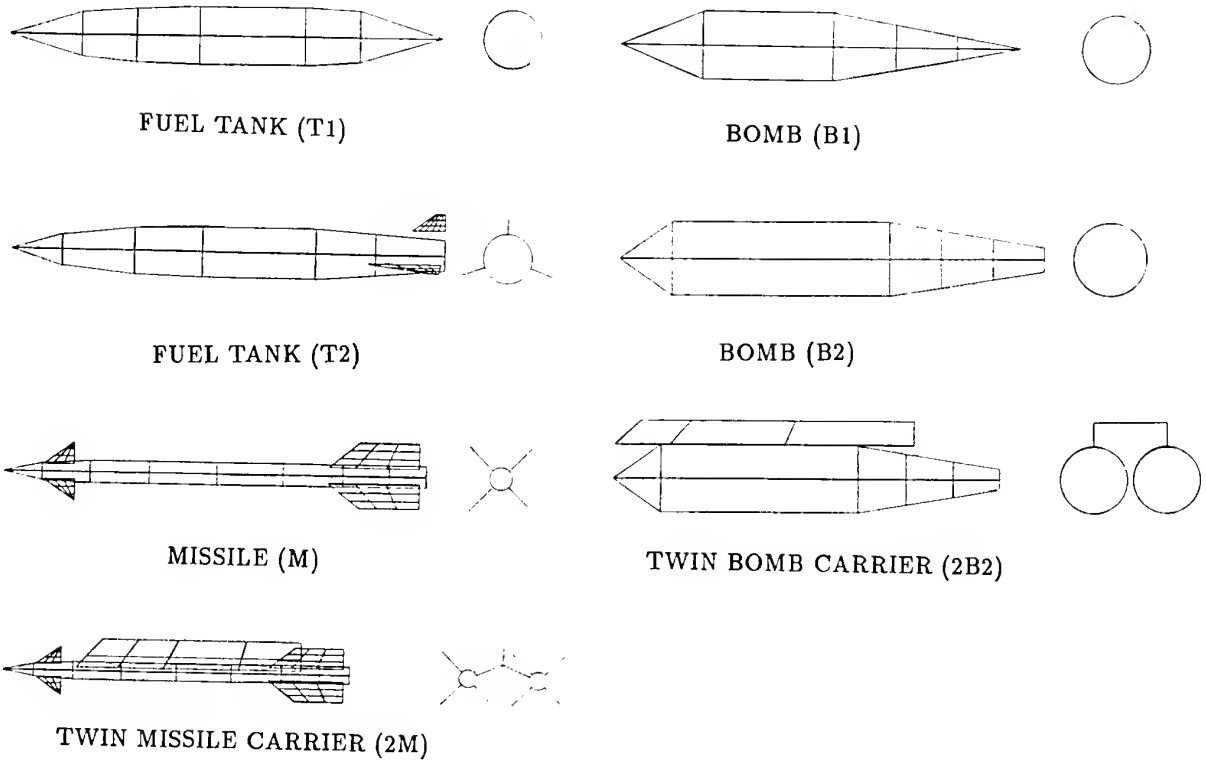

Figure 7: Stores unsteady aerodynamic models (not to scale)

Figure 8: Stores difficult to model with current methods

4 RESULTS OF "SINGLE STORE" CONFIGURATIONS

The 10 single store configurations have been considered in a first step to present results in a systematic way. Although the loads have been obtained for all pylon and aircraft monitoring stations, results are presented only for the pylon monitoring station that takes into account the contribution of store plus launcher. Loads have been obtained with and without store aerodynamics.

The loads envelopes displayed in figure 9 show a typical effect of the store unsteady aerodynamics on pylon loads. Continuous lines correspond to the case without store unsteady aerodynamics while dotted lines correspond to the case with aerodynamics. The larger envelopes correspond to all gust lengths of the tuned discrete gust. The small envelopes correspond to only considering the $25\bar{c}$ gust length case.

Some regulations [11]-[12] request for compliance with $25\bar{c}$ gust length only. Figure 9 shows that due to the small loads obtained in this particular case, to consider or not the store unsteady aerodynamics is a matter of minor importance.

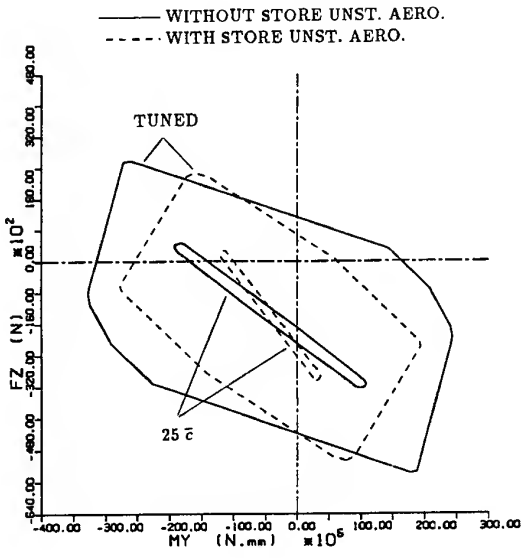

Figure 9: Effect of store unsteady aerodynamics on gust load envelopes

Figure 10 shows the effect of the store unsteady aerodynamics in the response to continuous turbulence. Continuous line is the case without store unsteady aerodynamics and dotted line is the case with aerodynamics.

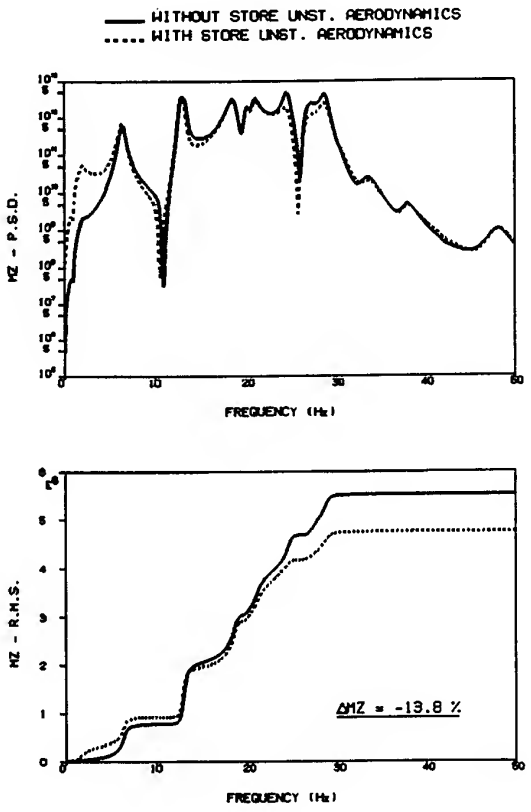

Figure 10: Effect of store unsteady aerodynamics on continuous turbulence response

From the envelopes (gust) or limit loads (turbulence), the effect of the unsteady aerodynamic modelling has been computed for each store-pylon combination and each load:

$$\Delta_{LOAD}(\%) = 100 \times \frac{LOAD_A - LOAD_0}{LOAD_0} \quad (9)$$

Where:

LOAD	Peak values (gust) or Limit loads (eq. 8) (turbulence)
A	"With Aerodynamics"
0	"Without Aerodynamics"

Table 2 displays the values obtained for the 10 single store configurations. The two figures in each box correspond to the influence in the tuned discrete gust response (above) and the influence in the continuous turbulence response (below). Negative values represent alleviating effect of considering aerodynamics while positive values represent an increase of loads.

	TYPE OF STORES									
	FUEL TANKS		MISSILES			BOMBS				
	T1	T2	M	2M		B1			B2	2B2
	CTR	CTR	STUB	O/B	STUB	I/B	CTR	O/B	O/B	I/B
ΔF_y (%)	4.4	4.6	-8.8	45.3	23.8	11.1	1.7	-8.5	-0.6	43.0
	0.6	2.6	-10.0	15.3	17.1	10.2	1.6	-10.1	-5.3	37.1
ΔF_z (%)	-7.9	-1.5	7.2	16.6	58.7	-1.1	0.9	-2.3	-1.3	-7.3
	-8.1	-3.9	2.9	5.9	35.5	-1.3	0.5	-2.3	-1.6	-7.1
ΔM_x (%)	4.0	4.8	6.1	60.2	17.0	9.6	1.7	-8.8	-1.0	38.9
	0.5	2.7	-8.4	20.2	-3.5	8.3	1.3	-10.1	-5.4	30.2
ΔM_y (%)	-17.3	-5.8	-5.0	-2.4	-20.9	-6.3	-6.9	-5.2	-6.0	-7.3
	-24.7	-4.2	-7.1	-7.9	-9.3	-1.3	-6.2	-3.3	-4.2	-6.8
ΔM_z (%)	17.0	6.6	-6.4	159.1	-21.7	6.5	30.9	27.1	2.8	7.0
	17.4	2.8	-13.8	44.6	-15.4	1.3	29.1	28.5	15.0	1.9

Table 2: Variation of gust/turbulence loads due to store unsteady aerodynamics for "single store" configurations

In general, results show that similar effects are obtained for both excitations tuned gust and continuous turbulence. It is remarkable that the effect is always alleviating for the M_y load. The largest store unsteady aerodynamics effects are obtained for the missiles and twin carriers, as was expected because of the presence of lifting surfaces embodied in the models of those stores. On the other hand, a small effect is reported for stores consisting basically on slender bodies. To get a better insight into the different aerodynamic contributions, the following sensitivity analyses have been performed:

- PRESENCE OF FINS IN FUEL TANKS.

  A tuned gust run was performed removing the fins in the fuel tank T2 model. Comparison of results with the run including the fins shows that the influence of fins is not significative.

- PRESENCE OF FINS AND CANARDS IN THE MISSILE.

  Two tuned gust runs were performed either removing the fins or the canards in the Missile M model. Comparison of results with the run including fins and canards show that all the effect is basically due to the canards and the influence of fins is not significative.

- PRESENCE OF CARRIER

  Two tuned gust runs were performed removing the aerodynamic model of the carrier but maintainig the close bodies in the twin missile 2M and twin store 2B2 carriers. Results show that although the influence of the close bodies is very important in both cases (bombs and missiles) the influence of the carrier itself should also be taken into account.

- SPANWISE POSITION OF SLENDER BODIES

  The store B1 is carried in three spanwise positions. Results from table 2 show the effect of store unsteady aerodynamics:

  - Increases on M_z with spanwise position.
  - Decrases on F_y and M_x with spanwise position.
  - Remains almost constant on F_z and M_y.

4.1 Effect on Wing Monitoring Stations

Usually, inclusion of stores produces an alleviation on wing gust/turbulence loads. Nevertheless, an example has been selected to illustrate that depending on the configuration and monitoring station, a wide variety of cases can occur, including increase of loads after store inclusion. The consideration of the store unsteady aerodynamics can contribute to expand the load envelopes.

The following plots show the comparison of results for three configurations:

- Clean wing (without missile).
- Missile M on stub pylon without store aerodynamics.
- Missile M on stub pylon with store aerodynamics.

Figure 11 shows the comparison for a typical tuned gust load envelope in the wing root monitoring station, far inboard the missile section. The influence of the missile inertia is small and the effect of the unsteady missile aerodynamics very reduced.

Figure 12 shows the comparison in the wing monitoring station located at the same missile position. The presence of the missile inertia substantially modifies the load envelope shape, producing additional critical points. The unsteady missile aerodynamics significantly contributes to enlarge the load envelope and therefore, if not included in the calculations, non conservative results can be obtained.

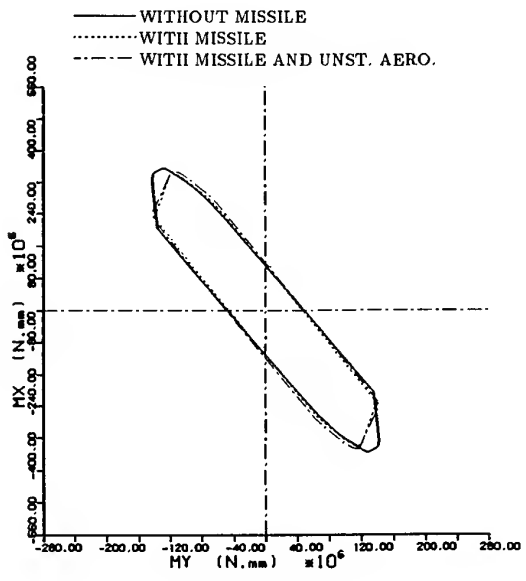

Figure 11: Wing root monitoring station

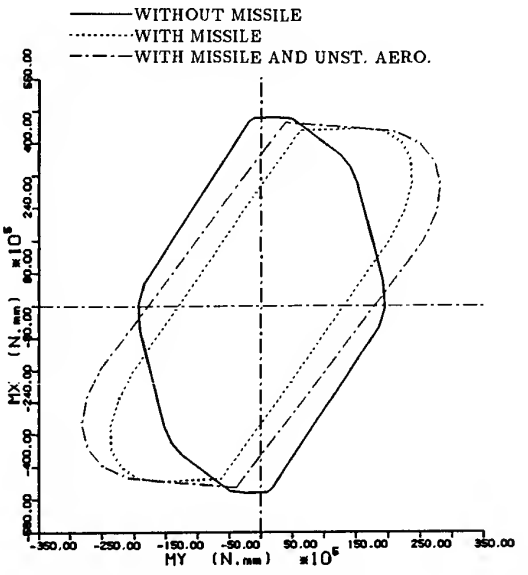

Figure 12: Wing 89% spanwise monitoring station

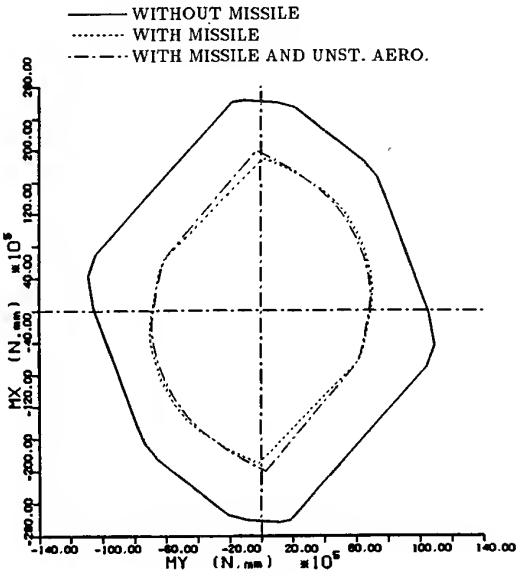

Figure 13: Wing 99% spanwise monitoring station

Figure 13 shows the comparison at a wing monitor station located outboard from the missile position. Comparison shows the clear alleviating effect of the missile inertia, only slightly modified by the missile unsteady aerodynamics.

5 RESULTS OF "MULTIPLE STORE" CONFIGURATIONS

In principle, it is assumed that the inertia added in the "multiple stores" configurations should alleviate the loads in each particular pylon already obtained with the "single store" configurations. Although in general the assumption is quite appropriate, some critical load cases coming from multiple stores configurations have been obtained.

Configurations with multiple stores can been arranged combining the stores of table 1. The maximum number of possible multiple store configurations including all possible combinations is in the order of hundreds. Nevertheless, a large reduction in the number of configurations can be achieved based on particular functional considerations (non-flight configurations, two or more failures in the release sequence, etc.). An additional reduction in the number of configurations to analyse can be obtained removing the configurations which loads are clearly covered by other configurations (lightest stores at each pylon).

The remaining "multiple stores" configurations have been analysed with and without store unsteady aerodynamics and the loads due to gust/turbulence response obtained. At the end, 6 "multiple stores critical configurations" have been obtained. A configuration is considered critical when it produces critical loads in at least one monitoring station. Loads are critical when overshoot the envelopes already produced by "single store" configurations.

	UNDER WING STORES			
	I/B	CTR	O/B	STUB
1	B1	B1	B1	M
2	2B2	T1	B2	M
3		T1	2M	M
4		T1		M
5	2B2			M
6			B1	M

Table 3: "Multiple Stores" Critical Configurations

An attempt has been made to reduce the amount of computation, trying to derive guidelines on which store unsteady aerodynamics should be considered and which can be removed in a multiple store configurations. Several runs have been performed with the 6 critical configurations considering a partial number of stores with unsteady aerodynamics instead of all of them. Table 4 shows a typical example of obtained results, corresponding to the first critical configuration. Again, percentages have been obtained following equation 9. In each box, values above represent the effect in tuned discrete gust and values below represent the effect in continuous turbulence. Negative values mean alleviating effect and positive values mean load increases. First block of the table presents the influence of store unsteady aerodynamics considering all the stores. Second block presents the results considering only the aerodynamics of the 3 bombs slender bodies. Third block presents the results considering only the missile aerodynamics.

AERO	Δ	UNST. AERO. EFFECT			
		I/B	CTR	O/B	STUB
3 Slen. + miss.	F_y (%)	-7.8	13.6	-10.9	-21.3
		-4.6	6.0	-9.9	-10.8
	F_z (%)	8.9	15.9	4.7	1.5
		2.8	6.4	-0.4	-2.7
	M_x (%)	-9.8	13.0	-10.9	25.9
		-4.6	5.6	-10.0	-19.6
	M_y (%)	4.4	-0.6	-6.2	-41.7
		0.3	-13.7	-3.8	-26.6
	M_z (%)	11.3	103.3	29.0	18.8
		16.8	21.5	-32.3	-26.9
3 Slen.	F_y (%)	-9.8	-3.3	-11.1	-2.2
		-5.7	-7.8	-12.1	-4.7
	F_z (%)	10.1	13.7	-2.8	-2.4
		7.5	5.6	-3.7	-3.1
	M_x (%)	-12.2	-3.7	-11.2	-1.3
		-5.5	-8.1	-12.3	-2.4
	M_y (%)	4.1	-8.4	-13.3	-4.8
		0.4	-8.8	-7.0	-3.6
	M_z (%)	2.2	104.9	28.5	-5.4
		17.6	22.5	-29.5	-3.0
miss.	F_y (%)	1.1	18.8	-0.8	-10.8
		0.6	18.5	1.1	-5.6
	F_z (%)	-1.5	3.5	8.1	2.9
		-4.6	1.5	3.7	0.2
	M_x (%)	1.1	19.2	-0.8	21.9
		0.6	18.4	1.1	-18.3
	M_y (%)	0.3	9.4	8.9	-36.1
		0.1	-4.6	3.6	-24.1
	M_z (%)	-6.5	4.6	2.6	11.9
		1.2	-1.2	-4.8	-24.1

Table 4: Variation of gust/turbulence loads due to store unsteady aerodynamics for a "multiple store" critical configuration

Inboard pylon results are relatively similar between first and second block indicating that the presence of missile aerodynamics at the stub pylon has a minor effect on the inboard pylon. Stub pylon results are relatively similar between first and third block indicating that the presence of missile aerodynamics is the main contribution to stub pylon loads.

In spite of the above expected considerations, table 4 shows no other clear guidelines. Therefore, the conclusion (confirmed with similar results with other configurations) should be that the store unsteady aerodynamics should be considered for all the stores in critical multiple store configurations.

6 SUMMARY OF RESULTS

So far, the effect of the store unsteady aerodynamics has been considered by comparing with the same situation without aerodynamics. When different configurations have been analysed, a range of values representing that effect are obtained, one for each configuration. When application of results have to be made to an actual aircraft to obtain the global effect per pylon basis, it is better to normalize the effects to the same value in each pylon. Figure 14 shows a histogram of the effects per pylon basis obtained with the expresion:

$$\Delta_{LOAD}(\%) = 100 \times \frac{(LOAD_A) - (LOAD_0)}{[MAX(LOAD_0)]} \quad (10)$$

Where:

LOAD	Peak values (gust) or Limit loads (eq. 8) (turbulence)
A	"With Aerodynamics"
0	"Without Aerodynamics"
MAX(LOAD)	Maximum Load in that pylon

The histogram represents the range of values of the store unsteady aerodynamics effect for all the configurations analysed with single or multiple stores. A table like table 5 with the maximum positive values (in form of factors) for each load on each pylon can be derived for this particular aircraft and could help to decide whether a new configuration should be analysed including store unsteady aerodynamics given the gust/turbulence loads without such aerodynamics.

	I/B	CTR	O/B	STUB
F_y	1.37	1.07	1.09	1.00
F_z	1.26	1.17	1.09	1.11
M_x	1.36	1.06	1.14	1.28
M_y	1.07	1.00	1.13	1.00
M_z	1.16	1.21	2.24	1.79

Table 5: Factors for pylon loads

The histogram shows larger influence of store unsteady aerodynamic than expected at the begining of this study, in both discrete tuned gust and continuous turbulence excitation. In general, comparison between the two types of excitation shows similar effects with the only exceptions of STUB pylon F_z, M_x and M_z.

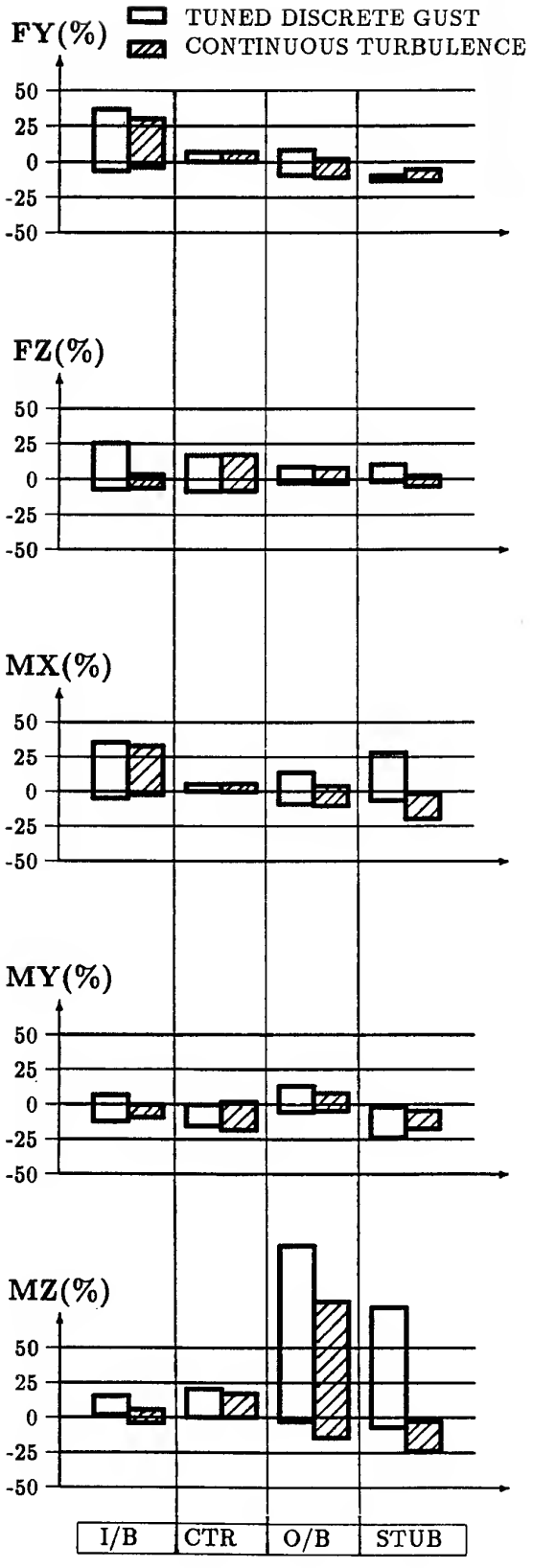

Figure 14: Histogram of Global Effects per Pylon

7 CONCLUDING REMARKS

An extensive analytical study of the effect of store unsteady aerodynamics on gust/turbulence response has been presented. The influence has been larger than expected in both discrete tuned gust and continuous turbulence. The effect in single store configurations is very similar for both excitations and also for multiple store configurations with the only exceptions of STUB pylon F_z, M_x and M_z.

In general, considering store unsteady aerodynamics alleviates the pylon M_y loads but there are not clear trends for the rest of loads.

"Single store" configurations results indicate that unsteady aerodynamics of stores with lifting surfaces, (missiles, twin carriers) have to be considered. Otherwise, non-conservative results can be obtained even for some wing monitoring stations close to the store position. For missiles models, the contribution of canards is the most significative with only limited influence of fins.

"Multiple store" configurations results indicate that it is necessary to include unsteady aerodynamics of all stores in critical configurations. Apart from this, no other clear guidelines can be derived from the results.

Current methods do not allow easy modelling of stores which control surfaces that are inside of interference body. Interference body section should match slender body maximum section, which in turn, should match store maximum section. Control surfaces close to longitudinal axis should be modelled translated outside the interference body with the associated problem of structural-aerodynamic interpolation. According with results presented in this paper, it will not be a serious problem with balistic bombs with fins, but it is likely to be a major problem with laser guided bombs with canards.

Extensions of the work performed herein can be application to engine nacelles or stores in supersonic regime.

8 REFERENCES

1. Sewall, J.L. and Woolston, D.S., "Preliminary Experimental Investigation of Effects of Aerodynamic Shape of Concentrated Weights on Flutter of a Straight Cantilever Wing". NACA RM L9E17, July, 1949.
2. Turner, C.D., "The Effect of Store Aerodynamics on Wing/Store Flutter". 5th Aircraft/Stores Compatibility Symposium, St. Louis, Missuri, 9-11 September 1980. (AIAA paper 81-0604).
3. Gockel, M.A. (Editor), MSC/NASTRAN Handbook for Dynamic Analysis, The MacNeal-Schwendler Corporation. 1983.
4. MSC/NASTRAN Handbook for Aeroelastic Analysis, Vols I and II, The MacNeal-Schwendler Corporation. 1987.
5. Rodden, W.P., Giesing, J.P. and Kalman, T.P., "Refinement of the Nonplanar Aspects of the Subsonic Doublet Lattice Lifting Surface Method", Journal of Aircraft, Vol. 9, No. 1, pp 69-73, January 1972.
6. Miles, J.W., "On Non-Steady Motion of Slender Bodies", The Aeronautical Quarterly, Vol. II, pp. 183-194, November 1950.
7. J.P. Giesing, T.P. Kalman, and W.P. Rodden, "Subsonic Steady and Oscillatory Aerodynamics for Multiple Interfering Wings and Bodies", Journal of Aircraft, Vol. 9, N0. 10, pp 693-702, October, 1972.
8. J.P. Giesing, T.P. Kalman, and W.P. Rodden, "Subsonic Unsteady Aerodynamics for General Configurations", Part II, AFFDL-TR-71-5.
9. Defence Standard 00-970, Design and Airworthiness Requirements for Service Aircraft. Issued April 87 - Amdt 5 Chapter 204.5. U.K. Ministry of Defence.
10. Military Specification MIL-A-87221 (USAF) 28 February 1985.
11. Military Specification MIL-A-8861B(AS) (USAF) 7 February 1986.
12. Federal Aviation Reguration- Part 25.
13. Newland, D.E., An introduction to Random Vibrations and Spectral Analysis. Longman, London 1983.

COMPARISON OF STOCHASTIC AND DETERMINISTIC NONLINEAR GUST ANALYSIS METHODS TO MEET CONTINUOUS TURBULENCE CRITERIA

Patrick J. Goggin
Senior Engineer/Scientist
McDonnell Douglas Aerospace - Transport Aircraft
3855 Lakewood Blvd
Long Beach, CA. 90846
United States

Summary

Current continuous turbulence Power Spectral Density (PSD) gust analysis methods are valid only for linear aircraft. In the past, many methods for the analysis of nonlinear aircraft to meet the current PSD gust criteria have been proposed. In this paper, three stochastic simulation based and one deterministic function based method are compared and evaluated for the compliance of nonlinear aircraft to the current continuous turbulence gust criteria. The aircraft configurations analyzed in this paper include a symmetric aircraft model coupled to a nonlinear gust load alleviation (GLA) system and an anti-symmetric aircraft model coupled to a nonlinear yaw damper system. Results from these four nonlinear methods are compared to linear closed and open-loop results as well as currently used linear approximation methods. Computing performance issues are addressed to provide the reader with a complete picture of the trade-off between the analysis accuracy and computing cost.

Nomenclature

Scalars

$\overline{A}_y$	Unit gust root-mean-square value of response y from linear PSD analysis
A, B, C	Constants used in the approximation of the cumulative probability distribution integral for the probability of exceedence criteria
b_1, b_2	Non-storm and storm scale parameters for probability distribution of root-mean-square gust velocity
C_1, C_2	Coefficients for linear regression fit
$h_y(t)$	Impulse response of the first system in Matched Filter Theory
$H_y(i\omega)$	Fourier transform of $h_y(t)$
K	Strength of impulse function used in the nonlinear Matched Filter Theory
k_{MFT}	Matched Filter Theory waveform normalization factor
N_0	Number of zero response crossings
$N(y)$	Number of crossings of response level y
P_1, P_2	Proportion of flight time spent in non-storm and storm turbulence
$P(y > y_d)$	Cumulative probability distribution function for y greater than y_d
$p(y)$	Probability density function for y
T_E	Maximum simulation time
t_0	Time shift for the Matched Filter Theory waveform
U_σ	Design gust velocity $U_\sigma = \eta\sigma_w$
Wg	Input gust time history
$x(t)$	Matched excitation waveform in Matched Filter Theory analysis
$X(i\omega)$	Fourier transform of $x(t)$
y_d	Design value of response y
$y(t)$	Time history of response y in Matched Filter Theory when excited by the matched excitation waveform.
$Y(i\omega)$	Fourier transform of $y(t)$
η	Peak to root-mean-square ratio
ω	Circular frequency (rad/sec)
ψ	Uniform random phase angle from 0 to 2π
$\Phi(\omega)$	Input turbulence power spectral density
σ_w	Root-mean-square gust intensity
σ_y	Root-mean-square value of response y

Subscripts

L	Linear
NL	Nonlinear

Superscripts

*	Complex conjugate

Introduction

All modern aircraft today utilize active control systems of some type during normal everyday operation. These include Yaw Dampers and Stability and Control Augmentation Systems (SCAS). Future aircraft will also include Maneuver Load Alleviation (MLA), Gust Load Alleviation (GLA), and Elastic Mode Suppression (EMS) systems. To properly account for the effects and benefits of such systems, methods which include the systems nonlinear behavior, such as saturation (control surface rate and deflection limitations) and nonlinear aerodynamics, must be used.

Certifying agencies require limit load analysis of the aircraft responding to continuous turbulence (CT) as well as discrete gust events (1-3). When the current continuous turbulence criteria was developed, one of the main assumptions was that the aircraft model was linear. This is demonstrated by the definition of $\overline{A}$ in the requirements as the unit gust root-mean-square (RMS) response level, as well as the specification for U_σ as combination of the RMS design gust intensity and a factor which transforms the response from a RMS to peak value.

On current aircraft programs, because of this linear assumption, gust load analyses are performed in the frequency domain. Typically when design or mission Power Spectral Density (PSD) and 1-cosine discrete gusts are analyzed, the nonlinear effects of the system (such as saturation) are side-stepped by reducing the gain of the control system until the saturation is eliminated. This is a conservative approach which reduces the full benefit of the active control system. Currently also, the effects of nonlinear aerodynamics cannot be properly modeled using frequency domain approaches, but correction factors are instead applied to the linear aerodynamics.

Actual aircraft designs are in fact nonlinear and for some of the new systems introduced on modern day aircraft, they are highly nonlinear. The analysis of these nonlinear systems for the current continuous turbulence criteria requires additional assumptions in order to determine the limit load or response levels. Satisfying the requirements of these certifying agencies when analyzing aircraft with highly nonlinear control systems will include determining the effects of these nonlinearities.

Paper presented at a Workshop on "Aircraft Loads due to Turbulence and their Impact on Design and Certification" held in Lillehammer, Norway on 5 May 1994.

Gould(4), Noback (5), Vinnecombe, Hockenhull and Dudman (6), and Scott, Pototzky, and Perry (7-9) have published procedures to comply with the design envelope requirement for nonlinear aircraft in the current continuous turbulence criteria. Goggin (10) includes some preliminary work performed to correlate stochastic linear and nonlinear time domain limit load results with those from traditional frequency domain PSD gust analyses.

This paper provides a brief overview of the procedures listed above, as well as a comparison of the results from these approaches for a large transport aircraft. Results for a vertical gust case with a nonlinear active gust load alleviation system and a lateral gust case with a nonlinear yaw damper control law will be compared and correlated with the linear results from the traditional frequency domain analyses.

Mathematical Model

Goggin (11) developed an extremely accurate state-space formulation of the flexible aircraft/active control system model. In this formulation, the unsteady aerodynamics are generated using Doublet Lattice theory and Slender Body theory with Interference effects developed by Giesing, Kalman and Rodden (12). The motion dependent aerodynamics are then approximated with a Rational Function Approximation (RFA) developed by Sevart (13) and Roger (14).

The unsteady gust forces are approximated by a RFA that was developed by Dykman (15). This form of RFA was demonstrated to be a much more accurate description of the unsteady gust forces, especially at higher frequencies and for components that are a considerable distance from the gust reference point. This would be true for tail forces on large transport aircraft.

The final equations of motion are formulated in modal coordinates and include the coupling of the flexible aircraft equations and the control law equations of motion. Loads are determined using a summation of force method to combine the inertial forces with the aerodynamic gust and motion induced forces.

Analysis capabilities for nonlinear systems include rate and deflection limitations for control surface deflection degrees of freedom, as well as two types of nonlinear time marching corrections for modifying the linear aerodynamic theory to match steady experimental nonlinear aerodynamic data. For further information on the formulation of the math model, nonlinear capabilities, or correlation of this math model with linear and nonlinear maneuver and 1-cosine gust excitations, see Reference 11.

Average Peak Criteria

Early analyses of nonlinear active control systems (ACS) were performed using what will be called the Average Peak Criteria (APC). This method was initially used by Gould(4) for the evaluation of the nonlinear characteristics of a GLA system on a version of the L-1011 aircraft. This procedure requires the time domain stochastic simulation of the output response quantities to be evaluated for many input root-mean-square (RMS) gust intensities. These response quantities were then processed to determine the average of a given number of peaks and the RMS of the response. Gould showed that the results from using one peak in this analysis and using three peaks produced essentially the same results.

When the peak response quantities are known for all of the responses, the peak-to-RMS ratio η is calculated for each response.

$$\eta = \frac{\text{Peak Response}}{\text{RMS Response}} \tag{1}$$

The peak gust velocity, U_e, for that response is derived from the peak-to-RMS ratio and the simulation RMS gust intensity σ_w.

$$U_e = \eta \sigma_w \tag{2}$$

After processing the results from many simulations using different RMS gust intensities, a table of peak load vs. peak gust intensity is established. This table then provides the design gust response when interpolated from using the design gust velocity.

For the analysis shown here in this paper, a modification of the above method was used due to the asymmetric nature of a spoiler based GLA system. When determining the peak and RMS load for a positive response quantity, only positive bending peaks were used, and only that part of the response time history that was positive was used when calculating the RMS response. Similarly, the negative peaks and negative parts of the time history were used when generating negative response quantities.

Probability of Exceedence Criteria

Noback (5) developed and evaluated another method for determining limit loads from a nonlinear aircraft using the design envelope criterion. In this paper this method will be referred to as the Probability of Exceedence Criteria (PEC). This method also requires a time domain stochastic simulation of the pertinent responses to be evaluated for a number of input RMS gust intensities. Noback suggests the use of three gust intensities which may be considerably less that the APC method. He based the criteria so that the probability of exceeding the design load in the nonlinear system would be the same as the probability of exceeding the design load in a linear system. For a linear Gaussian system, the probability density of the output y of that system is defined as:

$$p(y) = \frac{1}{\sqrt{2\pi}\,\sigma_y} e^{-1/2(y/\sigma_y)^2} \tag{3}$$

Where σ_y is the standard deviation of y.

Substituting $\sigma_y = \overline{A}_y \sigma_w$ and integrating the probability density function above some design load y_d will result in the probability distribution function for a given RMS gust intensity.

$$P(y > y_d, \sigma_w) = \int_{y_d}^{\infty} \frac{1}{\sqrt{2\pi}\,\overline{A}_y \sigma_w} e^{-1/2(y/\overline{A}_y \sigma_w)^2} dy = 0.5\, erfc\left\{ \frac{y_d}{\sqrt{2}\,\overline{A}_y \sigma_w} \right\} \tag{4}$$

This is the probability that a given design load, y_d, will be exceeded in a linear system when excited by a Gaussian input with a standard deviation of σ_w.

Now in the design envelope criteria, only U_e is specified and not σ_w. Noback introduces probability density of turbulence that is used in the mission analysis criteria and was initially developed by Press and Steiner(16).

$$p(\sigma_w) = \frac{P_1}{b_1}\sqrt{\frac{2}{\pi}}\, e^{-1/2(\sigma_w/b_1)^2} + \frac{P_2}{b_2}\sqrt{\frac{2}{\pi}}\, e^{-1/2(\sigma_w/b_2)^2} \tag{5}$$

Where P_1 and P_2 are the proportion of flight time spent in non-storm and storm turbulence and b_1 and b_2 are the non-storm and storm scale parameters in the probability distribution of root-mean-square gust velocity.

Neglecting the non-storm terms of turbulence and combining with Equation 4:

$$P(y > y_d) = \int_0^\infty p(\sigma_w)\, P(y > y_d, \sigma_w)\, d\sigma_w$$
$$= \int_0^\infty p(\sigma_w)\, 0.5\, erfc\left\{ \frac{y_d}{\sqrt{2}\, \bar{A}_y \sigma_w} \right\} d\sigma_w \qquad (6)$$
$$= \frac{P_2}{b_2} \sqrt{\frac{2}{\pi}} \int_0^\infty e^{-1/2(\sigma_w/b_2)^2}\, 0.5\, erfc\left\{ \frac{U_o}{\sqrt{2}\, \sigma_w} \right\} d\sigma_w$$

This is the probability that the design load y_d, for a linear system will be exceeded. Noback proposes that this may be approximated to be within 0.6% using:

$$P(y > y_d) \simeq P_2 \frac{e^{\frac{-U_o}{b_2}}}{\frac{2}{1 + \sqrt{U_o/b_2}} + \sqrt{2\pi U_o/b_2}} \qquad (7)$$

For nonlinear systems, the probability distribution function, $P(y > y_d, \sigma_w)$, is not known and must be determined numerically.

$$P(y > y_d) = \int_0^\infty p(\sigma_w)\, P(y > y_d, \sigma_w)\, d\sigma_w = \int_0^\infty Q(\sigma_w) d\sigma_w \qquad (8)$$

Noback suggests that for an estimate of the design load, y_{est}, the probability distribution function $P(y > y_{est}, \sigma_w)$ is evaluated for 3 input gust intensities. The integrand of Equation 8 is then approximated using the form:

$$Q(\sigma_w) \doteq A e^{-B^2 x^2 - C^2/x^2} \doteq p(\sigma_w)\, P(y > y_{est}, \sigma_w) \qquad (9)$$

and this equation is integrated analytically resulting in:

$$P(y > y_{est}) \doteq \frac{A\sqrt{\pi}}{2B} e^{-2BC} \qquad (10)$$

If this is performed for a few estimates of the design load, the design load can be found by interpolation using the probability of exceeding the design load in a linear system from Equation 7.

Due to the asymmetric nature of some types of aeroservoelastic systems, the probability distribution function is evaluated numerically for both positive and negative estimates of the design response level. For more details on this method see Reference 5.

Threshold Exceedence Count Criteria

Vinnecomb, Hockenhull and Dudman (6) developed another stochastic simulation based method which utilizes normalized exceedence counts as the defining criteria for the limit load level. In this paper this method will be referred to as the Threshold Exceedence Count Criteria (TEC). From Rice (17) the exceedence curve for a Gaussian system can be defined as:

$$N(y) = N_0 \exp\left\{ \frac{-y^2}{2\sigma_y^2} \right\} \qquad (11)$$

At the design load level, the number of exceedences is:

$$N(y_d) = N_0 \exp\left\{ \frac{-U_o^2}{2\sigma_w^2} \right\} \qquad (12)$$

Vinnecombe et. al. propose that for shorter simulations, the output exceedence curves will be biased on the statistics of the input gust time history and that the biasing of a linear reference model and the nonlinear model will be similarly distorted. An estimate of the limit load is then determined for these short simulations as:

$$\frac{N_{NL}(y_{d_{NL}})}{N_{0_{NL}}} = \frac{N_L(\bar{A}_{y_L} U_o)}{N_{0_L}} \qquad (13)$$

Note that if the output response remains Gaussian, then this remains consistent with the previous results derived by Rice in the limit.

$$N_L(\bar{A}_{y_L} U_o) \to N_{0_L} \exp\left\{ \frac{-U_o^2}{2\sigma_w^2} \right\}$$
$$N_{NL}(y_{d_{NL}}) \to N_{0_{NL}} \exp\left\{ \frac{-U_o^2}{2\sigma_w^2} \right\} \qquad (14)$$

In this analysis, a linear regression fit was used to smooth the data between linear and nonlinear reference models. At common normalized exceedence levels, the linear load from the linear reference model and the nonlinear load from the nonlinear model are plotted against each other. This data is then approximated using linear regression. Vinnecombe et. al. found for the type of nonlinearities under evaluation, that the linear regression fit accurately represented the data. As will be shown later in this paper, the linear regression accurately represents the type of nonlinearity used here as well. The form of the fit is:

$$y_{NL} = C_1 y_L + C_2 \qquad (15)$$

Where y_{NL} is the nonlinear load at a given normalized exceedence level and y_L is the linear load at the same normalized exceedence level. Vinnecombe et. al. generally used a peak-to-RMS ratio of 3, but also investigated the effect of other ratios. For more details on this method see Reference 6.

This method might have some advantages over the previous two described. First, if the results from various input gust intensities are very similar, then the nonlinear simulation may need only be performed for one input gust intensity on both the nonlinear and linear reference model. Secondly, if the input gust time history tends to bias the linear reference and nonlinear model similarly, especially near the limit load, then the simulation time might be able to be reduced.

Matched Filter Theory Criteria

Matched Filter Theory (MFT) has been under development during the last decade at NASA Langley for computing maximized and correlated gust loads and responses for both linear and nonlinear aircraft systems (7-9,18-19). For a linear aircraft model, the process behind MFT is shown in Figure 1 and is as follows:

A unit impulse function is used as input to a gust filter modeled after the atmospheric turbulence spectrum. The gust filter used for the results within this paper is documented in Reference 20. This is then used as the excitation of the linear aircraft model. The output will be called the impulse response and is designated by $h_y(t)$. The combination of the gust filter and the aircraft model here will be referred to as the first system.

The impulse response $h_y(t)$ is then normalized by a factor k_{MFT}, reversed, and shifted in time an amount t_0. This scaled, shifted, and reversed impulse response function $x(t)$ is referred to as the matched excitation waveform and is then used as input to the gust filter/aircraft model a second time. The combination of the gust filter and the aircraft model here will be referred to as the second system.

$$x(t) = \frac{1}{k_{MFT}} h_y(t_0 - t) \tag{16}$$

The output from the second system is then designated by $y(t)$. Note that for a linear system, the time response $y(t)$ will reach a maximum at exactly $t = t_0$. This is because for a linear system:

$$y(t) = \frac{1}{2\pi}\int_{-\infty}^{\infty} Y(i\omega)e^{i\omega t}d\omega = \frac{1}{2\pi}\int_{-\infty}^{\infty} X(i\omega)H_y(i\omega)e^{i\omega t}d\omega \tag{17}$$

$$X(i\omega) = \frac{H_y^*(i\omega)}{k_{MFT}} e^{-i\omega t_0} \tag{18}$$

$$y(t) = \frac{1}{2\pi k_{MFT}}\int_{-\infty}^{\infty} H_y(i\omega)H_y^*(i\omega)e^{i\omega(t-t_0)}d\omega \tag{19}$$

Now because this is an even function:

$$y(t) = \frac{1}{2\pi k_{MFT}}\int_{-\infty}^{\infty} H_y(i\omega)H_y^*(i\omega)\cos(\omega(t-t_0))d\omega \tag{20}$$

So the maximum occurs at time $t = t_0$. If k_{MFT} is selected as unity then the maximum of $y(t)$ will occur at t_0 and will be equal to A_y^2/π. The selection of k_{MFT} for the linear analysis is not very important, because for a linear system, the response $y(t)$ will be linearly proportional to the input $x(t)$. For the nonlinear analysis however, the selection of k_{MFT} is crucial.

For the MFT analysis, k_{MFT} is selected so as to create a waveform $x(t)$ that will be of unit energy. Jones (21) shows that this constraint on the input waveform enforces that all of the input waveforms will have an equal probability of occurrence. If k_{MFT} is selected such that:

$$k_{MFT} = \frac{1}{2\pi}\left\{\int_{-\infty}^{\infty} H_y(i\omega)H_y^*(i\omega)d\omega\right\}^{\frac{1}{2}} \tag{21}$$

then for a linear system $y_{max} = y(t_0) = \overline{A}_y$.

For nonlinear systems, Scott et. al. (7-9) has been actively researching methods to optimize the MFT waveform to obtain peak load levels. Two types of nonlinear MFT processes are currently documented in this research. The first type of optimization is what is referred to as the multi-dimensional search. This procedure uses Chebyshev polynomials for the approximation of the input MFT waveform. The coefficients of the polynomials are then used as the design variables in the optimization process with the energy of the MFT waveform constrained to unity. This nonlinear analysis is computationally expensive and will not be addressed further in this paper but the reader is encouraged to look into the references for more details of this procedure.

The second type of optimization is actually more of a trial and error search technique. This technique is referred to as the one-dimensional search method in the references and will be the only nonlinear MFT method documented in this paper. The one-dimensional search method is depicted in Figure 2 and is almost identical to the linear MFT process. The main differences are: 1) the strength of the impulse response in the first system is no longer unity but a variable (K), 2) a loop around the entire linear MFT analysis is created, and 3) in the the first and second systems for this analysis, the aircraft model is nonlinear.

If the nonlinear MFT analysis is executed for many impulse strengths (K), the resulting responses from each of these analyses can be searched through to generate a table of the maximum and minimum responses. Note that for a nonlinear analysis the maximum load y_{max} does not necessarily occur at t_0.

Scott et. al. showed that the results from the one-dimensional search closely approach those of the multi-dimensional optimized results at a fraction of the computing time (7). He recommends the use of the one dimensional search when using the MFT nonlinear analysis method.

Aircraft Model

The model used in this analysis is that of a wide body transport aircraft. This aircraft has 3 engines including one that is mounted in the vertical tail of the aircraft. The aircraft also has both upper and lower winglets. Seventeen elastic and three rigid body modes are used in the gust analyses as well as one rigid mode for each of the control surfaces that are utilized in the active control system. The vibration modes used in the analysis are generated using a beam-stick representation of the aircraft. The Doublet Lattice aerodynamic model of the aircraft is shown in Figure 3. All significant components of the aircraft are included. Wing engines and the tail engine are modeled using "ring wings" and the fuselage is modeled with Slender Body theory. The methods of Images and Interference Bodies are included to account for the wing-body interference. The steady and unsteady aerodynamics are modified to match the experimental values using weighting factors that remain constant with frequency.

The gust load alleviation (GLA) system that is included in the vertical gust analysis utilizes sensors at the center of gravity (CG) of the aircraft as well as accelerometers at the wingtips. The control law drives the outboard ailerons and spoilers. A pitch compensation loop also drives the inboard and outboard elevator to cancel the pitching forces that are generated by the wing control surfaces. The control law model used in this analysis has not been optimized to achieve the greatest reduction in loads but is included instead to provide a comparison of the nonlinear gust analysis methods.

Nonlinearities for the GLA system include aileron and spoiler rate and deflection limitations. The aileron in this GLA analysis is constrained to deflect between $\pm$ 20 degrees while the spoiler control surfaces are limited to 0.0 degrees trailing edge down (TED) and 30.0 degrees trailing edge up (TEU). The rate limitations included in these analyses are slightly more complicated and are not constant. The rate limitations are a function of the load on the actuator of the control surface. For the aileron, the no-load rate is $\pm$ 63.5 deg/sec and the half-load rate is $\pm$ 40.0 deg/sec. The spoiler no-load rate is $\pm$ 95.5 deg/sec and the half-load rate is $\pm$ 66.4 deg/sec. All of the deflection and rate limitations are maintained at the limit load level.

The nonlinear yaw damper model that is included in the lateral gust analysis utilizes roll attitude, lateral acceleration and yaw rate sensors up near the pilot station of the aircraft. This control law model drives the upper rudder control surface only and is typical of a failed yaw damper configuration. The analysis includes rate and deflection limitations similar to those used in the nonlinear GLA analysis. The rudder deflection was limited to $\pm$ 2.5 degrees in this analysis and the rudder rate was limited to $\pm$ 44.5 deg/sec at no-load and $\pm$ 30.0 deg/sec at half-load. As in the symmetric gust analysis, all of the deflection and rate limitations are maintained at the limit load level.

Analyses

The first aircraft configuration that will be examined in this paper is the symmetric case with the GLA active control system. Results will be shown for this case in both the open loop (GLA off) and closed loop (GLA on) configurations.

Unless otherwise noted in this paper, the stochastic simulation results use a maximum simulation time of 2500 seconds, the TEC analysis uses simulations excited by a RMS gust intensity derived from a peak-to-RMS ratio of 3.0, and the APC method uses the average of the highest 5 peaks. The peak gust velocity U_o for this analysis was 112.2 fps and this corresponds to a V_B flight condition within the 85.0 fps design envelope criterion. In the analysis method used here, the wing bending load sign convention is positive wing tip down.

The results from linear stochastic simulations and linear MFT analyses using the mathematical model described above are shown in tabular form for several loads and responses in Table 1. This table lists the differences in the unit gust RMS responses between the traditional linear frequency domain PSD analyses and the linear time domain analyses. As shown in the table, all of the responses for the stochastic simulation methods are within 4.5% and the results from the linear MFT analysis are within 2%.

An illustration of the accuracy of the state-space mathematical model is also shown in the comparison of frequency responses due to a harmonically oscillating one dimensional stationary gust field for two integrated loads and two physical Degree-Of-Freedom (DOF) accelerations. Figure 4 illustrates the frequency response of the wing root bending moment, Figure 5 is the horizontal tail root shear, Figure 6 is the C.G. vertical acceleration, and Figure 7 is the C.G. pitching acceleration. The frequency response data generated from the state-space model is shown with the solid line, and the data from the traditional frequency domain method is shown by the solid circles in these figures. As shown, the mathematical model is extremely accurate throughout the entire frequency range of interest. The higher frequency elastic modes in the analysis are captured with this accurate mathematical model as well as the lower frequency, rigid body and elastic modes.

A couple of representative probability functions that were used in the PEC analysis are shown in the next two figures. Figure 8 illustrates the probability functions for the wing root bending moment in the up-bending direction and Figure 9 shows the down-bending direction. Included in these figures are probability functions for the linear open loop analysis (shown with the X's), the linear closed loop analysis (shown with the triangles), and the results from three nonlinear simulations with different input RMS gust intensities (σ_w = 32.0, 37.4, and 44.9 fps). These figures also include markings that show where the probability functions were evaluated for use in the PEC analysis method. Within the range that these probability functions were used, the functions are smooth. This indicates that 2500 seconds of response time should be an adequate amount to be used in this method.

The next two figures show the corresponding numerically determined values of the integrand of Equation 8 in the PEC analysis method. Figure 10 is the integrand for the wing root up-bending load and Figure 11 is the integrand for the wing root down-bending load. Included in these figures are numerically evaluated values of the integrand for seven input RMS gust intensities as well as a curve representing the approximation of the integrand. The numerically evaluated values of the integrand are shown in these figures by the solid black circles and the approximation of the integrand is shown by the solid continuous line. The formula for the approximation of the integrand is shown by Equation 9. This approximation of the integrand was determined using the numerically evaluated integrand at three of the input RMS gust intensities (σ_w = 32.0, 37.4, and 44.9 fps). The value of b_2 for this symmetric flight condition is 11.25 so this corresponds to σ_w/b_2 values of 2.84, 3.32, and 4.0. The remaining four numerically evaluated points in this figure show that this integrand is properly represented with the use of this approximation.

Intermediate results from the TEC analysis are shown in the next four figures. These figures illustrate the threshold exceedence curves for the same wing root bending load. Figure 12 is for wing root up-bending, and Figure 13 is for wing root down-bending. Once again included in these figures are the linear open loop results (shown by the X's), the linear closed loop results (shown by the triangles) and the results from the same three nonlinear simulations that were described above. Markings are also shown in these figures to illustrate the regions within these curves which correspond to the limit load level. These exceedence curves are not as well behaved as the probability functions that were used earlier. As mentioned earlier, a linear regression fit was used in conjunction with these curves to smooth the exceedence data.

The next two figures illustrate the accuracy of the linear regression fit in smoothing the data from these threshold exceedence curves. Figure 14 illustrates a cross-plot of the wing root up-bending loads at common normalized exceedence levels and Figure 15 illustrates the same data for the wing root down-bending load. These curves were generated using the linear closed loop results and the results from the nonlinear simulation with a peak-to-RMS ratio of 3.0. In these figures, the solid circles represent the numerical results interpolated directly from the threshold exceedence curves. The solid line here represents the linear regression fit of these numerical results. Also shown in these figures are markings to show the area of the cross-plot that is used for the limit load determination. An equation is also included in these figures to represent relationship between the linear and nonlinear load results.

Intermediate results from the MFT analysis are shown next. Figure 16 illustrates the effect of the maximum wing up-bending load with the change in the impulse strength. Figure 17 shows the same information for the wing down-bending moment. In the results shown here for the MFT analysis, 21 impulse strengths were used for the wing up-bending analysis and 9 impulse strengths for the wing down-bending analysis. These impulse strengths were logarithmically spaced as shown by the solid circles in these two figures. Additional impulse strengths were used in the up-bending analysis to be assured that a peak was not overlooked in the one dimensional search process. This concern for accuracy will be discussed further later within this paper.

The next two figures illustrate a comparison of these four nonlinear CF methods and include two linear methods for contrast as well. Figure 18 illustrates the reduction of wing bending moment across the span of the wing for the up-bending loads. Figure 19 includes similar data for the wing down-bending loads. As shown by these figures, the linear closed loop analysis (solid line, no symbols) provides the lowest (unconservative) load levels across the span of the wing for both up and down-bending loads. The linear reduced gain method shown here is the currently used linear approximation method. Simply put, the control law gain is reduced in this method until both the control surface rates and deflections are within the prescribed limits. For the rate limitations at the limit load level, the no-load control surface rates have been used. As we can see in these figures, for this symmetric case, this method results in the highest (most conservative) loads.

The PEC and TEC results are very similar for both the wing up and down-bending loads and are within 3.5% across the span of the wing. The APC method for the wing up-bending

loads is within a couple percent of the PEC method, but for the down-bending loads, the APC method produced loads that are up to 12% lower (less conservative).

The MFT results are up to 5.5% lower than the PEC results for the wing up-bending analysis and up to 3.5% lower for the down-bending analysis. Many points were added to the original nine impulse strengths in the wing up-bending MFT analysis to provide assurance that the critical matched excitation waveform was found. The final number of impulse strengths used was 21. The MFT analysis will always approach the nonlinear limit load from the unconservative side, due to the constraint of the energy of the matched excitation waveform. In the nonlinear MFT one-dimensional search method, there is no guarantee that the critical matched excitation waveform will ever be found. It is believed in the MFT analysis shown here, that the critical matched excitation has not yet been obtained. Further use of another nonlinear MFT procedure such as the multi-dimensional optimization should show that both the wing up and down-bending loads will increase.

The APC method used here resulted in unconservative loads for the wing down-bending moments and further investigation into this behavior was needed. In the APC method, the peak-to-RMS ratio is recalculated for each input gust intensity. For the analysis shown here, the peak-to-RMS ratio for the wing up-bending loads remained fairly constant with changes in the input gust intensity. For the wing down-bending loads this was not the case. In the wing down-bending analysis, the peak-to-RMS ratios increased as the RMS gust intensity increased.

A modification to the APC criteria was included that generated the peak gust velocity U_e from the peak-to-RMS ratio calculated in the linear closed loop analysis. This modification to the APC method can, in certain special circumstances, be identical to the TEC method. The results from this modification are shown for the wing up-bending loads in Figure 20 and for the wing down-bending loads in Figure 21. As shown in these figures, the results from the APC method wing up-bending loads are relatively unchanged. The results from the APC method wing down-bending loads have increased and are now within 1.1% of the loads from the PEC method.

An investigation into the effect of the simulation gust intensity used in the TEC method is illustrated in the following two figures. In these two figures, the TEC method is analyzed using three input gust intensities and is compared to the PEC method. For the up-bending loads of Figure 22, the results from the TEC method with a peak-to-RMS ratio of 3.5 almost exactly matched the results from the PEC method. For the TEC results from the other two peak-to-RMS ratios, the results were about 3-5% higher (more conservative) across the span of the wing For the down-bending loads shown in Figure 23, the results from the TEC method using a peak-to-RMS ratio of 3.0 were almost identical to those from the PEC method. The results from the analyses using the remaining two peak-to-RMS ratios were with $\pm$ 1-2% of the PEC results.

An investigation into the amount of stochastic simulation time needed to obtain reasonable results from the TEC method was also performed. The results of this investigation are shown in the following two figures. In Figure 24, the effect of the maximum simulation time on the wing up-bending loads is illustrated. As shown in this figure, results from the 2500, 2000, and 1500 second simulations provide extremely similar results. When the maximum simulation time is reduced to 100 or 500 seconds, the results diverge and become about 5-6% less conservative.

A similar investigation is shown in Figure 25 for the wing down-bending loads. Once again, for the maximum simulation time of 2500, 2000, and 1500 seconds, the results are indistinguishable. For simulation times of 1000 and 500 seconds, the results also begin to diverge and become slightly less conservative.

The second aircraft configuration that is examined in this paper is an anti-symmetric case with a yaw damper (YD) active control system. Results are shown for this case in the closed loop (YD off) configuration only. Once again, unless otherwise noted in this paper, the stochastic simulation results use a maximum simulation time of 2500 seconds, the TEC analysis uses simulations excited by a RMS gust intensity derived from a peak-to-RMS ratio of 3.0, and the APC method uses the average of the highest 5 peaks. The peak gust velocity U_e for this analysis was also 112.2 fps corresponding to a V_B flight condition within 85.0 fps design envelope criterion.

Figure 26 illustrates a comparison of the four nonlinear CT analyses along with two linear analyses for the vertical tail integrated normal shear forces. Once again, the linear closed loop results are the lowest and most unconservative over most of the vertical tail span. The results from the linear reduced gain method result in integrated loads that are deemed to be the most conservative of the methods shown here. All of the nonlinear methods remain within about 3% across the span of the vertical tail except for the results from the APC method which are 8-12% lower than the other nonlinear methods in the region of the lower vertical tail.

Another investigation into the discrepancy between the APC and the other (TEC,PEC, and MFT) nonlinear CT analyses was performed. It was found, once again, that the peak-to-RMS ratio of the nonlinear simulations increased at the higher gust intensities. The APC method was modified again to use the peak-to-RMS ratio from the linear closed loop analysis and the results are shown in Figure 27. As shown in this figure, this modification to the APC method brought the results in line with the other three nonlinear CT methods.

Figure 28 illustrates the effect of different input RMS gust intensities used in the TEC method on the vertical tail normal shear forces. Figure 29 shows the effect of reducing the amount of simulation time used in the TEC method on the vertical tail normal shear forces. As shown in these two figures, the effect of input RMS gust intensity and simulation time for the anti-symmetric case are minimal within these reasonable bounds.

Computing Performance Issues

One of the major issues when discussing the use of these nonlinear gust analysis methods for use with "real world" problems is that of computing time (and effort) needed to analyze these problems. It is important to point out that for the APC, PEC and TEC methods that the computing time is relatively constant for any number of loads or responses that are evaluated, because the loads and responses can typically be determined at a much coarser time interval than the integration of the equations of motion. For the MFT analysis, the opposite is true. The computing time needed for the MFT analysis is almost linear to the number of output loads or responses that are requested in the analysis. This is because in the MFT analysis, the aircraft model is excited by a series of matched excitation waveforms that are derived from the impulse response functions of each load or response.

Included below is a brief description of the computing time needed to produce the results shown here. This description is not meant to necessarily be conclusive but instead should be used as a tool to show the relative amount of computing time that could be needed for real problems. The amount of simulation time required for the APC method is highly subjective and will not be discussed here.

For the symmetric gust analysis, the analysis included 15 wing load stations. 3 load components were determined at each of these load stations. 7 physical DOF accelerations were also included within this analysis. In the MFT analysis, the wing up-bending load analysis was performed using 21 input impulse strengths and the wing down bending analysis used 9 input impulse strengths. The simulation of the first system in the MFT analysis was performed for 10 seconds using the impulse function and the simulation of the second system was performed for 15 seconds using each of the matched excitation waveforms. When we add up all of the simulation time needed for this analysis we can see that this equals (21+9)*1*10 + (21+9)*(45+7)*15 = 23,700 simulation seconds. The first term in the equation is the amount of simulation time needed in the first system and the second term is the amount of simulation time needed in the second system.

For the PEC method, four simulations were needed. Three of the simulations were needed for the nonlinear analysis of the PEC method and one linear baseline simulation was required to correlate the time domain method to the results from the linear frequency domain methods. The amount of time for the PEC method was 2500 seconds per simulation. Thus the total amount of simulation time required for the PEC method shown here was 10,000 seconds.

For the TEC method, two simulations were needed. One linear baseline and one nonlinear simulation. The results from the TEC method showed that the reasonable results were obtained when simulation times of 1500 to 2500 seconds were used. Thus for the TEC method, the amount of simulation time ranges from 3000 to 5000 seconds.

For the anti-symmetric case shown in this paper, the computing time used for the PEC and TEC analyses was the same as that used in the symmetric analysis. For the MFT analysis, the amount of simulation time was much lower. This was due to the fact that the number of loads and responses under analysis was reduced (7 vertical tail load stations, 3 components of load per station, and 8 physical DOF accelerations), only 11 impulse strengths were used in the one-dimensional search process (instead of 21 and 9 for the symmetric analysis), and also due to the symmetry of this nonlinearity. When we add up the simulation time needed for this analysis we can see that this equals 11*1*10 + 11*(21+8)*15 = 4,895 simulation seconds.

A tabular comparison of the simulation time required for these analyses is shown in Table 2. It is important to note here that the analyses performed for this paper included only a small subset of the loads and responses on the aircraft. Typical production gust analyses will require the analysis of many more responses and the computing time for the MFT analysis will increase accordingly.

Conclusion

The nonlinear continuous turbulence analyses are currently extremely expensive to use. More research is needed into methods that reduce the cost of these analyses. The use of the nonlinear gust analysis methods should only be after performing an exhaustive filtering of the flight conditions using linear methods and approximation techniques.

For the analyses shown here in this paper, the TEC method illustrated a slightly conservative behavior while requiring the least amount of simulation time. It is believed that the PEC method is the most accurate of those shown in this paper but the computing cost of this method is at least double that of the TEC method. Comparisons of the two methods should be performed for a representative condition to be assured of the conservative nature of the TEC method. A sensitivity analysis should also be performed both with gust intensity and amount of simulation time that is required in the TEC method.

Correlated loads are difficult if not impossible to determine using methods based on the TEC and PEC methods. Correlated load conditions may be determined using the MFT analysis methods for a small group of loads or responses. Some scaling of the results from the MFT analyses will need to be performed to eliminate the unconservative nature of the analysis.

References

1. "Federal Aviation Regulations - FAR", Part 25, Airworthiness Standards, Transport Aircraft Category, Department of Transportation, Federal Aviation Administration.
2. "Joint Aviation Requirements - JAR", Part 25, Large Aeroplanes, Joint Airworthiness Authorities.
3. "Military Specification", MIL-A-8861, Airplane Strength and Rigidity Flight Loads.
4. Gould, J. D., "Effect of Active Control System Nonlinearities on the L-1011-3 (ACS) Design Gust Loads", AIAA Paper No. 85-0755, Proceedings of the AIAA/ ASME/ ASCE/ AHS 26th Structures, Structural Dynamics, and Materials Conference, Part 2, pps 468-476, Orlando, FL, April 15-17, 1985.
5. Noback, R., "Definition of P.S.D. - Design Loads for Nonlinear Aircraft", NLR TP 89016 U, Netherlands, 1989.
6. Vinnicombe, G., Hockenhull, M., and Dudman, A. E., "Gust Analysis of an Aircraft with Highly Nonlinear Systems Interaction", Presented to Gust Specialists Meeting, Mobile, Alabama, April 1989.
7. Scott, R. C.,Pototzky, A. S., and Perry, B., "Further Studies Using Matched Filter Theory and Stochastic Simulation for Gust Loads Prediction", AIAA Paper No. 93-1365-CP, Proceedings of the AIAA/ ASME/ ASCE/ AHS 34th Structures, Structural Dynamics, and Materials Conference, Part 1, pps 604-616, LaJolla, CA, April 19-22, 1993.
8. Scott, R. C.,Pototzky, A. S., and Perry, B., "Determining Design Gust Loads for Nonlinear Aircraft -- Similarity Between Methods Based on Matched Filter Theory and Stochastic Simulation", NASA TM 107614, April, 1992.
9. Scott, R. C.,Pototzky, A. S., and Perry, B., "Maximized Gust Loads for a Nonlinear Airplane Using Matched Filter Theory and Constrained Optimization" NASA TM 104138, Sept., 1991.
10. Goggin, P., "Progress at Douglas Aircraft in Nonlinear P.S.D. Gust Analysis", Presented to Gust Specialists Meeting LaJolla, CA, April 1993,
11. Goggin, P., "A General Gust and Maneuver Load Analysis Method to Account for the Effects of Active Control Saturation and Nonlinear Aerodynamics", Presented to Gust Specialists Meeting and AIAA Dynamics Specialists Conference, Dallas, Texas, April 1992, AIAA Paper No. 92-2126.

12. Giesing, J. P., Kalman, T. P., and Rodden, W. P., "Subsonic Unsteady Aerodynamics for General Configurations: Part II, Vol. I, Application of the Doublet Lattice Method and Method of Images To Lifting Surface/Body Interference", Air Force Flight Dynamics Laboratory TR-71-5, 1971.
13. Sevart F. D., "Development of Active Flutter Suppression Wind Tunnel Testing Technology", Air Force Flight Dynamics Laboratory, TR-74-124, Jan. 1975.
14. Roger, K. L., "Airplane Math Modeling Methods for Active Control Design", AGARD-CP-228, August 1977.
15. Dykman, J., "An Approximate Transient Gust Force Derived From Phase Shifted Rational Function Approximations to Doublet Lattice Harmonic Gust Coefficients", MDC92K0283, February 1992.
16. Press, H., and Steiner, R., "An Approach to the Problem of Estimating Severe and Repeated Gust Loads for Missile Operations", NACA TN-4332, Sept. 1958.
17. Rice, S. O., "Mathematical Analysis of Random Noise", Bell System Technical Journal, Vol. XXIII, No. 3, July 1944, pp. 282-332, and Vol. XXIV, No. 1, Jan. 1945, PP. 46 156; also, in Wax, N., Selected papers on Noise and Stochastic Processes, Dover, New York, 1954.
18. Pototzky, A. S., Zeiler, T. A., and Perry, B.,"Maximum Dynamic Responses Using Matched Filter Theory and Random Process Theory", NASA TM 100653, Sept., 1988.
19. Pototzky, A. S., Zeiler, T. A., and Perry, B.,"Calculating Time-Correlated Gust Loads Using Matched Filter and Random Process Theories", Journal of Aircraft, Vol. 28, No. 5, ppgs. 346-352, May, 1991.
20. Hoblit, F. M.,"Gust Loads on Aircraft: Concepts and Applications", Washington, D.C., American Institute of Aeronautics and Astronautics, 1988, (ISBN 0 - 930403 - 45 - 2), pps 169-171.
21. Jones, J. G., "On the Implementation of Power-Spectral Procedures by the Method of Equivalent Deterministic Variables", Part-I Analytical Background, Royal Aircraft Establishment, Farnborough, England, UK, RAE-TM-FS(F) 485, July, 1982.

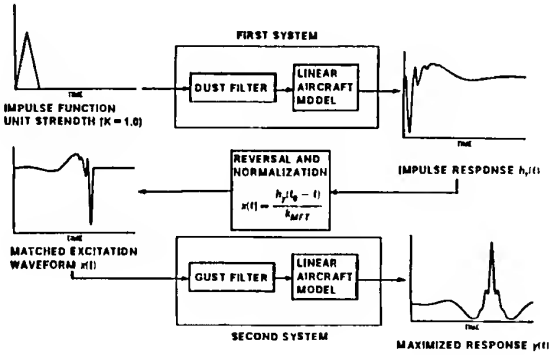

Figure 1. Flowchart of the Linear MFT Process

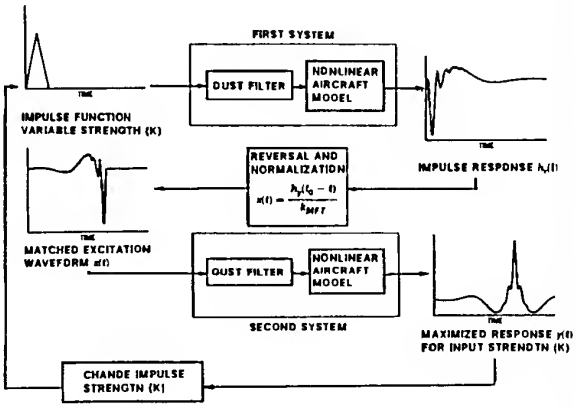

Figure 2. Flowchart of the Non-Linear MFT Process

	Open Loop		Closed Loop	
Response	SS	MFT	SS	MFT
C.G. Vert. Accel.	+4.1%	+0.8%	+4.3%	+1.0%
C.G. Pitch Accel.	+4.1%	+1.1%	+4.1%	+1.7%
Wing Tip Norm Accel	+1.3%	−0.4%	+2.5%	+1.3%
Wing Root Bending	+2.8%	+0.2%	+3.8%	+0.6%
Wing Mid-Span Bending	+2.8%	–	+3.4%	+0.6%
Aft Fuselage Vert Bending	+2.5%	–	+3.9%	+0.5%
Horiz Tail Root Shear	+4.4%	+0.4%	+2.7%	+0.5%

SS and MFT refer to Stochastic Simulation and Matched Filter Theory results respectively.

Table 1. Comparison of Time Domain and Frequency Domain Results

Analysis	Symmetric Case Simulation Time	Anti-Symmetric Case Simulation Time
MFT	23,700 sec.	4,895 sec.
PEC	10,000 sec.	10,000 sec.
TEC	3,000-5,000 sec.	3,000-5,000 sec.

Table 2. Comparison of Simulation Time Needed for Nonlinear Gust Analyses

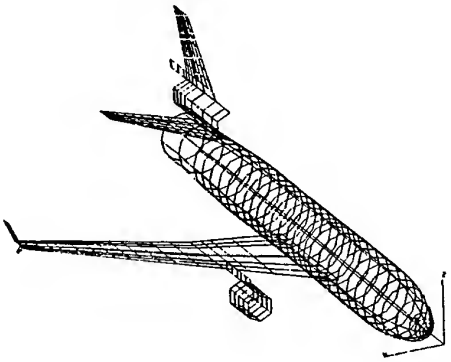

Figure 3. Doublet Lattice Model of a Large Transport Aircraft

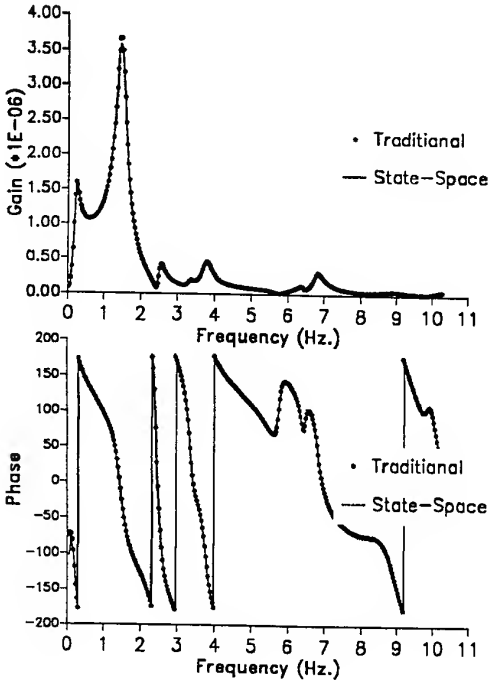

Figure 4. Frequency Response of Wing Root Bending Moment from a Vertical Gust

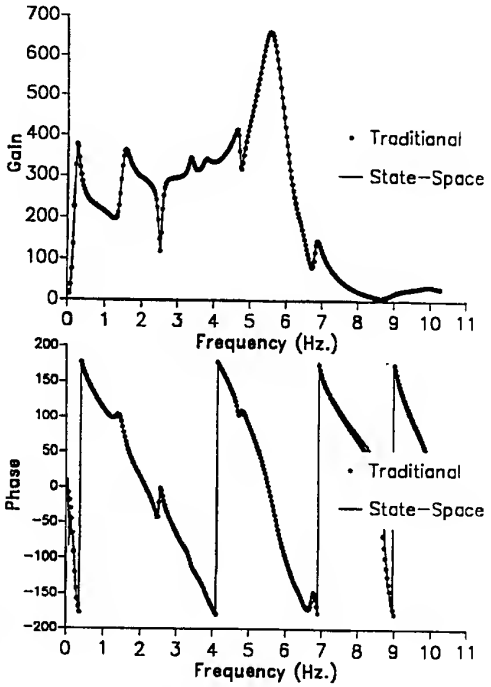

Figure 5. Frequency Response of Horizontal Tail Root Shear from a Vertical Gust

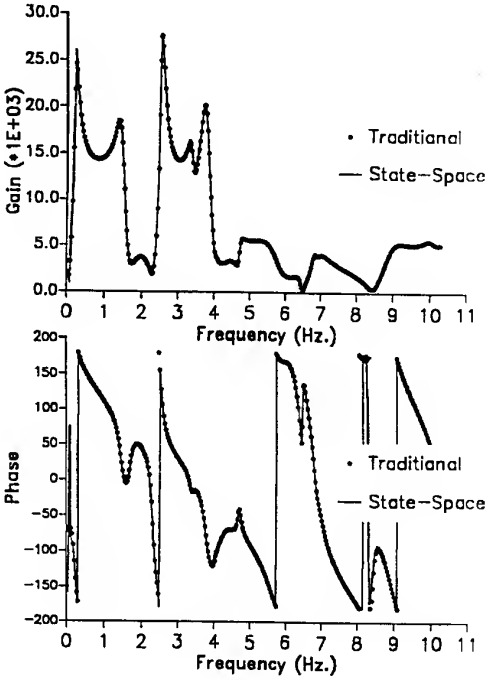

Figure 6. Frequency Response of C.G. Vertical Acceleration from a Vertical Gust

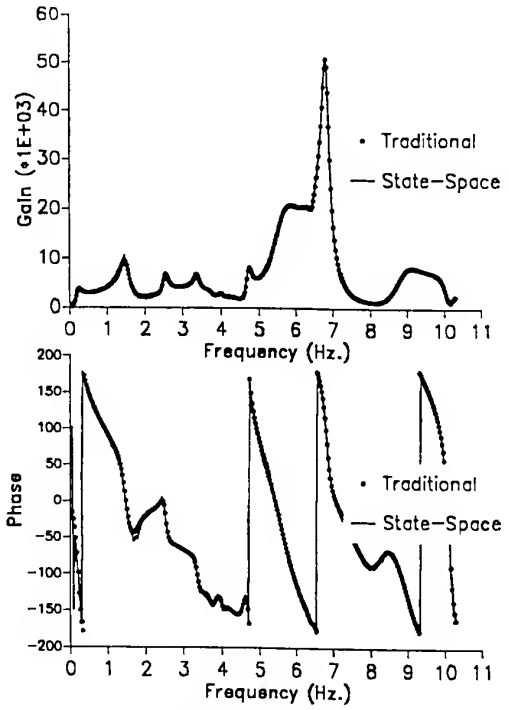

Figure 7. Frequency Response of C.G. Pitching Acceleration from a Vertical Gust

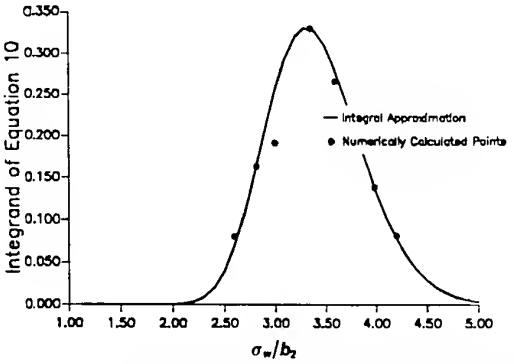

Figure 10. Approximation of the PEC Probability Integral for Wing Root Up-bending

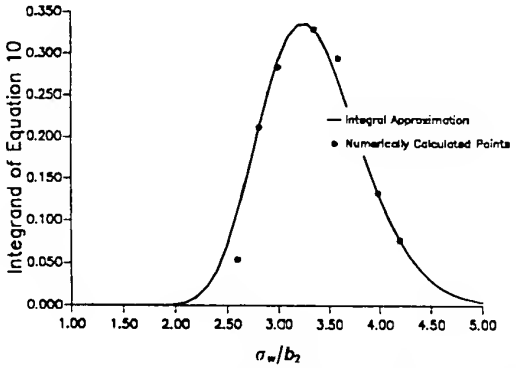

Figure 11. Approximation of the PEC Probability Integral for Wing Root Down-bending

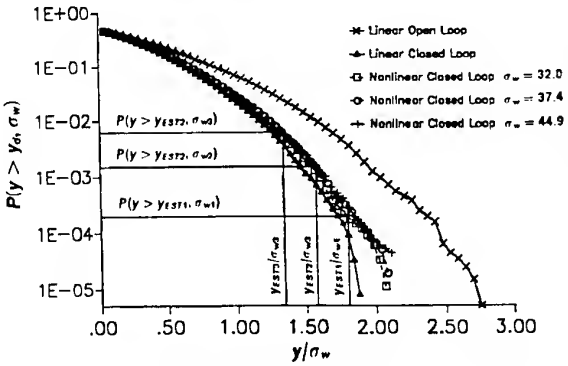

Figure 8. Cumulative Probability Functions for Wing Root Up-bending

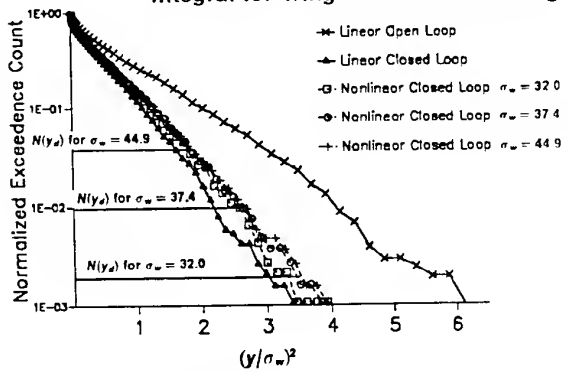

Figure 12. Exceedence Curves for Wing Root Up-Bending

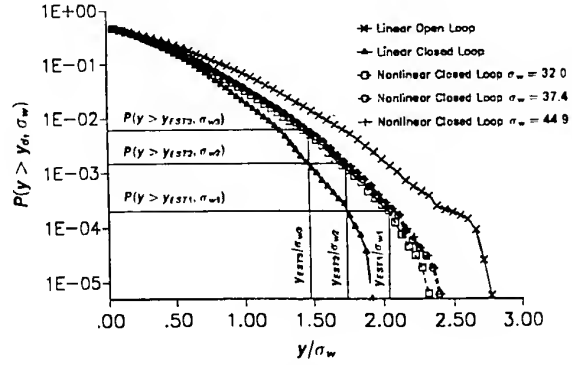

Figure 9. Cumulative Probability Functions for Wing Root Down-bending

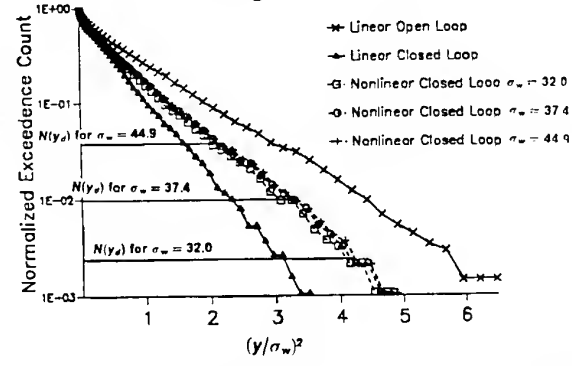

Figure 13. Exceedence Curves for Wing Root Down-Bending

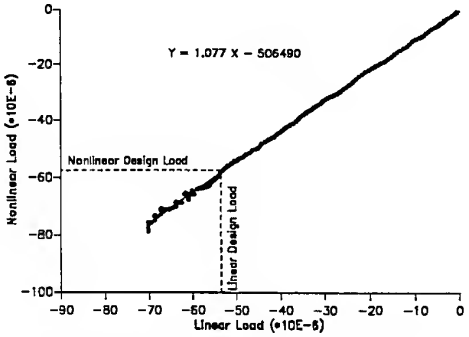

Figure 14. Linear Regression Fit of the Exceedence Data for Wing Root Up-bending

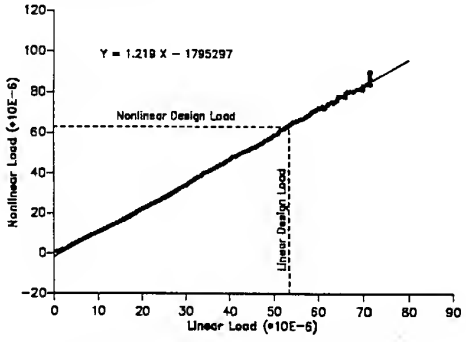

Figure 15. Linear Regression Fit of the Exceedence Data for Wing Root Down-bending

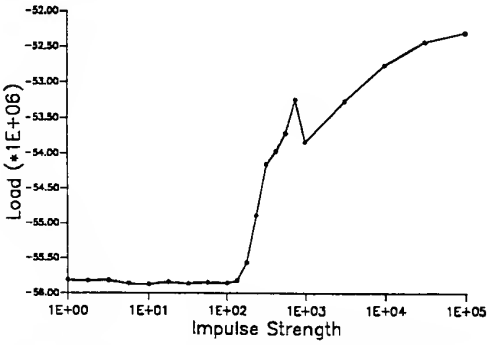

Figure 16. Effect of Impulse Strength on Nonlinear MFT Wing Root Up-Bending Load

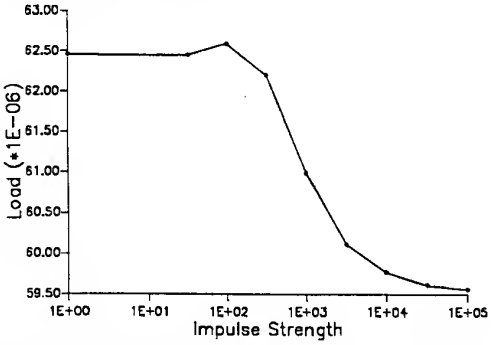

Figure 17. Effect of Impulse Strength on Nonlinear MFT Wing Root Down-Bending Load

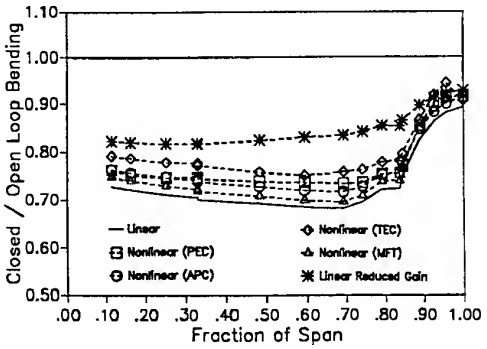

Figure 18. Comparison of Four Nonlinear Gust Analyses for Wing Up-Bending Loads

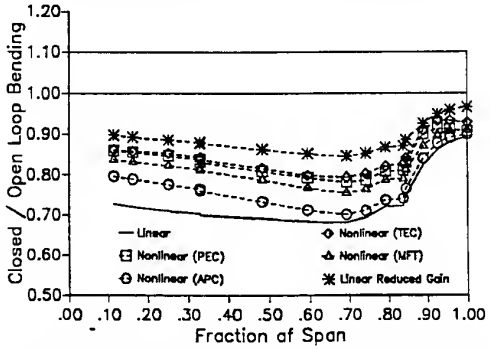

Figure 19. Comparison of Four Nonlinear Gust Analyses for Wing Down-Bending Loads

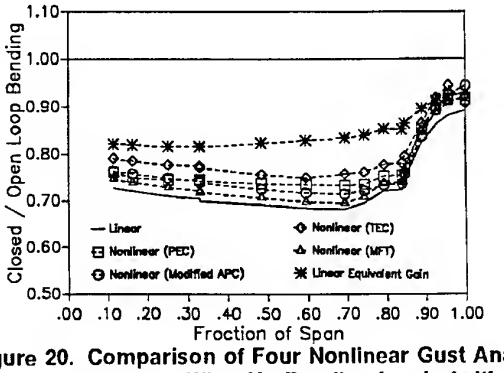

Figure 20. Comparison of Four Nonlinear Gust Analyses for Wing Up-Bending Loads (with Modified APC Method)

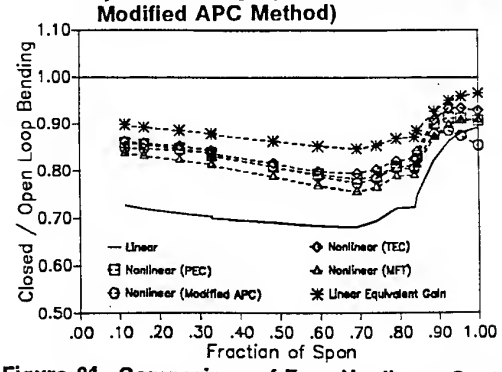

Figure 21. Comparison of Four Nonlinear Gust Analyses for Wing Down-Bending Loads (with Modified APC Method)

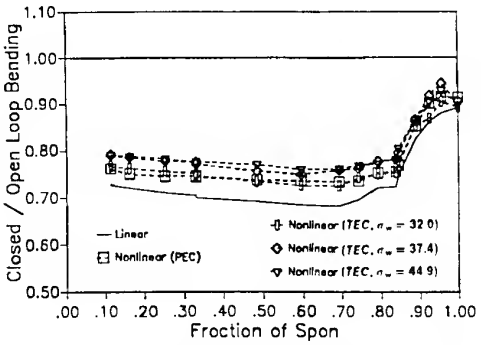

Figure 22. Effect of Input RMS Gust Intensity on TEC Results for Wing Up-Bending

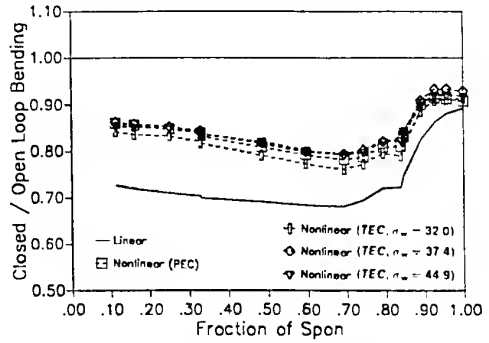

Figure 23. Effect of Input RMS Gust Intensity on TEC Results for Wing Down-Bending

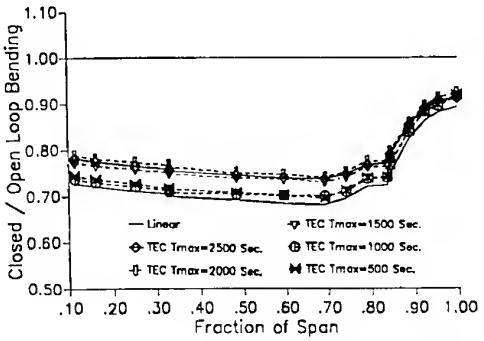

Figure 24. Effect of Simulation Time on TEC Results for Wing Up-Bending

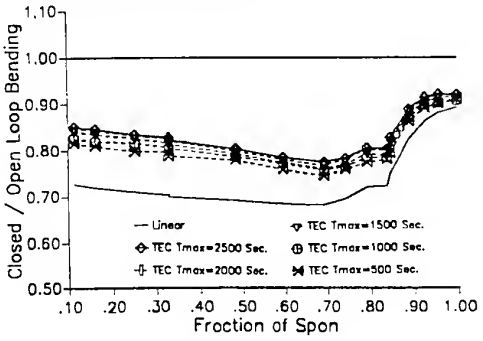

Figure 25. Effect of Simulation Time on TEC Results for Wing Down-Bending

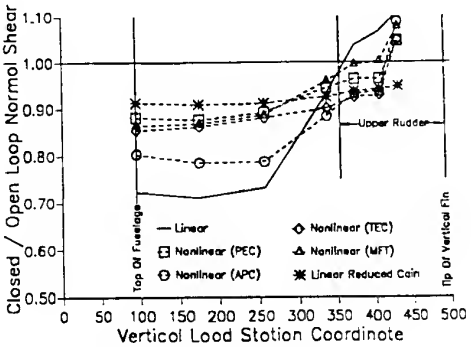

Figure 26. Comparison of Four Nonlinear Gust Analyses for Vertical Tail Shear Forces

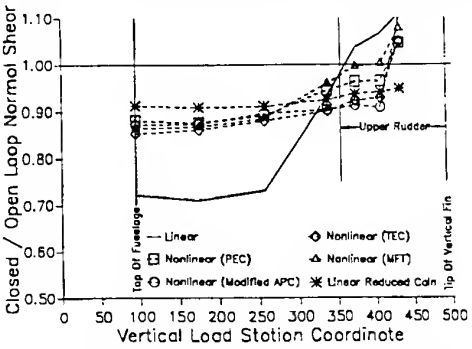

Figure 27. Comparison of Four Nonlinear Gust Analyses for Vertical Tail Shear Forces (with Modified APC Method)

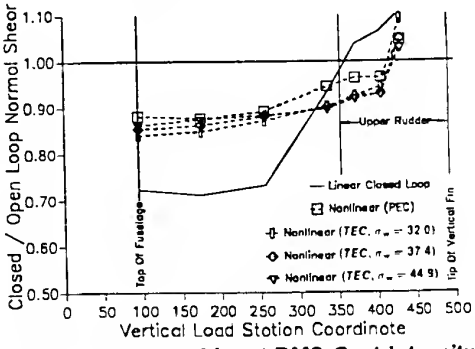

Figure 28. Effect of Input RMS Gust Intensity on Results from TEC Method for Vertical Tail Shear Forces

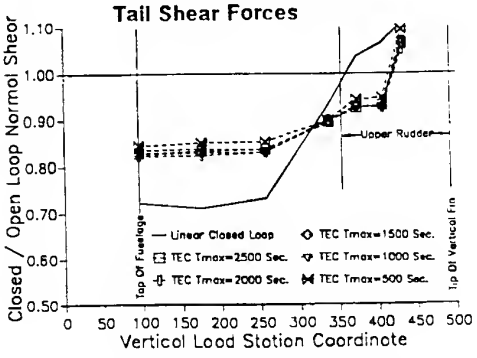

Figure 29. Effect of Simulation Time on Results from TEC Method for Vertical Tail Shear Forces

Design Limit Loads Based Upon Statistical Discrete Gust Methodology

D. L. Hull
Engineering Specialist
Aircraft Structural Integrity, Dept 178
Cessna Aircraft Company
P.O. Box 7704
Wichita, Kansas 67277-7704 USA

1. SUMMARY

Statistical Discrete Gust (SDG) methodology for extreme turbulence provides the basis of a design criterion that accounts for: (1) the statistical nature of design level turbulence; (2) the effects of lightly damped aircraft responses; (3) critical responses that may have significant frequency separation; and (4) the effects of nonlinear control systems. The criterion would eliminate the need for multiple design criteria and could increase the structural efficiency of new aircraft. The increased efficiency would be the result of having equally probable design limit loads for all gust critical components of the aircraft.

2. LIST OF SYMBOLS

$\overline{A}$	Standard deviation
E_i	i^{th} Extreme value of a response
EAS	Equivalent airspeed
F_g	Flight profile alleviation factor
H	Gust development length, ft
P_k	SDG probability factor
RB	Rigid Body
U	Maximum velocity for SDG ramp gusts, ft/sec (TAS)
U_J	Intensity factor for JAR gusts , ft/sec(TAS)/$ft^{1/6}$
U_{ref}	Reference gust velocity, ft/sec (EAS)
U_0	SDG gust intensity factor, ft/sec(TAS)/$ft^{1/6}$ for extreme turbulence ft/sec(TAS)/$ft^{1/3}$ for continuous turbulence
U_σ	Continuous turbulence design intensity, ft/sec
TAS	True airspeed
$\overline{\gamma}$	SDG design amplitude
σ	air density ratio

3. INTRODUCTION

Analyses of a swept wing business jet with fuselage mounted engines has raised questions about existing design gust criteria. Areas have been identified where existing criteria may not provide levels of safety comparable to those for aircraft having frequency response characteristics that differ from those of the business jet. To alleviate this concern a design criterion has been developed based upon the SDG model of extreme turbulence. This development has followed verification of the equivalency of power spectral density (PSD) and SDG results for linear systems in continuous turbulence[1] and the extension of the SDG model to include extreme turbulence[2,3]. This paper concentrates on the results obtained from SDG methodology for a particular aircraft and comparison of the results with those from present criteria. However, a brief discussion of SDG-PSD equivalency is included since the continuous turbulence methodology is directly applicable to extreme turbulence.

3.1 Continuous Turbulence

Present criteria specify use of the von Kármán turbulence spectrum with 2,500 feet as the characteristic scale of turbulence. With this model for PSD analyses and unity for the turbulence intensity in each analysis, the relationship between PSD and SDG results is given by:

$$\overline{\gamma} = 10.4\overline{A} \tag{1}$$

Equation 1 is consistent with units of feet and seconds. Other units of distance will require adjustment of the constant, 10.4. The constant must be adjusted by the cube root of the conversion factor between feet and the desired unit of measure. This relationship has been satisfied to a reasonable degree of accuracy by deleting one assumption included in references 1 and 4. The assumption that a gust profile consisting of either one, two, four, or eight (1-cos) ramp gusts would adequately define the critical profile for a given load or response has been found to be inappropriate. The number of ramps in a critical profile may take on any value, and may even be greater than eight for lightly damped modes.

The basic SDG model represents continuous turbulence as a series of non-overlapping (1-cos) ramp gusts of alternating sign. The maximum velocity for the j^{th} ramp gust is a function of gust intensity, U_0, and the gust development length, H_j.

$$U_j = U_0 \cdot H_j^{1/3} \tag{2}$$

Using this relationship and the principle of superposition for linear systems, aircraft responses are calculated for a family of ramp gusts of varying development length. For each desired load and response the extreme values of alternating sign, E_i, resulting from the family of ramp gusts are identified. The identification of these extreme values requires a peak tracking routine. However, that routine will not be described here since peak tracking can be accomplished by several methods and it is not necessary when using the SDG model of extreme turbulence.

Once the extreme values have been determined, they are selected in descending order of magnitude with alternating sign. The times of occurrence and the gust development lengths associated with each extreme value are retained to form the critical profile and to assure the ramps do not overlap. The design amplitude, $\overline{\gamma}$, for a given load or response is the maximum of the peak responses, γ_k, resulting from profiles consisting of k ramps.

$$\gamma_k = P_k \sum_{i=1}^{k} |E_i| \qquad \text{for k= 1 to n} \tag{3}$$

Paper presented at a Workshop on "Aircraft Loads due to Turbulence and their Impact on Design and Certification" held in Lillehammer, Norway on 5 May 1994.

The probability factors, P_k, take on values of 1.0 for k=1 and $1/(0.88\sqrt{k})$ for k>1. The constant, n, is the number of extreme values retained from the response analyses. The probability factors maintain a constant probability of exceedance for gust patterns consisting of multiple ramps. The design amplitude is then:

$$\bar{\gamma} = \max(\gamma_1, \gamma_2, \gamma_3, \ldots, \gamma_n) \quad (4)$$

Development lengths for the family of gusts must cover a sufficient range to assure finding maximum values of $\bar{\gamma}$ for each of the loads and responses. For vertical gusts a development length range of 30 to 500 feet is usually adequate. Lateral gust analyses may require development lengths greater than 1000 feet to accommodate lightly damped dutch roll modes. Each gust response analysis must extend over a sufficient period of time to provide the necessary number of extreme values for calculation of $\bar{\gamma}$. The duration of each analysis may vary from two to three seconds for vertical gusts; while it may be 15 seconds or more for lateral gust analyses.

Equation 1 is satisfied within two percent when unit values of U_0 and U_σ are used and gust development lengths are chosen such that the gust velocity increases approximately two percent for each succeeding ramp gust in the SDG analysis. Thus the validity of SDG methodology for linear systems in continuous turbulence has been verified.

Verification of the equivalency between SDG and PSD analyses of linear systems in continuous turbulence and the extension of the SDG model to extreme turbulence has led to a practical means of predicting aircraft limit loads reflecting the statistical nature of design level atmospheric turbulence.

3.2 Extreme Turbulence

Extension of the SDG model to extreme turbulence requires an alternate power law for the maximum gust velocity and a set of probability factors that reflect the intermittent nature of the turbulence. For extreme turbulence the relationship between the maximum gust velocity and development length for the j^{th} ramp gust is given by:

$$U_j = U_0 \cdot H_j^{1/6} \quad (5)$$

At present, provisional values (obtained from J .G. Jones, DRA Farnborough) are being used for the factors that maintain a constant probability of exceedance for multiple ramp profiles. The values for P_1, P_2 and P_3 are 1.0, 0.75 and 0.48, respectively. The number of ramp gusts forming a critical profile is restricted to either one or two; since

$$0.75\sum_{i=1}^{2}|E_i| > 0.48\sum_{i=1}^{3}|E_i| \quad (6)$$

for the worst case, $E_1=E_2=E_3$. This restriction to the gust shape leads to simplification of the SDG methodology described above for continuous turbulence. A maximum of two extreme values is required to define critical gust profiles and these values must be of opposite sign to satisfy the requirement for ramp gusts of alternating sign. Thus, overall maximum and minimum values from the complete family of gusts analyzed are all that are required. This eliminates the need for peak tracking routines and reduces the magnitude of the computations for SDG gust analyses to a level similar to that required for the JAR 25.341, Amendment 91/1 discrete gust. Computation time is increased slightly for lateral gust analyses to accommodate the dutch roll response of the aircraft. Details of SDG methodology for extreme turbulence are outlined in the Appendix. The following discussion of gust load analyses based upon present discrete gust and continuous turbulence criteria and a SDG criterion illustrates the benefits provided by a statistical model of extreme turbulence.

4. DISCUSSION

Gust load analyses using continuous turbulence methods (either SDG or PSD) maximize contributions to structural loads from rigid body and elastic responses of the aircraft. However, there are two undesirable characteristics resulting from using a model of continuous turbulence for design limit loads. First, for relatively high frequency responses that are critical for short gust development lengths, the design values for U_σ yield gust velocities that are much lower than what is required to represent design levels of extreme turbulence. Again, it is the extreme turbulence that has the potential to cause structural overload and failure. Secondly, for lightly damped low frequency responses that are critical for long gust development lengths the continuous turbulence model yields extremely high gust velocities for design values of U_σ. The combination of light damping and high gust velocities yield exaggerated values for limit loads.

Scaling the continuous turbulence model to design levels does not account for changes in the nature of turbulence with increasing intensity. Incremental gust velocities associated with the continuous turbulence model increase rather slowly with increasing development length ($H^{1/3}$ power law). On the other hand, velocities associated with extreme turbulence increase rapidly at short development lengths but at a much lower rate for longer development lengths ($H^{1/6}$ power law). Unless the character of extreme turbulence is accounted for, gust induced limit loads will not have equal probability of exceedance.

Results presented in this section are based upon gust loads analyses of a swept wing business jet with fuselage mounted engines. Two other aircraft (a straight wing business jet and a transport with four wing-mounted engines) have been analyzed. When the differing response characteristics are taken into consideration, SDG analysis results for those aircraft are consistent with the results presented below. Analyses are based upon JAR 25.341 Amendment 91/1 discrete gust and FAR Part 25 Appendix G continuous turbulence requirements, and a SDG model with the gust intensity factor derived from U_{ref}, the JAR 25.341 reference gust velocity. SDG modeling provides a statistical representation of the turbulence that caused the extreme events from which values of U_{ref} were derived. The SDG extreme turbulence model is applied for design speeds V_B, V_C and V_D, with the gust intensity reduced 50 percent for speed V_D. Pending further study, design speed V_B is retained to assure that the effects of very lightly damped rigid body modes are taken into account. However, the design gust intensity is unchanged from that for speed V_C. This will be discussed further in the paragraphs on loads due to lateral turbulence.

Design gust intensities for discrete gust loads analyses are compared in terms of gust intensity factors U_0 and U_J for the

SDG and JAR discrete gusts, respectively. The factors are defined in terms of true airspeed by:

$$U_0 = U_{ref} / 350^{1/6} / \sqrt{\sigma} \quad (7)$$

and

$$U_J = F_g \cdot U_{ref} / 350^{1/6} / \sqrt{\sigma} \quad (8)$$

The design gust intensity factors are illustrated in Figure 1 with the probability factors applied to the SDG intensities. Even though intensities for JAR gusts are greater than those for the two-ramp SDG profile, the resulting loads are consistently greater for the SDG method. The shape of the two-ramp SDG profile has a significant influence on the magnitude of the gust induced structural loads. The altitude variation of design gust intensities for the two discrete gust models also contributes to the differences in the design limit loads presented in the following paragraphs.

Comparison of design level extreme and continuous turbulence is facilitated by using SDG models for both types of turbulence. Gust intensity factors equivalent to the design values of U_σ for continuous turbulence PSD analyses are given by:

$$U_0 = U_\sigma / 10.4 \quad (9)$$

The gust intensity factors for extreme and continuous turbulence have different units. Therefore, the following comparisons will be in terms of true gust velocity. Present design level velocities for continuous turbulence and those selected for use with the SDG extreme turbulence model are compared in Figure 2. The design gust velocities are for single ramp gusts having development lengths of 350 feet. The variation of design velocities with altitude illustrated in Figure 2 is a major contributor to differences in limit loads resulting from SDG extreme and continuous turbulence models.

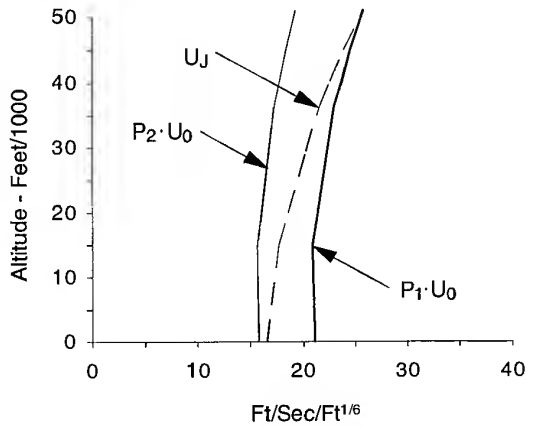

Figure 1 Design Gust Intensity Factors for Discrete Gust Analyses

For vertical turbulence, an upper limit for critical ramp lengths is approximately 350 feet. For lateral turbulence critical ramp lengths tend to be somewhat greater and may exceed 1000 feet for both extreme turbulence and continuous turbulence. The actual critical development lengths will depend upon the amount of damping present in the dutch roll mode. For a development length of 1000 feet, extreme turbulence maximum gust velocities are 19 percent greater than those shown in Figure 2; while for continuous turbulence maximum velocities are 42 percent greater than those shown. The long gust development lengths for continuous turbulence, the associated high gust velocities and light damping of the dutch roll mode yield very conservative limit loads for components such as the aft fuselage and vertical fin. Representative loads for the wing and horizontal stabilizer due to vertical turbulence and vertical fin loads due to lateral turbulence are compared in the following paragraphs.

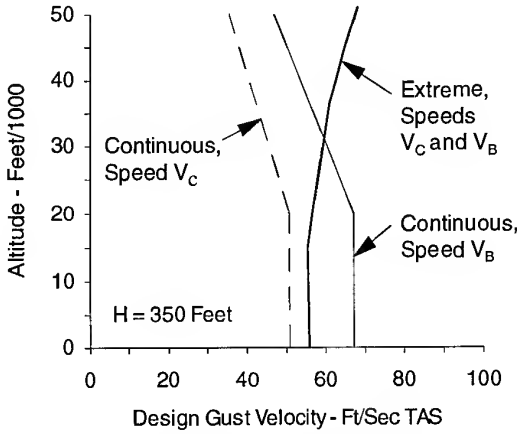

Figure 2 Example Design Gust Velocities for Extreme and Continuous Turbulence

4.1 Vertical Turbulence

Discrete gust analyses yield maximum positive wing bending (wing tips up) for flight at maximum dynamic pressure and maximum mach for speed V_C. For this flight condition, SDG methodology was used for continuous turbulence analyses. This provides results in a form comparable to those from discrete gust analyses. Critical gust profiles for this flight condition are shown in Figure 3 for the two discrete gust models and for continuous turbulence. The same maximum gust velocity was chosen for the continuous turbulence analysis as that for the SDG extreme turbulence analysis. This provides a direct comparison of the two analyses without introducing variations due to criteria. Using the same maximum gust velocity for both analyses serves to illustrate the similarities and difference between the two models.

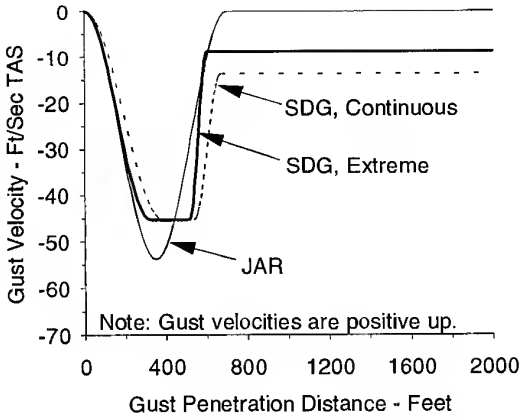

Figure 3 Critical Gust Profiles for Wing Root Vertical Bending Moment, Positive Tip Up

It can be seen from Figure 3 that critical SDG profiles for continuous turbulence and extreme turbulence have similar shapes. Each profile begins with a relatively long ramp and ends with a shorter ramp. The long initial ramp and the overall duration of the gust provide maximum excitation of the short period mode; while the shorter ramp provides maximum excitation of the elastic modes. Gust velocity envelopes corresponding to these profiles are illustrated in Figure 4.

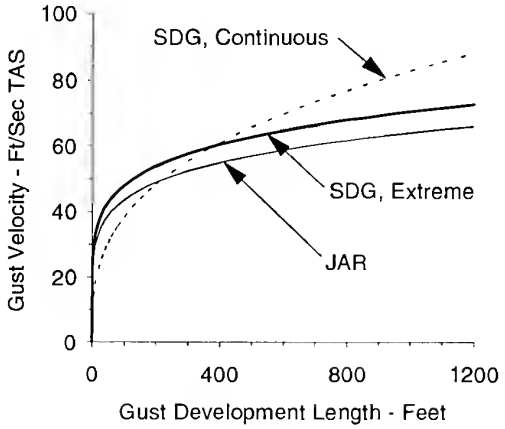

Figure 4 Gust Velocity Envelopes at the Altitude for Critical Discrete Gust Loads

Wing root bending moments due to the critical SDG profiles are illustrated in Figure 5. The variation of the bending moment with gust penetration distance illustrates the differences between the extreme and continuous turbulence models. Compared to the extreme turbulence results the continuous turbulence model produces lower bending moment contributions from both the short period mode and the elastic modes. The loads from the extreme turbulence analysis are 14 percent greater than those from the continuous turbulence analysis. This, even though the maximum gust velocities are the same. The continuous turbulence intensity in this example corresponds to a U_σ value of 86.2 ft/sec (which is 27 percent greater than that required for design speed V_C by FAR Part 25 Appendix G).

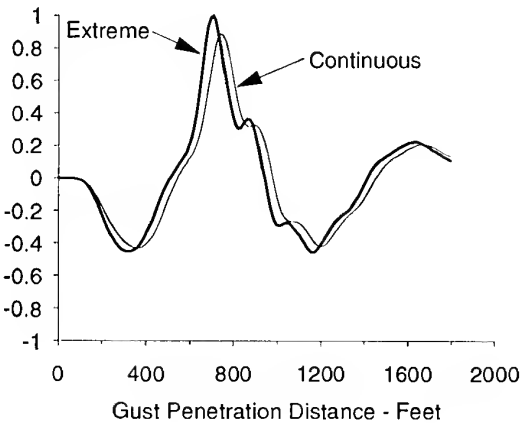

Figure 5 Normalized Incremental Wing Bending Moment Due to Critical SDG Profiles

The bending moments shown in Figure 6 for the JAR analysis show no elastic mode contribution resulting from the profile yielding the maximum bending moment. This is due to the significant separation between the frequencies of the elastic modes and the rigid body short period mode. The bending moment response for the maximum contribution from the elastic modes yields only 91 percent of the moment resulting from the critical JAR profile. SDG methodology, on the other hand, maximizes the contributions of both rigid body and elastic modes of the aircraft. As a result the maximum bending moment from the SDG analysis is 16 percent greater than that from the JAR analysis. The SDG loads are greater even though the JAR gust velocity is 19 percent greater than that for the SDG analysis. These results illustrate the importance of gust shape in the determination of design limit loads.

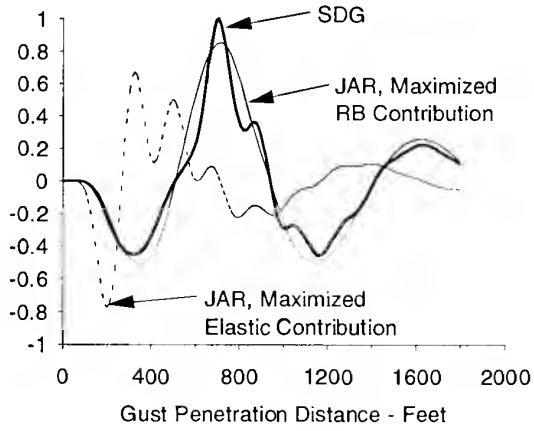

Figure 6 Normalized Incremental Wing Bending Moment Due to SDG and JAR Discrete Gust Profiles

For aircraft with lower frequency wing bending modes the JAR profile may yield significant elastic contribution to critical incremental loads. For example, JAR analyses yielded ineremental wing bending moments for the four-engine transport that were slightly greater than those from the SDG analysis. However, the maximum velocity for the JAR gust was approximately 20 percent greater than that for the SDG critical profile. The JAR profile will usually yield wing bending moments greater than those from the SDG extreme turbulence model only if the maximum gust velocity is significantly greater than the velocity for the two-ramp SDG profile. However, depending upon the response characteristics of particular aircraft, some wing bending moments are critical for a one-ramp SDG profile. In that case the velocity for the SDG profile will generally be greater than that for the JAR profile.

4.1.1 Design Limit Loads

Normalized design limit loads at the root of the wing and horizontal stabilizer are shown in Figures 7 through 10 for the three analysis methods. All loads have been normalized by the results from SDG analyses. The majority of the SDG loads due to vertical gusts are greater than those from JAR and PSD analyses. Exceptions to this occur because the design levels of turbulence for the three turbulence models vary significantly with altitude. Because of these altitude variations, the JAR and PSD results for torsion, shown in Figure 7, exceed those from the SDG analysis. The critical value of tor-

sion from the JAR analyses occurs at high altitude where the maximum gust velocity is much greater than that for the critical two-component SDG profile. The critical positive torsion from PSD analyses occurs at low altitude and speed V_B where, according to FAR Part 25 Appendix G, U_σ has a value of 99 ft/sec.

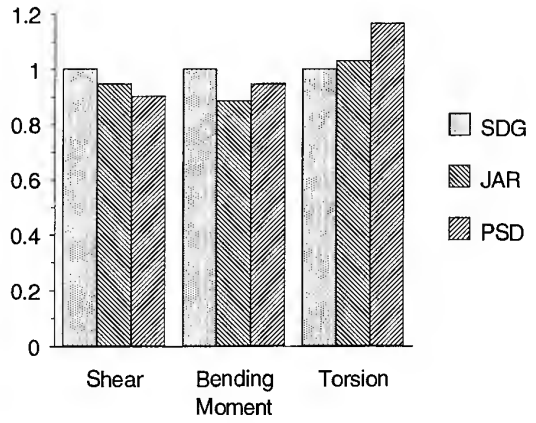

Figure 7 Normalized Positive Wing Root Limit Loads Due to Vertical Turbulence

The negative wing loads shown in Figure 8 are also influenced by the distribution of design gust intensities versus altitude. Down loading on the wing tends to be critical for light weight configurations flying at maximum dynamic pressure (sea level and design speed V_C). The SDG gust intensity decreases very little at low altitude as can be seen in Figure 1. However, at low altitude, the JAR gust velocities are reduced significantly by the flight profile alleviation factor. For this particular aircraft, down loading of the wing due to the SDG extreme turbulence model tends to be critical for single-ramp gusts. As can be seen from the data in Figure 1, SDG intensities for single-ramp profiles are greater than the JAR intensities at all altitudes. At low altitude the JAR design gust intensities are relatively low which causes down loading of the wing to become critical at a higher altitude. Because of the critical single-ramp SDG profile and the low JAR gust intensities at the lower altitudes, JAR loads are somewhat less than those from SDG analyses. The light weight configurations have minimum fuel in the wing. The reduced mass yields increased frequencies for the elastic modes. PSD loads are reduced because of these increased frequencies. The reduced critical gust development lengths associated with the increased frequencies yield relatively low design gust velocities .

The negative horizontal stabilizer loads (downward loading) illustrated in Figure 9 follow the same trend as the positive wing loads. Here again the torsional moments from the JAR analysis exceed the SDG results. The critical condition for JAR torsion is at high altitude, where the JAR gust velocity is as much as 33 percent greater than that for the critical two-ramp SDG profile. PSD loads are relatively low because of the relatively high frequencies of the elastic modes.

The variation of steady-state balancing tail loads with flight condition has a significant influence on the positive (upward loading) horizontal stabilizer loads illustrated in Figure 10. In this case the net load represents the difference between steady-state and incremental loads. The JAR loads are critical for higher altitudes where the gust intensities are greater, while the SDG and PSD loads are critical for lower altitudes.

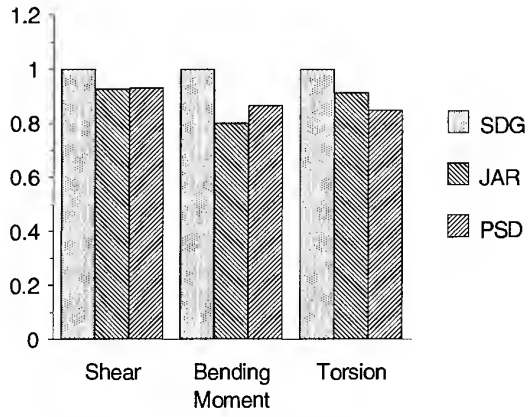

Figure 8 Normalized Negative Wing Root Limit Loads Due to Vertical Turbulence

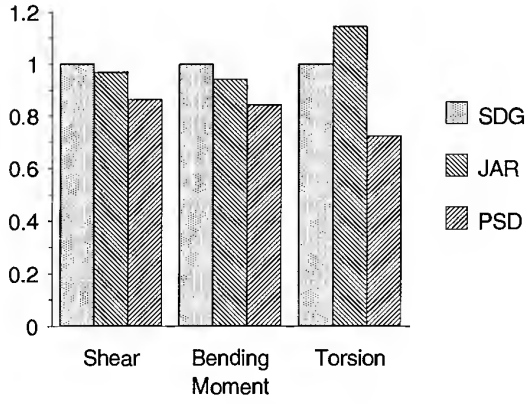

Figure 9 Normalized Negative Horizontal Stabilizer Root Limit Loads Due to Vertical Turbulence

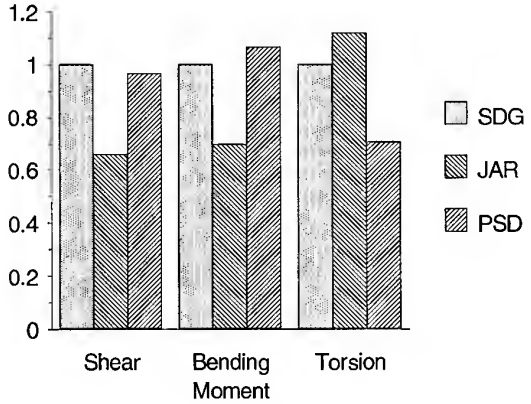

Figure 10 Normalized Positive Horizontal Stabilizer Root Limit Loads Due to Vertical Turbulence

4.2 Lateral Turbulence

SDG continuous turbulence analyses were performed for vertical fin lateral bending moment to provide data comparable to extreme turbulence results. The critical condition for bending moment at the root of the vertical fin due to continuous turbulence is at low altitude and design speed V_B. Typical critical profiles for the two types of turbulence are illustrated in Figure 11. The continuous turbulence profile is made up of six ramps having development lengths of 1,363 feet and one ramp with a length of 912 feet. On the basis of a U_σ value of 99 ft/sec the maximum gust velocity for the longer ramp is 105 ft/sec and 92 ft/sec for the short ramp. For a gust profile consisting of seven ramps, the probability factor, P_7, reduces the maximum incremental velocities to 45 and 40 ft/sec respectively, for the long and short ramps. In contrast, the extreme turbulence critical profile is formed from one ramp with a development length of 997 feet, followed by a second ramp with a length of 89 feet. The maximum velocity associated with this profile is 53 feet per second.

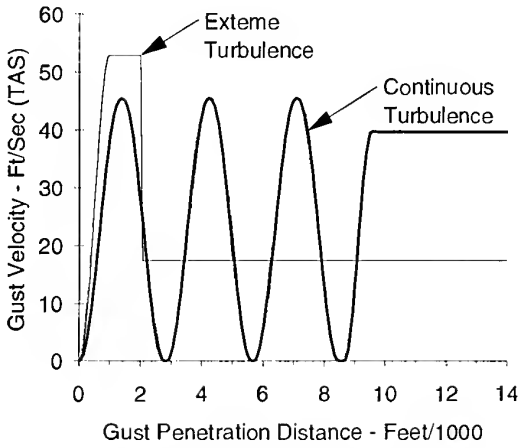

Figure 11 Typical SDG Critical Profiles for Fin Lateral Bending Moment

The bending moments resulting from the critical profiles are illustrated in Figure 12. For continuous turbulence, maximum bending moment occurs at a distance of 9,528 feet into the gust pattern. The long development lengths in the critical continuous turbulence profile cause the critical bending moments to be entirely due to rigid body response characteristics of the aircraft. In contrast, the extreme turbulence profile provides excitation of both the elastic modes and rigid body modes. The maximum bending moment for extreme turbulence occurs at a gust penetration distance of 2,213 feet, compared to the distance of 9,528 feet for the critical continuous turbulence profile. The JAR gust was not included in this comparison because the maximum development length of 350 feet fails to provide significant excitation of the dutch roll mode.

Considering the bending moment data for the wing (Figure 5) and the vertical fin data in Figure 12; the question must be raised as to whether or not gust loads analyses based on a model of continuous turbulence should be required for design limit loads. While the continuous turbulence model (at intensity levels well below those being used for design limit loads) is appropriate for defining fatigue loads, it clearly does not represent the nature of the extreme turbulence that is likely to cause structural overload and failure.

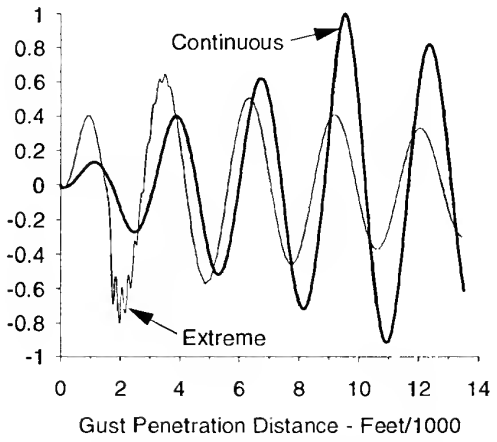

Figure 12 Normalized Vertical Fin Lateral Bending Moment Due to Critical SDG Profiles

4.2.1 Design Limit Loads

The normalized design limit loads in Figure 13 for the vertical fin illustrate the influence of a lightly damped dutch roll mode on design limit loads. The SDG model of extreme turbulence accommodates the light damping of the dutch roll mode by virtue of the variable gust shape. Vertical fin design limit loads from the extreme turbulence analyses have the same probability of exceedance as those for the other aircraft components. The results from PSD analyses illustrate the effects of complex gust profiles and the large values of U_σ at low altitude (99 ft/sec for design speed V_B). The continuous turbulence intensity level for design speed V_B is 32 percent greater than that for speed V_C. If this increased intensity was eliminated for speed V_B, the difference between the SDG and PSD limit loads in Figure 12 would be reduced significantly. Elimination of the increased intensity for speed V_B does not imply the elimination of speed V_B as a design condition. Very lightly damped rigid body modes may cause critical loads at speeds lower than V_C. This is an area that should receive additional study before considering the elimination of speed V_B as a design condition.

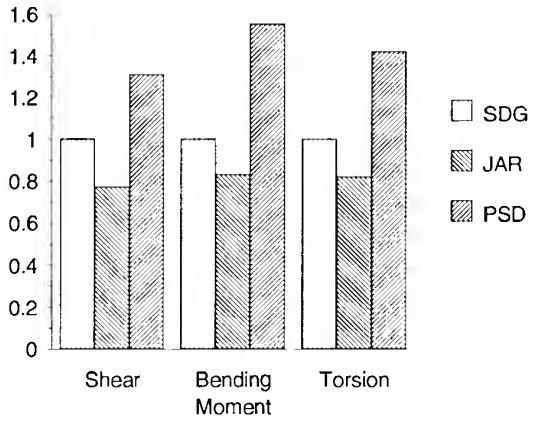

Figure 13 Normalized Fin Root Limit Loads Due to Lateral Turbulence

4.3 Design Gust Intensity

The gust intensity factors used with the SDG model of extreme turbulence were derived from, U_{ref}, the reference gust velocity of JAR 25.341 Amendment 91/1. The reference gust velocity was derived from an accumulation of extreme event data collected during normal commercial airline operations. This derivation included the design cruise speeds of aircraft that normally cruise in various altitude bands. The use of these design cruise speeds causes a deviation from the statistics of the measured data; but results in conservative values for design gust intensities. The limit loads due to SDG extreme turbulence presented in previous sections have been described as having equal probability of exceedance for all components of the aircraft. However, this is true only at any given altitude, since the gust intensity factors were derived from U_{ref}.

Design gust intensity factors would more accurately reflect the statistics of the measured data if the flight speeds and the time spent in a specific altitude range by the data collecting aircraft were used in the derivation. The design values would then reflect the statistics of the recorded events. Thus, the altitude variation of design gust intensities would reflect the statistical nature of extreme turbulence as weighted by normal airline operations.

As stated earlier, the probability factors used with the SDG model of extreme turbulence are provisional. These values should be re-evaluated and revised (if required) for use in an official SDG based design gust criterion.

4.4 Nonlinear systems

The preceding discussion was restricted to procedures and results for analysis of linear systems. The process, however, is readily extended to nonlinear systems. SDG methodology for extreme turbulence is well suited for the development of gust load alleviation systems since it readily accommodates control system nonlinearities. The computational effort increases significantly because the search for worst case loads must span the applicable range of gust development lengths for each of the two possible ramp gusts and the distance between the ramps. However, computational effort can be reduced by combining a systematic (hill-climbing) search for the worst case with an element of randomization so the search will not stop at a local maxima, rather than finding the global maxima[4].

Nonlinear automatic control systems designed to reduce loads induced by extreme (design level) turbulence must also operate satisfactorily in continuous turbulence. Therefore, the effects of any nonlinear systems must be evaluated for appropriate levels of continuous turbulence. SDG methodology for continuous turbulence, used with the search technique described in Reference 4, is a practical means of performing this evaluation.

5. CONCLUSIONS

While existing gust load criteria have yielded satisfactory levels of flight safety, it can be seen from the data presented above that SDG extreme turbulence methodology produces levels of dynamic response that are not provided by either the variable development length (1-cos) discrete gust or continuous turbulence methods. The degree of variation between loads predicted by the three methods is a function of the response characteristics of the individual aircraft. The results presented above may represent an extreme for commercial aircraft because of the relatively wide separation between rigid body and elastic mode frequencies. SDG modeling accommodates this frequency separation and yields equally probable loads for all components of the aircraft. Results from analyses of other aircraft may not show as much variation between methods. However, SDG methodology is the only one of the three analysis methods that produces consistent results for all aircraft. This is the result of maximizing both rigid body and elastic responses due to a statistical model of extreme turbulence, regardless of the frequency response characteristics of a particular aircraft.

A design criterion based upon the SDG model of extreme turbulence has several advantages over the discrete gust and continuous turbulence criteria presently in use. It uses a statistical model of the type of turbulence that is likely to produce structural overload and failure. It is independent of the aircraft configuration. It provides equally probable limit loads, which provide the potential for improved structural efficiency of the aircraft. It would reduce the engineering effort required for certification by eliminating the need for multiple requirements for design limit loads due to turbulence.

The next step in the evolution of criteria for design limit loads due to turbulence should be the acceptance of SDG methodology for extreme turbulence. The process of acceptance should include a review of the design gust intensities and the probability factors that maintain a constant probability of exceedance for critical gust profiles consisting of more than one ramp gust.

6. REFERENCES

1. Jones, J.G., "A Unified Procedure for Meeting Power-Spectral-Density and Statistical Discrete Gust Requirements for Flight in Atmospheric Turbulence," *Proc. AIAA/ASME/ASCE/AHS 27th Structures, Structural Dynamics and Materials Conference* , 1986, pp 646-652.
2. Jones, J.G., et al, "Fractal Properties of Inertial-range Turbulence With Implications for Aircraft Response," *Aeronautical Journal*, October 1988, pp 301-308.
3. Foster G.W. and Jones, J.G., "Analysis of Atmospheric Turbulence Measurements By Spectral and Discrete-gust Methods," *Aeronautical Journal*, May 1989, pp 162- 176.
4. Jones, J.G., "Statistical-Discrete-Gust Method for Predicting Aircraft Loads and Dynamic Response," *Journal of Aircraft*, Vol. 26, No. 4, 1989, pp. 382-392.

APPENDIX

Statistical Discrete Gust Methodology for Design Limit Loads

The SDG model of extreme (design level) turbulence represents equally probable critical gust profiles with one (1-cos) ramp gust or two such gusts of alternating sign. The maximum incremental velocity for a single ramp is a function of the gust intensity factor, U_0, and its development length, H, and is given by:

$$U = U_0 \cdot H^{1/6} \qquad \text{Ft/Sec (TAS)} \qquad \text{(A-1)}$$

For the present, a definition for the gust intensity factor based on the reference gust velocity of JAR 25.341, Amendment 91/1 is suggested.

$$U_0 = U_{ref} / 350^{1/6} / \sqrt{\sigma}, \quad \text{Ft/Sec(TAS)/Ft}^{1/6} \qquad \text{(A-2)}$$

The velocity profile for each ramp gust, is given as a function of gust penetration distance, s, the maximum velocity, U, and the gust development length, H.

$$u(s) = \frac{U}{2}\left(1 - \cos\frac{\pi s}{H}\right) \qquad \text{for } 0 < s < H \qquad \text{(A-3)}$$

and

$$u(s) = U \qquad \text{for } s \geq H \qquad \text{(A-4)}$$

To maintain a constant probability of exceedance for the more complex two-ramp critical profiles, a probability factor, P_2, is applied to the incremental velocities. A provisional value of 0.75 is currently being used for P_2.

For the general case, worst case loads for extreme turbulence are determined by varying the development length for a single ramp profile and the development lengths and spacing of ramp gusts of alternating sign in a two-ramp gust profile. Superposition of results from a family of single ramp gust is used to determine worst case loads and responses and the associated critical gust profiles for linear systems. Development lengths for the family of ramp gusts must satisfy two requirements. First, the range of development lengths must be broad enough to assure maximum excitation of both rigid body and elastic modes of the aircraft. Second, the spacing of the development lengths must be sufficiently close to assure finding the required extreme values. The following guidelines are suggested for use in initial analyses. However, the response characteristics of a particular aircraft will dictate the required range and spacing of the development lengths defining the family of gusts.

Minimum development length,	15 feet
Maximum development length,	
vertical gusts	400 feet
lateral gusts	1,200 feet
Incremental development length,	12 %

Response analyses for each member of the family of ramp gusts will yield maximum and minimum values of opposite sign for desired loads and responses. Since the most complex SDG extreme turbulence profile consists of two ramp gusts of alternating sign; only the overall maximum and minimum extreme values (E_1 and E_2) are required to define worst case loads and responses. The design amplitude, $\bar{\gamma}$, for a given load or response is the maximum of the peak values, γ_k, resulting from one and two ramp critical profiles.

$$\gamma_k = P_k \sum_{i=1}^{k} |E_i| \qquad \text{for } k=1,2 \qquad \text{(A-5)}$$

P_1 and P_2 have values of 1.0 and 0.75, respectively. The design amplitude is then;

$$\bar{\gamma} = \max(\gamma_1, \gamma_2) \qquad \text{(A-6)}$$

Associated with the extreme values, E_1 and E_2, values are gust development lengths, H_1 and H_2, and times of occurrence, T_1 and T_2. These times and development lengths are used to define critical profiles and (if desired) determined if any overlapping of ramps in a two-ramp profile has occurred. Critical two-ramp profiles are defined by superimposing the ramp gusts with alternating signs such that the extreme values will add to form the worst case value for the load or response. The critical profile begins with the ramp, H_2, causing the second extreme value, E_2, followed at the appropriate time by the ramp, H_1, (with opposite sign) that caused the first extreme value, E_1. The time to start the second ramp, T_s, is given by:

$$T_s = T_2 - T_1 \qquad \text{(A-7)}$$

The possibility of overlapping ramps is checked by comparing the times at which the initial ramp ends, T_i, and the time at which the final ramp begins, T_f. For non-overlapping ramps:

$$T_f - T_i > 0 \qquad \text{(A-8)}$$

Experience has shown that overlap does not occur except when one of the extreme values is the result of inertia loads caused by gust loading on other parts of the aircraft. In the case where local extreme values are the result of local gust loads, overlap has not been observed. However, one case of apparent overlap has been encountered. For a configuration with a highly swept wing and low wing loading the first extreme values of shear and bending moment near the wing tip were due to inertia loads. These inertia loads resulted from the inboard portion of the wing penetrating the gust and generating significant rigid body acceleration before the outboard wing encountered significant gust loading. The result is inertia loads of larger magnitude than the loads associated with dynamic overshoot of loads due to local gust loading. This condition has not been encountered for a critical load case. However, if such loads were present for critical conditions, they would be used in the calculation of $\bar{\gamma}$, because this is a real loading condition. The overlap of gust ramps resulting from this kind of loading is not considered to be a violation of the SDG model because the initial extreme value is not the result of local gust loading.

A REVIEW OF GUST LOAD CALCULATION METHODS AT de HAVILLAND

John Glaser

de Havilland Inc., 123 Garratt Blvd., Downsview
Ontario, CANADA, M3K 1Y5

SUMMARY

The development of an analysis system for the routine calculation of gust response loads is reviewed in some detail in this report. While the system provides adequate design strength margins, a more robust and effective system would reduce user workload, computer costs and analysis time. It is suggested that other analysis systems could benefit similarly, particularly when considering the demands imposed by highly nonlinear aircraft systems, the trend toward full finite element structural dynamic models and the relentless quest for structural efficiency. It is proposed that improvements in analysis systems could evolve from the collective experience in gust loads methodologies acquired within the aeronautical community. To capitalize on that collective experience, it is recommended that a working group of gust load specialists be formed to assemble and evaluate current and promising methods for calculating gust loads and to recommend standardized airplane test cases, both rigid and elastic, for validating analysis methods and results.

1 INTRODUCTION

This paper is not about the modeling of atmospheric turbulence or the modeling of aircraft structures; these matters, although extremely important, have been and will continue to be investigated by such bodies as the AGARD Structures and Materials Panel (SMP), the FAA-hosted Gust Specialists' Meetings, the AIAA/ ASME/ASCE/AHS/ASC Structures, Structural Dynamics and Materials Conferences, and the International Modal Analysis Conferences (IMAC) to mention a few.

Rather, the purpose of this paper is to focus attention on the methods used for calculating response loads given that models for atmospheric turbulence and the airplane structure have been defined. Loads methods for highly nonlinear aircraft in continuous turbulence fall within this category but will not be discussed here; this problem is currently receiving considerable attention by the FAA-hosted Gust Specialists' meetings and other groups.

Figure 1 provides a flow diagram for the method used at de Havilland. We begin by assuming linearity and set up the flight dynamic and structural dynamic equations of motion for the airplane in terms of its rigid and elastic modes of vibration. Frequency response functions (FRFs) for modal coordinates and hence for loads are calculated assuming flight through one dimensional sine wave gust fields. We can then continue in the frequency domain to calculate loads for continuous turbulence (usually von Karman) or we can transform into the time domain to obtain loads for a step gust from which versed sine or (1-cos) gust responses can be calculated using the convolution integral.

As we look more deeply into the process we find that a number of analytical assumptions and computational procedures are required to calculate gust response loads, each having their influence on user workload, computer requirements, analysis time and the results obtained. This paper will describe some of the approaches taken by de Havilland in developing its gust loads analysis system. This review is presented with the hope that it will stimulate renewed attention within the aeronautical community on this important aspect of the gust loads analysis problem.

The basis of experience for this report is de Havilland's family of turboprop commuter airplanes with maximum take-off weights ranging from 30,000 to 45,000 pounds (13,500 to 20,500 kg), with maximum design cruise speeds of about 250 kts eas and with maximum design altitudes of 25,000 feet (7,500 m). The analysis models for these aircraft were developed using stick models for the structure and unsteady strip theory aerodynamics with Yates corrections (Ref. 1).

2 SETTING UP THE EQUATIONS OF MOTION - SIMULATING FLIGHT DYNAMICS

Limited accountability was the first method used at de Havilland (some 30 years ago) to include elastic responses due to gust encounter. The gust model used was discrete with versed sine shape. The general approach was to compare elastic-to-rigid gust response ratios for the new design with those of an acceptable ref-

Paper presented at a Workshop on "Aircraft Loads due to Turbulence and their Impact on Design and Certification" held in Lillehammer, Norway on 5 May 1994.

erence airplane and to augment the prevailing gust criteria loads by the increase in dynamic factor, if present. The aircraft model used included only rigid body heave and first wing bending modes; there was no attempt to include flight dynamics in the gust calculations in those days.

Flight dynamics first became important at de Havilland with the introduction of the continuous turbulence criterion of FAR Part 25, Appendix G, because of the relatively high energy at low frequencies that characterize continuous turbulence models. Our first approach to simulate combined flight dynamic and structural dynamic effects was to write the equations of motion in a body fixed coordinate system. However, because we ran into some analytical difficulties which we felt could not be resolved in the time available, we quickly retreated to the customary space fixed coordinate system.

Good flight stability characteristics (phugoid, short period, dutch roll) were achieved in the space fixed system by manually adjusting some of the aerodynamic terms in the flight dynamic matrix. This method was subsequently automated by introducing a so-called "sky hook" - a single aerodynamic panel - located at the aircraft cg to achieve the flight stability characteristics required. Consistent with the manual adjustment method, the sky hook was arranged to affect only the flight dynamic equations (ie, panel forces did no work in elastic modes). While the sky hook method was simple to implement, we felt uneasy with the approach because of the inconsistency introduced between rigid and elastic degrees of freedom.

Our current approach for setting up the combined equations is to distribute a set of aerodynamic panels over the length of the fuselage that affect rigid and elastic modes consistently and that provide the flight stability characteristics required. While clearly an improvement over the sky hook method, we are still not satisfied because the aerodynamic coefficient distribution required for flight stability does not agree well with fuselage aerodynamic test data.

Some vertical gust loads results for continuous turbulence are presented in Table 1 for three flight dynamic simulation methods; no attempt to simulate stability, the sky hook method and the fuselage panel method. The results show that simulating flight stability is important and that it matters how that simulation is achieved.

3 GUST LOAD RESPONSE CALCULATIONS

The Mission Analysis Method and N_o

As part of our evaluation of the Mission Analysis method of Appendix G, we ran into some difficulty in establishing an acceptable method for defining N_o, the number of zero crossings in unit time. This parameter is calculated from a definite integral over frequency with convergence depending on the specific formulation of the Sears function used. With guidance from Refs. 2 and 3, we investigated the acceleration response for the case of a rigid airplane free in heave only. We found that converged values for N_o could be obtained using approximations to the Sears function that decayed as k^{-2} or faster, for large values of k, where k is the reduced frequency. For example, the two-term Kussner approximation for the incompressible Sears function (Ref. 4), gave a value for N_o of 2.3 whereas the Houbolt compressible formulation (Ref. 3) gave 2.6. Reference 2 suggests that physically more realistic values of N_o are obtained if the integration is truncated at a frequency corresponding to 95% of the converged value of $\bar{A}$, the response magnitude due to unit root-mean-square (rms) gust intensity. Using this definition, the values obtained for N_o were 0.85 and 0.81, respectively. Due to the ambiguity in defining N_o and for more compelling philosophical reasons regarding the use of Mission Analysis for defining design loads, we decided very early to adopt the Design Envelope method of Appendix G.

The foregoing investigation on N_o caused us to wonder what effect the various Sears function approximations (Fig. 2) might have on loads. This is shown in Table 2 for an elastic airplane. The results have been normalized with respect to Fung's formulation which gives a very close approximation to the exact, incompressible Sears function (Ref. 5). Compared to Fung, the results are noted to vary from +3% to -6%. Houbolt's compressible formulation (Ref. 3) for M=0 is also observed to be in good agreement with Fung. Time did not permit our investigation into lifting surface formulations for Sears functions.

The Force Summation Method and Other Methods for Calculating Loads

As mentioned earlier, our first method for taking elastic effects into account required the calculation of elastic to rigid gust response ratios. This required the use of a Force Summation Method (Refs. 6, 7, and 8) as it is the only method that can be used to calculate response loads for a rigid aircraft. For a variety of reasons, Force Sum-

mation remains the preferred method for calculating loads at de Havilland as well as at most airplane manufacturers (based on a survey conducted by the AGARD SMP). Furthermore, simplified rigid airplane analysis models can be used to provide important checks on results and it is always useful to keep a "calibrated" eye on elastic-to-rigid response ratios as a reality check.

Another very attractive reason for using the Force Summation method is that fewer modes need to be carried to obtain converged dynamic load results than for methods such as Mode Acceleration or Mode Displacement (Ref. 6). This is illustrated in Fig. 3 for wing root and horizontal tail root shear, bending moment and torque loads. Note that in some cases, the Mode Displacement method has not converged fully even with 80 elastic modes and frequencies up to approximately 300 Hz. Furthermore, it is difficult to know whether convergence has actually been achieved when using that method.

4 DISCRETE GUST LOADS AND BALANCED LOADS

Transforming The Frequency Response Function

For calculating discrete gust loads, the procedure used at de Havilland is to first calculate the response for a unit step gust from a Fourier transformation of the frequency response function and to use the convolution integral to obtain the load response for any arbitrary gust pattern of interest (Fig. 1).

It can be shown (Ref. 9) that the response, A(t), to a unit step gust can be calculated from the following transformation expression:

$$A(t) = R(0) + \frac{2}{\pi}\int_0^\infty \frac{I(\omega)\cos\omega t}{\omega} d\omega \qquad (1)$$

where $H(\omega) = R(\omega) + iI(\omega)$ is the frequency response function for the particular load of interest, ω is the circular frequency, t is time and $i = \sqrt{-1}$.

Due to the rigid body modes, $H(\omega)$ is not well defined at $\omega = 0$. This problem is addressed (Ref. 10) by setting $R(0) = R(\varepsilon)$ and $I(0) = 0$, and by assuming linear variations in their values over the frequency range 0 to ε. Here, ε is a small value of ω, and is determined by computational experimentation so that expected behaviours for A(t) are obtained at large values of time, t. For example, loads should converge to zero and velocities to constant values.

The application of the convolution integral for calculating the response to an arbitrary discrete gust profile is straightforward and requires no comment. However, it should be noted that some gust patterns, such as the familiar versed sine, can mask inaccuracies that may exist in the step response function at $t = 0$ and $t \to \infty$ before convolution is applied. This process for calculating transient loads is subjective and tedious; a more robust methodology would improve effectiveness.

Balanced Loads

The need for balanced loads became important when the Stress Group at de Havilland requested time correlated, externally applied load distributions for their calculations. In this context, balanced loads means that the externally applied load distribution, including inertia reactions, produces no residual force or moment when integrated over the whole airplane.

This requirement exposed several new problems.

(1) We first discovered an inconsistency in our application of the force summation method for calculating frequency response functions which, once realized, was easily resolved.

(2) The sky hook method for achieving required flight stability characteristics (already discounted for other reasons as explained above) produced discrete and sometimes significant loads at the aircraft cg that were difficult to rationalize when calculating internal loads. This reinforced our resolve to establish realistic aerodynamic distributions for both flight stability and loads.

(3) The Stress Group's method for calculating internal loads for the fuselage expected shear distributions only whereas the Loads Group provided both local shear and bending moment. This was a process problem that was easily resolved once realized.

In summary, the degree of balance achieved for an aircraft in free flight provides a useful test on the loads methods used.

5 CONTINUOUS TURBULENCE, BALANCED LOADS AND THE SDG METHOD

When it came time to calculate Design Envelope loads, we were confronted with a new problem: how to define balanced load sets for flight in random turbulence for which there is no time basis for correlation.

By way of a solution, we undertook an investigation of J. G. Jones' Statistical Discrete Gust (SDG) method (Ref. 11). This method gave loads approximating those obtained for the Design Envelope method, once the design gust intensity was calibrated (Chapter VI, Ref. 12). Being a time domain method, time correlated and hence balanced load distributions could be defined to provide a solution to our problem. The SDG method had other attractions as well; for example, it could be used to represent other (more realistic) models of atmospheric turbulence (discrete or continuous) and, being a time-domain method, it could be used for calculating Design Envelope loads for aircraft with highly nonlinear systems.

In the end, however, the SDG method was not used at de Havilland for design because a parallel study based on Noback's work (Ref. 13) showed that balanced load distributions for random turbulence could in fact be defined using correlation coefficients. Therefore, the effort to validate the SDG method for design and certification was avoided. With reference to Fig. 3, it should be noted that balanced load conditions are always obtained irrespective of the number of modes carried.

The SDG method, as proposed at the time, was generally concluded to be overly complex for constructing critical gust patterns. While a simpler formulation has since been proposed (not formally documented to date), due to limited resources, we have not had an opportunity to evaluate this new proposal. Although we believe that the SDG method and other similar methods merit further evaluation, we wish to express our concern about the general level of complexity that these new methods require. Complex methods are costly to implement and validate and their standardized application in industry to achieve consistent results will be virtually impossible unless standardized algorithms are made generally available.

Currently, a NASA-developed code for determining critical discrete gust patterns for von Karman continuous turbulence has been made available for evaluation (Ref. 14). The method is based on Matched Filter Theory and is applicable to airplanes with linear and nonlinear systems. The effectiveness of this development and distribution approach should be monitored because it could prove to be an effective means for the standardization of complex computational methods within the aeronautical community.

6 AERODYNAMIC CORRECTION FACTORS

Aerodynamic corrections are used to modify strip or doublet lattice aerodynamic formulations to account for the effects of three-dimensionality, viscosity, or transonic flow. Generally, these corrections derive from wind tunnel data or more sophisticated aerodynamic codes. The correction method used at de Havilland applies factors to the derivatives and cross-derivatives for each streamwise strip. This approach was recently applied in showing compliance with the new requirement for control surface loads, JAR 25.391, introduced by JAR Amendment 91/1.

Two other aerodynamic correction methods are summarized by T. Noll (Ref. 15) viz: applying correction factors to airfoil section properties and applying correction factors to the pressures or downwashes on individual boxes. Due to limited resources, these alternate aerodynamic correction methods have not been evaluated at de Havilland to date.

7 DISCUSSION

This report has reviewed the development of an analysis system for calculating gust loads and has indicated some of the difficulties experienced in developing that system. Due to high development costs, the preferred approach of evaluating all methods and choosing the best could not be pursued; rather, we made what appeared to be rational decisions on methodology at the outset and built our system accordingly. The end result, although acceptable for design safety, requires considerable diligence on the part of the user with the obvious consequent impact on program costs and schedule.

While our analysis system would benefit from revisions in the methods used, we believe other systems could benefit similarly, particularly in view of some emerging requirements and trends. Consider the following:

- The design of aircraft with highly nonlinear systems (active controls) which will require more complex and computer costly analysis routines,

- The trend toward full finite element structural dynamic models to achieve more efficient structural designs and design processes.

- The ever increasing need to reduce design cost and cycle time while developing more efficient structures.

In summary, we perceive a two-fold need; the need for more effective gust load analysis systems to design efficient structures within tight schedules, and the need to validate the results of the analysis systems used.

8 RECOMMENDATIONS

Especially over the last 10 years, considerable experience has been acquired in the development and application of routine gust load calculation methods. While this experience resides mostly with the end users in industry, considerable contribution and insight have emanated from Research Institutes as well. It is therefore evident that, if further gains are to be made in gust loads analysis methods, a united participation of the experts in the field will be required.

It is therefore recommended that a working group of gust loads experts from Industry and Research Institutes be formed and that this working group take into consideration the following recommendations as a basis for its terms of reference. Before proceeding further, it should be emphasized that it is not the intention of this proposal that a single, standardized analysis system evolve from the deliberations of such a working group but that more effective analysis systems tailored to specific needs be defined and validated from a digest of the collective experience accumulated by the experts in the field.

(1) As a first step toward achieving more effective analysis systems for routine gust load computations, it is recommended that a compendium of currently used and promising methods be assembled that would provide a detailed definition of each method giving its advantages, disadvantages, limitations and examples of results. This compendium should consider the following very different approaches:

- The method for setting up and solving the equations of motion for an elastic airplane in body-fixed coordinates as presented in Ref. 16 by Waszak and Schmidt of Purdue University.
- The procedure presented by Lusebrink and Sonder of Deutsche Airbus (Chapter V, Ref. 10) which sets up and solves the equations of motion in the time domain using indicial unsteady aerodynamic formulations.
- The procedure presented in Ref. 17 by Anthony Pototzky and Boyd Perry III of NASA Langley which sets up and solves s-plane and state space formulations of the equations of motion.
- The procedure presented in Ref. 18 by Ph. Nicot and C. Petiau of Dassault Aviation which sets up and solves the equations of motion using a loads basis method as opposed to the more common modes basis method.

(2) It is recommended that standard test cases be defined to provide a basis for validating newly developed analysis methodologies or to verify problem setups using established analysis systems. One standard case that has proven invaluable is the so-called Pratt gust formula (FAR 25.341) that gives the discrete gust load factor for a rigid aircraft with freedom in heave only. Additional standard cases that include other rigid body freedoms and structural flexibility should also be considered in order to achieve more comprehensive validations.

ACKNOWLEDGEMENTS

To Jack Grabowski and Duan Qian for preparing the results and for the stimulating discussions they sparked.

REFERENCES

1. Yates, E. Carson, Jr., "Modified-Strip-Analysis Method for Predicting Wing Flutter at Subsonic to Hypersonic Speeds", Journal of Aircraft, Vol.3, No. 1, Jan.-Feb., 1966, pp. 25-29.

2. Houbolt, J. C., "Design Manual for Vertical Gusts Based on Power Spectral Techniques" AFFDL-TR-70-106, December, 1970.

3. Yates, J.E., and Houbolt, J.C., "On the Aerodynamic Forces of Oscillating Two-Dimensional Lifting Surfaces", AFOSR TR-71-1079, December 1970.

4. Giesing, Joseph P., Rodden, William P. and Stahl, Bernhard, "Sears Function and Lifting Surface Theory for Harmonic Gust Fields", Journal of Aircraft, May-June 1970.

5 Fung, Y. C., *An Introduction to the Theory of Aeroelasticity*, Galcit Aeronautical Series, John Wiley & Sons, 1955.

6. Mar, J.W., Pian, H.H., and Calligeros, J.M., "A Note on Methods for the Determination of Transient Stresses", Journal of the Aeronautical Sciences, January, 1956.

7. Bisplinghoff, Raymond L. and Ashley, Holt, *Principles of Aeroelasticity*, John Wiley and Sons, Inc., 1962.

8. Parthasarathy, Alwar, "Force-Sum Method for Dynamic Stresses in MSC/NASTRAN Aeroelastic Analysis", MSC 1991 World Users' Conference, March 11-15, 1991.

9. Mitchell, C.G.B., "Calculation of the Response of a Flexible Aircraft to Harmonic and Discrete Gusts by a Transform Method", RAE TR65264, November 1965.

10. Cox, R. A., "A Comparative Study of Aircraft Gust Analysis Procedures", The Aeronautical Journal of the Royal Aeronautical Society, October, 1970.

11. Jones, J.G., "The Statistical Discrete Gust (SDG) Method in its Developed Form", presented at the 30th AIAA Structures, Dynamics and Materials Conference, Mobile Alabama, AIAA 89-1375-CP, April 1989.

12. Manual on the Flight of Flexible Aircraft in Turbulence, AGARD-AG-317, May, 1991.

13. Noback, R., The Generation of Equal Probability Design Load Conditions Using P.S.D.-Techniques, NLR TR 85014 L, 1985.

14. Perry, Boyd, III, "MFB1DS and User's Instructions", Aeroelasticity Branch, Structural Dynamics Division, NASA Langley Research Center, MS 340, Hampton VA 23665-5225.

15. Noll, Thomas E., "Aeroservoelasticity", AIAA-90-1073-CP, 1990.

16. Waszak, Martin R., and Schmidt, David K., "Flight Dynamics of Aeroelastic Vehicles", Journal Of Aircraft, June, 1988.

17. Pototzky, Anthony S. and Perry, B., III, "Dynamic Loads Analyses of Flexible Airplanes - New and Existing Techniques", AIAA Paper No. 85-0808, Presented at AIAA/ASME/ASCE/AHS 26th Structures, Structural Dynamics and Materials Conference, Orlando Florida, April 15-17, 1985.

18. Nicot, Ph., and Petiau, C., "Aeroelasticity Analysis using Finite Element Models", Dassault Aviation, European Forum on Aeroelasticity and Structural Dynamics, Aix La Chapelle, April 1989.

TABLE 1 EFFECT OF FLIGHT DYNAMIC SIMULATION ON LOADS

CONTINUOUS TURBULENCE VERTICAL GUST RESULTS ELASTIC AIRPLANE

		FLIGHT DYNAMIC SIMULATION METHOD		
		NO SIMULATION WING + TAIL AERO ONLY	SKY HOOK	FUSELAGE PANELS
WING ROOT RESPONSE	VERTICAL SHEAR	1.00	.94	.91
	VERTICAL BM	1.00	.95	.95
	TORQUE	1.00	.99	1.01
HORIZONTAL TAIL ROOT RESPONSE	VERTICAL SHEAR	1.00	1.10	1.17
	VERTICAL BM	1.00	1.10	1.16
	TORQUE	1.00	.87	.92
FLIGHT STABILITY	FREQUENCY Hz	.82	.53	.53
	DAMPING RATIO	.33	.50	.52

TABLE 2 EFFECT OF SEARS FUNCTION APPROXIMATIONS ON LOADS

CONTINUOUS TURBULENCE VERTICAL GUST RESULTS ELASTIC AIRPLANE

	SEARS APPROXIMATION	WING ROOT			HORIZONTAL TAIL ROOT		
		SHEAR	BM	TORQUE	SHEAR	BM	TORQUE
INCOMPRESSIBLE	FUNG	1.00	1.00	1.00	1.00	1.00	1.00
	2-TERM KUSSNER	1.03	1.03	1.01	1.03	1.03	1.03
	3-TERM KUSSNER	1.00	1.00	1.00	1.00	1.00	1.00
	LIEPMANN	0.95	0.96	0.94	0.96	0.95	0.95
COMPRESSIBLE *	HOUBOLT M=0	0.99	0.99	1.01	0.99	0.99	1.01
	HOUBOLT M=.48	0.95	0.95	0.89	0.95	0.94	0.91

* CONSTANT LIFT-CURVE SLOPE THROUGHOUT

FIG. 1 GUST RESPONSE CALCULATION FLOW DIAGRAM

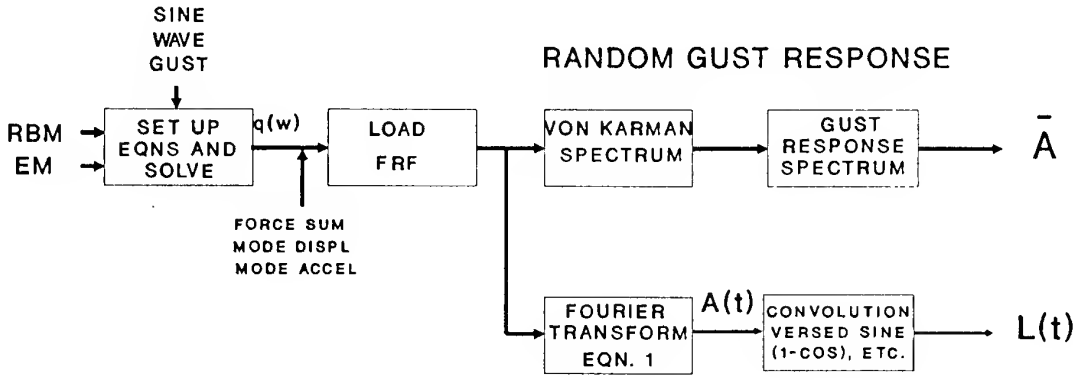

RBM = RIGID BODY MODES
EM = ELASTIC MODES
q(w) = MODAL COORDINATE SOLUTION
FRF = FREQUENCY RESPONSE FUNCTION
$\bar{A}$ = RESPONSE FOR UNIT RMS GUST
A(t) = RESPONSE FOR UNIT STEP GUST
L(t) = DISCRETE GUST LOAD vs TIME

FIG. 2 COMPARISON OF SEARS FUNCTIONS

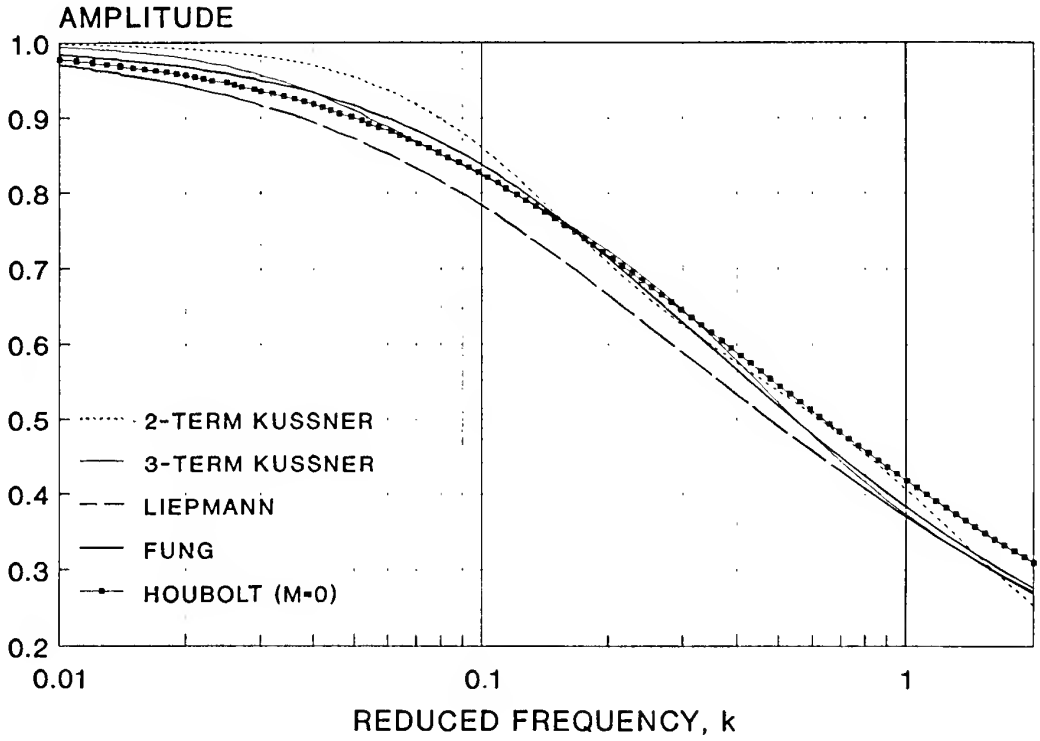

FIG. 3 LOAD CONVERGENCE WITH MODES CARRIED

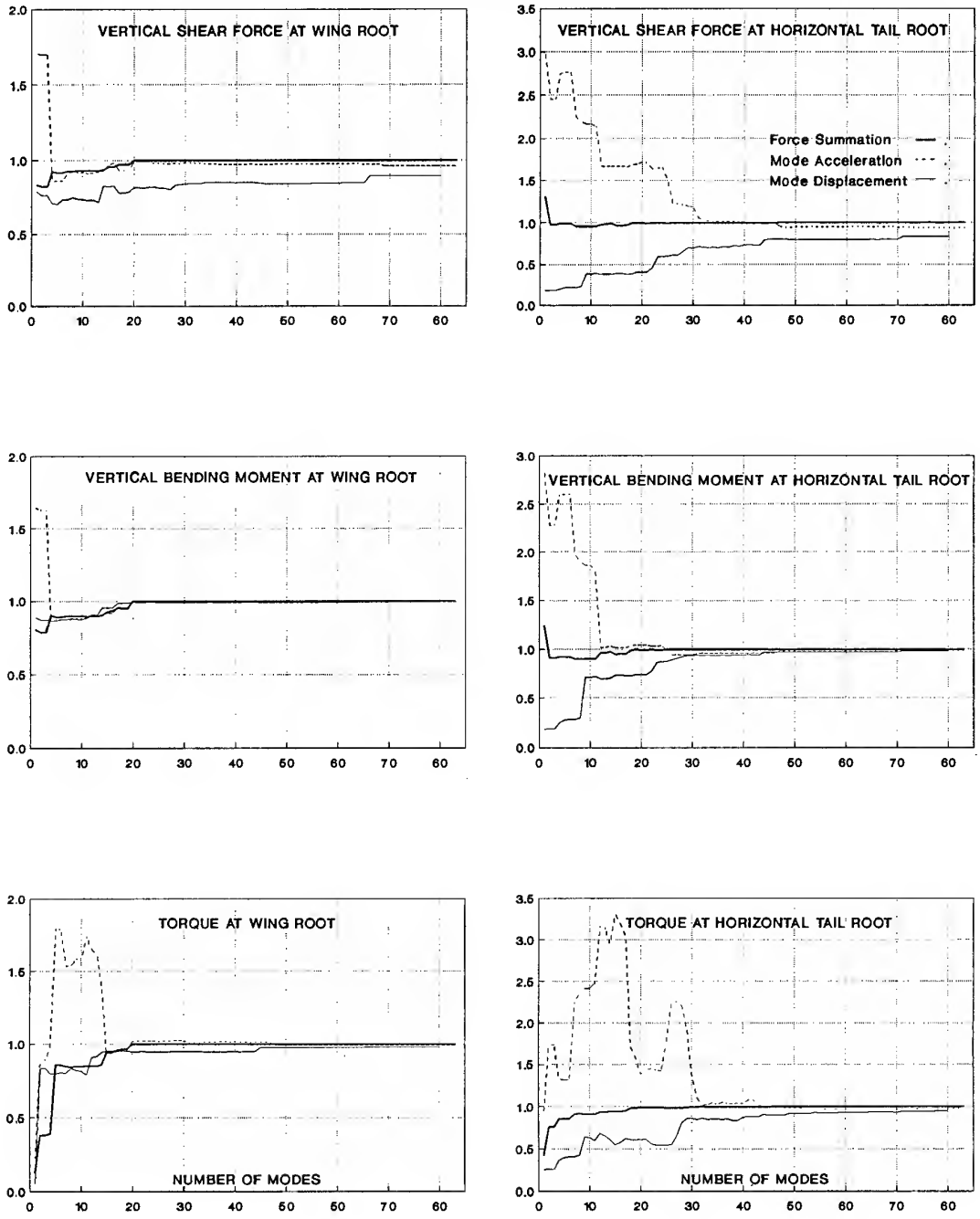

SPECIAL EFFECTS OF GUST LOADS ON MILITARY AIRCRAFT

by

Dr. John C. Houbolt
Chief Aeronautical Scientist (retired)
NASA Langley Research Center
Hampton Va. 23681

ABSTRACT

In the operation of airplanes, atmospheric turbulence creates a broad spectrum of problems. The nature of these problems is presented in this paper. Those that are common to both the commercial carriers and to the military fleet are discussed first. Attention is then focused on the problems that are of special concern in military operations. An aim is to bring out the need for continued effort in the gust research area.

GENERAL

The flight of aircraft through rough air has been studied for many years, but is still of major importance. Upon examination, one finds the breadth of the problems created somewhat surprising. In general terms, ***severe*** turbulence has been of concern because of the control "upset" problem and because of its influence on the static design strength of the airplane; ***moderate*** turbulence is of concern because it leads to problems in achieving precise flight and is a major source of fatigue damage to the structure. Many reviews have been written to bring out the specific problems created by turbulence. The points made are valid even to this day. A look at some of these points serves well to illuminate the extent and nature of the flight problems that are created by atmospheric turbulence. Back in 1964 alone, there were 8,500 pilot reports of turbulence encounter of the unanticipated clear air variety. Of these 2,060 (about 25%) were of ***severe*** nature, 135 were ***extreme***.

Generally, turbulence encounter affects all aviation activities, including defense and civil operation, in the following ways:

a) Mission cancellation and diversion around turbulence

Paper presented at a Workshop on "Aircraft Loads due to Turbulence and their Impact on Design and Certification" held in Lillehammer, Norway on 5 May 1994.

b) Increased aircraft inspection

c) Temporary loss of aircraft control; resultant injury to passengers and crew requiring compensation or medical treatment

d) Shortening of aircraft life time due to metal fatigue

e) Need for special aircrew training

f) Shortage of airspace due to increased number of "baby jets"

Certain aspects unique to civil and military operation are also present. In 1964, for civil aircraft alone, it is estimated that due to injury, diversions, training, information and inspection, a total expense of $18,000,000 was involved due to turbulence encounter. This figure does not include loss of the use of grounded aircraft, loss of time due to injuries, or expense of settling claims. Also the increase in number of general aviation jets, operating in the 20-40,000 foot environment, where restrictions vertically and horizontally may be imposed at times due to turbulence, result in increased economic concern to operators.

Military aircraft have experienced numerous accidents and incidents because of turbulence. Additional difficulties presented to military operations include:

a) Hazards in air-to-air refueling

b) Reduced available airspace for conducting simulated missions

c) Degradation of reconnaissance sensor and bombing accuracies

d) (More as discussed in a later section)

The cost of turbulence to DOD operations is difficult to evaluate, but estimates for the 3-year 1963-1965 period due to aircraft lost and damaged are placed at around $30,000,000. Costs of special inspections, minor repairs, minor injuries, and for special training are not known. In addition, value cannot be placed on loss of pilots or on the effect on actual combat missions due to lack of advanced information on the location of clear air turbulence.

GUST RESEARCH EFFORT

We list here in brief fashion the nature of the research effort that has been underway for years to understand and solve the problems that arise from gust encounter. It is convenient to list the studies in four broad categories.

Turbulence measurement: This effort has involved three main sources. Low altitude measurement on tall towers, specific research flights on well instrumented airplanes to measure the turbulence, and through means of special recorders in aircraft to measure turbulence encounter and severity during routine scheduled flights.

Turbulence modeling: By analytical studies, and through use of the turbulence measurements, mathematical modeling of turbulence has been made. The modeling has been in terms of at least four related aspects: the concept of discrete or isolated type gust encounter, the concept of continuous (random) turbulence encounter form, the establishment of turbulence design severity levels, and the determination of the time spent in turbulence.

Airplane response analysis due to turbulence: Here studies are made to determine how the airplane responds to turbulence. Modeling consists of representing the airplane by various structural degrees of freedom, and of using non-steady aerodynamics to account for the airplane motion and gust penetration effects. The results sought are the maximum loads, acceleration, stresses, and load encounter curves for airplane fatigue analysis and life prediction. In turn these results are used to design the structural members, particularly the wing, and to design special devices such as gust loads alleviation systems.

Specifications and regulations: The research studies do not directly write the specifications or regulations. However the studies are fed as guidelines to the regulators so that they can use the findings to establish the design specifications and procedures for turbulence encounter that ultimately appear in the regulations.

ADDED SPECIAL MILITARY PROBLEMS

Some of the turbulence problems that are special for military aircraft have been mentioned in the preceding sections. By way of emphasis we list here certain problems of turbulence encounter that are of particular concern, some of which are unique to military type aircraft.

Turbulence encounter has a marked effect on degrading the structural life of the aircraft (this has become to be known as the aging aircraft problem). In fact, gust encounter accounts for 40-50% of the damage hours of the structure.

In low level missions, which is of particular significance to military operations, but where turbulence can be rather severe and prevalent, damage hours build up ten times more rapidly than in higher altitude flight.

T-tailed aircraft take a rather rough beating during air-refueling operations due to turbulence generated by the tanker aircraft.

Gust alleviation systems are often needed to control airplane motion, such as yaw dampers. These devices are also needed to improve the ride comfort for the pilot, and to improve sensor capability and bombing accuracy.

We note that the items listed in this section are in need of greater research effort.

We also note that, whereas turbulence causes the most damage to the wings, the ground to air cycle (fuselage pressurization) creates most of the damage hours to the fuselage.

CLOSURE

For possible use to obtain a quick overview of this report, or for presentation purposes, the contents of this report are summarized in three condensed listings in the three pages that follow.

THE PROBLEMS DUE TO ATMOSPHERIC GUSTS

SEVERE

- Jet upsets
- In flight failures after out-of-control
- Overstressing
- Aircraft disappeared in servere turbulence

CIVIL SECTOR

- Cancel and diversions
- Information
- Training
- Injury
- Inspection

} $20,000,000 / Year

Not Included:

- Loss of use of grounded aircraft
- Loss of time due to injuries
- Overhead of settling claims

MILITARY

Civil Problem Plus:

- Hazards of air-to-air refueling
- Reduced airspace to conduct simulated missions
- Degradation in reconnaissance sensors and bombing accuracies

LOSS AND DAMAGE - $30,000,000 / Year

Costs Not Included:

- Special inspections
- Minor repairs
- Minor injuries
- Special training
- Loss of pilots and crew
- Effect on combat missions

GUST RESEARCH EFFORT

TURBULENCE MEASUREMENT

- Research flights to measure turbulence
- Recorders in aircraft to measure turbulence encounter and severity during routine scheduled flights

TURBULENCE MODELING

From Measurements Establish Mathematical Modeling

- Discrete or isolated type gust encounter
- Continuous (random) turbulence encounter
- Turbulence design severity levels
- Time in turbulence

AIRPLANE RESPONSE ANALYSIS DUE TO TURBULENCE

- Maximum loads, acceleration, and stresses
- Load encounter curves for airplane fatigue analysis and life prediction
- Design of structural members, particularly the wing
- Design of gust load alleviation systems

SPECS AND REGULATIONS

- Establish design specifications and procedures for turbulence encounter-to appear in regulations

ADDED SPECIAL MILITARY PROBLEMS

MARKED EFFECT ON DEGRADING STRUCTURAL LIFE OF THE AIRCRAFT (THE AGING AIRCRAFT PROBLEM)

GUSTS ACCOUNT FOR 40-50% OF THE DAMAGE HOURS OF THE STRUCTURE

IN LOW LEVEL MISSIONS DAMAGE HOURS BUILD UP 10 X MORE RAPIDLY

T-TAILED AIRCRAFT TAKE A ROUGH BEATING DURING AIR-REFUELING (TURBULENCE FROM THE TANKER AND THE ATMOSPHERE)

GUST ALLEVIATION IS NEEDED TO CONTROL AIRPLANE MOTION AND STRUCTURAL MODES, FOR RIDE COMFORT, AND FOR SENSOR AND BOMBING ACCURACY

NOTE: GROUND TO AIR CYCLE (FUSELAGE PRESSURIZATION) CREATES MOST OF THE DAMAGE HOURS TO THE FUSELAGE

REPORT DOCUMENTATION PAGE

1. Recipient's Reference	2. Originator's Reference	3. Further Reference	4. Security Classification of Document
	AGARD-R-798	ISBN 92-836-0002-9	UNCLASSIFIED

5. Originator Advisory Group for Aerospace Research and Development
North Atlantic Treaty Organization
7 rue Ancelle, 92200 Neuilly-sur-Seine, France

6. Title

Aircraft Loads due to Turbulence and
their Impact on Design and Certification

7. Presented at

Workshop held in Lillehammer, Norway, 5 May 1994

8. Author(s)/Editor(s)	9. Date
Various	December 1994
10. Author's/Editor's Address	**11. Pages**
Various	96

12. Distribution Statement There are no restrictions on the distribution of this document. Information about the availability of this and other AGARD unclassified publications is given on the back cover.

13. Keywords/Descriptors

Aircraft	Atmospheric disturbances
Flight loads	Design
Aerodynamic loads	Certification
Turbulence	

14. Abstract

The AGARD Structures and Materials Panel has always been heavily involved in the field of the effects of atmospheric disturbances on the behaviour of aircraft. The Panel organized a Workshop on the theme "Aircraft Loads due to Turbulence and their Impact on Design and Certification". This Workshop was held on 5 May 1994. This document reproduces the papers presented.

AGARD-R-798
Advisory Group for Aerospace Research and Development
North Atlantic Treaty Organization
AIRCRAFT LOADS DUE TO TURBULENCE AND THEIR IMPACT ON DESIGN AND CERTIFICATION
Published December 1994
96 pages

The AGARD Structures and Materials Panel has always been heavily involved in the field of the effects of atmospheric disturbances on the behaviour of aircraft. The Panel organized a Workshop on the theme "Aircraft Loads due to Turbulence and their Impact on Design and Certification". This Workshop was held on 5 May 1994. This document reproduces the papers presented.

ISBN 92-836-0002-9

AGARD-R-798

Aircraft
Flight loads
Aerodynamic loads
Turbulence
Atmospheric disturbances
Design
Certification

AGARD-R-798
Advisory Group for Aerospace Research and Development
North Atlantic Treaty Organization
AIRCRAFT LOADS DUE TO TURBULENCE AND THEIR IMPACT ON DESIGN AND CERTIFICATION
Published December 1994
96 pages

The AGARD Structures and Materials Panel has always been heavily involved in the field of the effects of atmospheric disturbances on the behaviour of aircraft. The Panel organized a Workshop on the theme "Aircraft Loads due to Turbulence and their Impact on Design and Certification". This Workshop was held on 5 May 1994. This document reproduces the papers presented.

ISBN 92-836-0002-9

AGARD-R-798

Aircraft
Flight loads
Aerodynamic loads
Turbulence
Atmospheric disturbances
Design
Certification

AGARD-R-798
Advisory Group for Aerospace Research and Development
North Atlantic Treaty Organization
AIRCRAFT LOADS DUE TO TURBULENCE AND THEIR IMPACT ON DESIGN AND CERTIFICATION
Published December 1994
96 pages

The AGARD Structures and Materials Panel has always been heavily involved in the field of the effects of atmospheric disturbances on the behaviour of aircraft. The Panel organized a Workshop on the theme "Aircraft Loads due to Turbulence and their Impact on Design and Certification". This Workshop was held on 5 May 1994. This document reproduces the papers presented.

ISBN 92-836-0002-9

AGARD-R-798

Aircraft
Flight loads
Aerodynamic loads
Turbulence
Atmospheric disturbances
Design
Certification

AGARD

NATO - OTAN

7 RUE ANCELLE • 92200 NEUILLY-SUR-SEINE

FRANCE

Télécopie (1)47.38.57.99 • Télex 610 176

DIFFUSION DES PUBLICATIONS

AGARD NON CLASSIFIEES

Aucun stock de publications n'a existé à AGARD. A partir de 1993, AGARD détiendra un stock limité des publications associées aux cycles de conférences et cours spéciaux ainsi que les AGARDographies et les rapports des groupes de travail, organisés et publiés à partir de 1993 inclus. Les demandes de renseignements doivent être adressées à AGARD par lettre ou par fax à l'adresse indiquée ci-dessus. *Veuillez ne pas téléphoner.* La diffusion initiale de toutes les publications de l'AGARD est effectuée auprès des pays membres de l'OTAN par l'intermédiaire des centres de distribution nationaux indiqués ci-dessous. Des exemplaires supplémentaires peuvent parfois être obtenus auprès de ces centres (à l'exception des Etats-Unis). Si vous souhaitez recevoir toutes les publications de l'AGARD, ou simplement celles qui concernent certains Panels, vous pouvez demander à être inclu sur la liste d'envoi de l'un de ces centres. Les publications de l'AGARD sont en vente auprès des agences indiquées ci-dessous, sous forme de photocopie ou de microfiche.

CENTRES DE DIFFUSION NATIONAUX

ALLEMAGNE
Fachinformationszentrum,
Karlsruhe
D-76344 Eggenstein-Leopoldshafen 2

BELGIQUE
Coordonnateur AGARD-VSL
Etat-major de la Force aérienne
Quartier Reine Elisabeth
Rue d'Evere, 1140 Bruxelles

CANADA
Directeur du Service des renseignements scientifiques
Ministère de la Défense nationale
Ottawa, Ontario K1A 0K2

DANEMARK
Danish Defence Research Establishment
Ryvangs Allé 1
P.O. Box 2715
DK-2100 Copenhagen Ø

ESPAGNE
INTA (AGARD Publications)
Pintor Rosales 34
28008 Madrid

ETATS-UNIS
NASA Headquarters
Code JOB-1
Washington, D.C. 20546

FRANCE
O.N.E.R.A. (Direction)
29, Avenue de la Division Leclerc
92322 Châtillon Cedex

GRECE
Hellenic Air Force
Air War College
Scientific and Technical Library
Dekelia Air Force Base
Dekelia, Athens TGA 1010

ISLANDE
Director of Aviation
c/o Flugrad
Reykjavik

ITALIE
Aeronautica Militare
Ufficio del Delegato Nazionale all'AGARD
Aeroporto Pratica di Mare
00040 Pomezia (Roma)

LUXEMBOURG
Voir Belgique

NORVEGE
Norwegian Defence Research Establishment
Attn: Biblioteket
P.O. Box 25
N-2007 Kjeller

PAYS-BAS
Netherlands Delegation to AGARD
National Aerospace Laboratory NLR
P.O. Box 90502
1006 BM Amsterdam

PORTUGAL
Força Aérea Portuguesa
Centro de Documentação e Informação
Alfragide
2700 Amadora

ROYAUME-UNI
Defence Research Information Centre
Kentigern House
65 Brown Street
Glasgow G2 8EX

TURQUIE
Millî Savunma Başkanliği (MSB)
ARGE Dairesi Başkanliği (MSB)
06650 Bakanliklar-Ankara

Le centre de distribution national des Etats-Unis ne détient PAS de stocks des publications de l'AGARD.
D'éventuelles demandes de photocopies doivent être formulées directement auprès du NASA Center for AeroSpace Information (CASI) à l'adresse ci-dessous. Toute notification de changement d'adresse doit être fait également auprès de CASI.

AGENCES DE VENTE

NASA Center for
AeroSpace Information (CASI)
800 Elkridge Landing Road
Linthicum Heights, MD 21090-2934
Etats-Unis

ESA/Information Retrieval Service
European Space Agency
10, rue Mario Nikis
75015 Paris
France

The British Library
Document Supply Division
Boston Spa, Wetherby
West Yorkshire LS23 7BQ
Royaume-Uni

Les demandes de microfiches ou de photocopies de documents AGARD (y compris les demandes faites auprès du CASI) doivent comporter la dénomination AGARD, ainsi que le numéro de série d'AGARD (par exemple AGARD-AG-315). Des informations analogues, telles que le titre et la date de publication sont souhaitables. Veuiller noter qu'il y a lieu de spécifier AGARD-R-nnn et AGARD-AR-nnn lors de la commande des rapports AGARD et des rapports consultatifs AGARD respectivement. Des références bibliographiques complètes ainsi que des résumés des publications AGARD figurent dans les journaux suivants:

Scientific and Technical Aerospace Reports (STAR)
publié par la NASA Scientific and Technical
Information Division
NASA Headquarters (JTT)
Washington D.C. 20546
Etats-Unis

Government Reports Announcements and Index (GRA&I)
publié par le National Technical Information Service
Springfield
Virginia 22161
Etats-Unis
(accessible également en mode interactif dans la base de
données bibliographiques en ligne du NTIS, et sur CD-ROM)

Imprimé par le Groupe Communication Canada
45, boul. Sacré-Cœur, Hull (Québec), Canada K1A 0S7

AGARD

NATO OTAN

7 RUE ANCELLE • 92200 NEUILLY-SUR-SEINE

FRANCE

Telefax (1)47.38.57.99 • Telex 610 176

DISTRIBUTION OF UNCLASSIFIED

AGARD PUBLICATIONS

AGARD holds limited quantities of the publications that accompanied Lecture Series and Special Courses held in 1993 or later, and of AGARDographs and Working Group reports published from 1993 onward. For details, write or send a telefax to the address given above. *Please do not telephone.*

AGARD does not hold stocks of publications that accompanied earlier Lecture Series or Courses or of any other publications. Initial distribution of all AGARD publications is made to NATO nations through the National Distribution Centres listed below. Further copies are sometimes available from these centres (except in the United States). If you have a need to receive all AGARD publications, or just those relating to one or more specific AGARD Panels, they may be willing to include you (or your organisation) on their distribution list. AGARD publications may be purchased from the Sales Agencies listed below, in photocopy or microfiche form.

NATIONAL DISTRIBUTION CENTRES

BELGIUM
Coordonnateur AGARD — VSL
Etat-major de la Force aérienne
Quartier Reine Elisabeth
Rue d'Evere, 1140 Bruxelles

CANADA
Director Scientific Information Services
Dept of National Defence
Ottawa, Ontario K1A 0K2

DENMARK
Danish Defence Research Establishment
Ryvangs Allé 1
P.O. Box 2715
DK-2100 Copenhagen Ø

FRANCE
O.N.E.R.A. (Direction)
29 Avenue de la Division Leclerc
92322 Châtillon Cedex

GERMANY
Fachinformationszentrum
Karlsruhe
D-76344 Eggenstein-Leopoldshafen 2

GREECE
Hellenic Air Force
Air War College
Scientific and Technical Library
Dekelia Air Force Base
Dekelia, Athens TGA 1010

ICELAND
Director of Aviation
c/o Flugrad
Reykjavik

ITALY
Aeronautica Militare
Ufficio del Delegato Nazionale all'AGARD
Aeroporto Pratica di Mare
00040 Pomezia (Roma)

LUXEMBOURG
See Belgium

NETHERLANDS
Netherlands Delegation to AGARD
National Aerospace Laboratory, NLR
P.O. Box 90502
1006 BM Amsterdam

NORWAY
Norwegian Defence Research Establishment
Attn: Biblioteket
P.O. Box 25
N-2007 Kjeller

PORTUGAL
Força Aérea Portuguesa
Centro de Documentação e Informação
Alfragide
2700 Amadora

SPAIN
INTA (AGARD Publications)
Pintor Rosales 34
28008 Madrid

TURKEY
Milli Savunma Başkanliği (MSB)
ARGE Dairesi Başkanliği (MSB)
06650 Bakanliklar-Ankara

UNITED KINGDOM
Defence Research Information Centre
Kentigern House
65 Brown Street
Glasgow G2 8EX

UNITED STATES
NASA Headquarters
Code JOB-1
Washington, D.C. 20546

The United States National Distribution Centre does NOT hold stocks of AGARD publications.
Applications for copies should be made direct to the NASA Center for AeroSpace Information (CASI) at the address below.
Change of address requests should also go to CASI.

SALES AGENCIES

NASA Center for
AeroSpace Information (CASI)
800 Elkridge Landing Road
Linthicum Heights, MD 21090-2934
United States

ESA/Information Retrieval Service
European Space Agency
10, rue Mario Nikis
75015 Paris
France

The British Library
Document Supply Centre
Boston Spa, Wetherby
West Yorkshire LS23 7BQ
United Kingdom

Requests for microfiches or photocopies of AGARD documents (including requests to CASI) should include the word 'AGARD' and the AGARD serial number (for example AGARD-AG-315). Collateral information such as title and publication date is desirable. Note that AGARD Reports and Advisory Reports should be specified as AGARD-R-nnn and AGARD-AR-nnn, respectively. Full bibliographical references and abstracts of AGARD publications are given in the following journals:

Scientific and Technical Aerospace Reports (STAR)
published by NASA Scientific and Technical
Information Division
NASA Headquarters (JTT)
Washington D.C. 20546
United States

Government Reports Announcements and Index (GRA&I)
published by the National Technical Information Service
Springfield
Virginia 22161
United States
(also available online in the NTIS Bibliographic
Database or on CD-ROM)

Printed by Canada Communication Group
45 Sacré-Cœur Blvd., Hull (Québec), Canada K1A 0S7

ISBN 92-836-0002-9